COLD TOLERANCE AND SEASONAL GENE EXPRESSION IN *DENDROCTONUS PONDEROSAE*

by

Jordie D. Fraser

B.Sc. University of Northern British Columbia, 2007

THESIS SUBMITTED IN PARTIAL FULFILLMENT OF
THE REQUIREMENTS FOR THE DEGREE OF
MASTER OF SCIENCE
IN
NATURAL RESOURCES AND ENVIRONMENTAL STUDIES
IN BIOLOGY

THE UNIVERSITY OF NORTHERN BRITISH COLUMBIA

April 2011

Your file Votre référence
ISBN: 978-0-494-75167-1
Our file Notre référence
ISBN: 978-0-494-75167-1

Abstract

Several aspects pertaining to quantification of seasonal *Dendroctonus ponderosae* gene expression, specifically, obtaining measures of insect RNA integrity and selection of stable endogenous controls are discussed. mRNA transcript levels indicate glycerol production in *D. ponderosae* occurs through both glycogenolytic, gluconeogenic and potentially glyceroneogenic pathways, but not from metabolism of lipids. A two-week lag period between fall glycogen phosphorylase and phosphoenolpyruvate carboxykinase transcript up-regulation indicates gluconeogenesis may serve as a secondary glycerol-production process, subsequent to the potential exhaustion of the primary glycogenolytic source; a successive "one-two punch" of glycerol production. Glycerol kinase is found to be present within *D. ponderosae* and its mRNA transcript levels increased in the autumn, along with those of triosephosphate isomerase and glycerol-3-phosphate dehydrogenase, suggesting that glycerol is produced from dihydroxyacetone phosphate intermediate. Constant alcohol dehydrogenase transcript levels indicates that a glyceraldehyde-3-phosphate intermediate is not involved in production of glycerol in *D. ponderosae*.

TABLE OF CONTENTS

Abstract		ii
Table of Contents		iii
List of Tables		vii
List of Figures		viii
Dedication		xiv
Acknowledgement		xv
Chapter One: Introduction		
1.1	Temperature and Mountain Pine Beetle Ecology	1
1.1.1	Mountain Pine Beetle Life Cycle	1
1.1.2	Mountain Pine Beetle Development & Voltism	1
1.1.3	Mountain Pine Beetle Quiescence	2
1.2	Mechanisms of Cold Tolerance in Insects	3
1.2.1	Freeze Tolerance and Freeze Avoidance	3
1.2.2	Anahydrobiosis	5
1.2.3	Vitrification	6
1.2.4	Freeze Tolerance	6
1.2.5	Freeze Avoidance	7
1.2.6	Mechanism Cross-over	8
1.3	Mechanisms of Cold Tolerance in Mountain Pine Beetle	10
1.3.1	Indication of Cold Avoidant Mechanisms	10
1.4	Gene Expression & Methodology	12
1.4.1	Gene Expression	12
1.4.2	Reverse Transcription Polymerase Chain Reaction (RT-qPCR)	13
1.4.3	RNA Integrity & Gene Expression	17
1.4.4	Slab Gel Electrophoresis	18
1.4.5	Microfluidic Capillary Electrophoresis (MCE)	18
1.4.6	28S/18S Measure of RNA Integrity	20
1.4.7	MCE Measures of RNA Integrity	21
1.5	Objectives	22
1.6	Bibliography	22
Chapter Two: RNA Integrity and Gene Expression in *Dendroctonus ponderosae*		
2.1	Introduction	29
2.2	Methods	34
2.2.1	Sample Collection and Preparation	34
2.2.2	Total RNA Extractions	34
2.2.3	Sample Assessment and Pooling of Total RNA Extractions	35
2.2.4	Thermal Treatment of Pooled Sample Aliquots	35

2.2.5	Integrity Assessment of Thermally Treated Aliquots	36
2.2.6	Reverse Transcription Reactions	39
2.2.7	Quantitative PCR & Fold Change Determination	39
2.2.8	Statistical Analysis	42
2.3	Results	44
2.3.1	Integrity Assessment of Thermally Treated RNA Aliquots	44
2.3.1.1	Integrity Assessment by Slab Gel Electrophoresis	47
2.3.1.2	Integrity Assessment by Microfluidic Capillary Electrophoresis (MCE)	48
2.3.2	Area Quotient Determination	49
2.3.3	Apparent mRNA n-Fold Expression Decrease	51
2.3.4	Thermal Threshold Determination	53
2.4	Discussion	56
2.5	Conclusion	59
2.6	Bibliography	60
2.7	Appendix	63

Chapter 3: Evaluation of Reverse Transcription-Quantitative Polymerase Chain Reaction (RT-qPCR) Reference Genes for Seasonal Cold Tolerance Gene Expression Studies in *Dendroctonus ponderosae*

3.1	Introduction	64
3.2	Methods	67
3.2.1	Sample Collection and Preparation	67
3.2.2	Total RNA Extractions	67
3.2.3	Reverse Transcription Reactions	68
3.2.3.1	Pooled cDNA	68
3.2.3.2	Dataset Samples	69
3.2.4	Bioinformatics and Primer and Probe Design	70
3.3.2.5	Primer Specificity and PCR Reaction Optimization	71
3.2.6	qPCR Reaction Optimization	73
3.2.6.1	Annealing Temperature Optimization	73
3.2.6.2	Primer Concentration Optimization	74
3.2.6.3	Dynamic Linear Range (DLR) and Reference Gene Amplification Efficiency Determination (E)	75
3.2.7	qPCR Dataset Reactions and Sample Analysis	76
3.2.8	Assessment of Genomic DNA (gDNA) Contamination	77
3.2.9	Reference Gene Expression Stability Determination	77
3.3	Results	79
3.3.1	Primer Design and Specificity Validation	79
3.3.2	RT-qPCR Reaction Optimization	84
3.3.3	Dynamic Linear Range (DLR) and Reference Gene Amplification Efficiency Determination (E)	84
3.3.4	geNorm Input and Output	87
3.4	Discussion	92
3.5	Conclusions	100
3.6	Bibliography	101

Chapter 4: Seasonal Transcript Accumulation of Glycerol Biosynthetic Genes in *Dendroctonus ponderosae*

4.1	Introduction	104
4.2	Methods	110
4.2.1	RT-qPCR and Temperature	110
4.2.2	GOI mRNA Expression Determination	113
4.2.3	Graphical and Statistical Analysis	113
4.3	Results	115
4.3.1	Primer Design and Specificity Validation	115
4.3.2	RT-qPCR Reaction Optimization	117
4.3.3	Dynamic Linear Range (DLR) and GOI Amplification Efficiency Determination (E)	117
4.3.5	Temperature Data	120
4.3.5.1	Fall 2008	120
4.3.5.2	Spring 2009	120
4.3.6	GOI mRNA Expression Results	121
4.3.6.1	GOI Associated with Major Energetic Storage Molecule Metabolism	121
4.3.6.1.1	Triacylglycerol Lipase (TAGL)	121
4.3.6.1.2	Glycogen Phosphorylase (GP)	123
4.3.6.2	GOI Associated with the Gluconeogenesis	126
4.3.6.2.1	Phosphoenolpyruvate Carboxykinase (PEPCK)	126
4.3.6.2.2	Fructose-1,6-bisphosphatase (FBP)	129
4.3.6.3	GOI Involved in Glycogenesis	132
4.3.6.3.1	Glycogen Synthase (GS)	132
4.3.6.4	GOI Associated with Substrate Intermediates Involved in Glycerol Metabolism	135
4.3.6.4.1	Alcohol Dehydrogenase (ADH)	135
4.3.6.4.2	Triosephosphate Isomerase (TPI)	137
4.3.6.4.3	Glycerol-3-phosphate Dehydrogenase (G3PDH)	140
4.3.6.4.4	Glycerol Kinase (GK)	143
4.3.6.5	GOI Associated with the Pentose Phosphate Pathway	146
4.3.6.5.1	6-Phosphoglucolactonase (6-PGL)	146
4.3.6.5.2	Glucose-6-phosphate dehydrogenase (G6PDH)	148
4.3.6.6	GOI Associated with the Citric Acid Cycle	150
4.3.6.6.1	Pyruvate kinase (PK)	150
4.3.6.6.2	Citrate synthase (CS)	152
4.4	Discussion	154
4.4.1	Introduction to Challenges of GOI Analysis	154
4.4.1.1	Diapause, Quiescence and Overwintering Development	154
4.4.1.2	Fasting	156
4.4.1.3	Hypoxia and Anoxia	157
4.4.2	Glycerol Metabolism Involves Both Glycogenolysis and Gluconeogenesis	157
4.4.3	Glycerol is Not Reconverted to Glycogen by Glycogenesis	162

4.4.4	Glycerol is Metabolized from a DHAP Intermediate and by Glyceroneogenesis	163
4.4.5	Glycerol Production Does Not Involve the Pentose Phosphate Pathway	167
4.4.6	During Glycerol Production, the Citric Acid Cycle Remains Unaffected	168
4.5	Conclusion	170
4.6	Bibliography	171

Chapter 5: Conclusion

5.1	Summary	177

Appendix 180

LIST OF TABLES

Table 2.1. Primer sequence and properties of three target genes employed to evaluate how the integrity of seven thermally treated *D. ponderosae* total RNA aliquots influences mRNA quantification by RT-qPCR 40

Table 2.2. Hydrolysis probe sequences of three target genes employed to evaluate how the integrity of seven thermally treated *D. ponderosae* total RNA aliquots influences mRNA quantification by RT-qPCR 41

Table 2.3 – Area quotients: average ratio of late phase area to early phase area for thermally treated RNA aliquots 50

Table 3.1. Primer sequence and properties used in evaluation of seven candidate RT-qPCR reference genes employed to investigate seasonal cold tolerance in *D. ponderosae*. 80

Table 3.2. Hydrolysis probe sequence used in evaluation of four candidate RT-qPCR reference genes employed to investigate seasonal cold tolerance in *D. ponderosae*. 81

Table 3.3. Candidate reference genes for normalization of GOIs associated with seasonal cold tolerance in *D. ponderosae* listed according to their respective stability as determined by geNorm. An overall stability ranking including all study treatments was produced. Rankings were further differentiated by treatment, as defined by the collection date during Fall 2008 period of study. Bold-faced type indicates the number of reference genes required to achieve a pair-wise variation just below or closest to 0.15 and the number of *D. ponderosae* biological replicates composing a treatment group are reported. 88

Table 3.4. Candidate reference genes for normalization of GOIs associated with seasonal cold tolerance in *D. ponderosae* listed according to their respective stability as determined by geNorm. Rankings differentiated by treatment, as defined by the collection date during Spring 2009 period of study. Bold-faced type indicates the number of reference genes required to achieve a pair-wise variation just below or closest to 0.15 and the number of *D. ponderosae* biological replicates composing a treatment group are reported. 89

Table 4.1. Primer sequence and properties used in evaluation of fourteen RT-qPCR genes of interest (GOI) employed to investigate seasonal cold tolerance in *D. ponderosae*. 111

Table 4.2. Hydrolysis probe sequence used in evaluation of fourteen RT-qPCR genes of interest (GOI) employed to investigate seasonal cold tolerance in *D. ponderosae*. 112

LIST OF FIGURES

Figure 2.1 – Definition of early phase and late phase interval bounds. The early phase was defined as the electropherogram interval starting after the 5S peak (~28-seconds) through to the beginning of the 18S peak (~41-seconds). Early phase area was selected for RNA integrity investigation as it provides a region of the electropherogram that can be expected to produce limited fluorescence (i.e. possess few RNA fragments of this size), resulting in a small early phase area. The late phase was defined as the electropherogram interval starting at the beginning of the 18S peak (~41-seconds) through to the end of the 18S peak (~42-seconds). Composed of the interval where the expected migration location of both the 18S and 28S fragments occur, the late phase area was selected for RNA integrity investigation as it provides a region of the electropherogram that can be expected to produce the majority (~70-85%) of the fluorescence detected from the whole electropherogram. Similar to a 28S/18S ratio, the ratio of late phase area to early phase area, referred to as an area quotient, can serve as a proxy measure of RNA integrity for samples of insect origin. 38

Figure 2.2 – Assessment of total RNA integrity (for sample #9) by microfluidic capillary electrophoresis (MCE) and slab gel electrophoresis. Ten pooled *D. ponderosae* total RNA samples were thermally treated in a thermocycler (MJ Mini, Biorad, USA) at 90°C for one of the following minute time intervals: 0, 30, 60, 90, 180, 300 or 420. (A) Digital microfluidic capillary electrophoresis RNA gel produced from loading 100ng of total RNA from each of the thermally treated aliquots for each pooled sample and a eukaryotic RNA standard onto a Experion StdSens RNA Microchip (BioRad, USA). (B) Agarose gel (1.5%, run for 45 minutes at 120V) produced from loading 800ng of each thermally treated RNA aliquot for a pooled sample and 75ng of 1kB DNA ladder (Invitrogen, USA). Electrophoresized slab gels were stained for 40 minutes with SYBR Green II RNA Gel Stain (Invitrogen, USA) using a 1:10,000 dilution of stock reagent as per reagent manual. Gels were visualized on a transilluminator at 300nm with a specialized filter. (C) Thermally treated RNA aliquot electropherograms produced by MEC methods. Electropherograms are displayed from 20 to 50 seconds and at variable fluorescence (RU) units. 45

Figure 2.3 – Mean n-fold mRNA apparent expression decreases for thermally treated total RNA aliqots, relative to mRNA expression of an untreated aliquot, using TBP primers and probes. A one-way ANOVA was conducted with mean n-fold mRNA expression decreases significantly different from the mRNA expression for the untreated sample denoted (* = $p<0.05$; *** = $p<0.001$). 52

Figure 2.4 - Assessment of total RNA integrity by microfluidic capillary electrophoresis (MCE). A pooled 20 May, 2009 *D. ponderosae* total RNA sample was split into equal volume aliquots and thermally treated in a thermocycler (MJ Mini, Biorad, USA) for two minutes at one of the following temperatures: 10°C, 20°C, 30°C, 40°C, 50°C or 60°C. (A) Digital microfluidic capillary electrophoresis RNA gel produced from loading 100ng of total RNA from each of the thermally treated aliquots onto an Experion StdSens RNA Microchip (BioRad, USA). (B) Thermally treated RNA aliquot electropherograms produced by MEC methods. Electropherograms are displayed from 20 to 50 seconds and at variable fluorescence (RU) units. 55

Figure 2.5 - 1.5% agarose gel (45 minutes at 120V) produced from loading 400ng of each thermally treated RNA aliquot for a pooled sample and 75ng of 1kB DNA ladder (Invitrogen, USA) and visualized on a transilluminator at 300nm. 63

Figure 3.1. Agarose gel (1.5%) run for 1 hour showing PCR product for succinate dehydrogenase (SuDH) optimized at three different magnesium chloride concentrations and two annealing temperatures. Note SuDH primers produced a single, amplicon-specific band of expected base pair size as determined by sequencing results (Table 3.1). 83

Figure 3.2. Standard curve produced for Actin (ACT) by use of serial dilution. Concentration of pooled cDNA template was quantified by fluorometry and total cDNA input for RT-qPCR reactions calculated for each serial (1/5) dilution. Dilutions possessing standard deviations greater than 0.5 for technical replicates were eliminated from the standard curve (Applied Biosystems 2008). 86

Figure 3.3. geNorm pair-wise variation analysis using forward addition to determine the optimal number of reference genes required to contribute to a normalization factor. For the dataset composed of *D. ponderosae* biological replicates from all treatment groups (n=62), four reference genes were required to achieve a pair-wise variation below 0.15. Accurate normalization of GOIs associated with seasonal cold tolerance in *D. ponderosae* is therefore best achieved from a normalization factor made up of ACT, YWHAZ, RPII, and PBD expression data (Table 3.2). 91

Figure 3.4. Developmental variation illustrated as a mechanism explaining expression stability rank variation for 19 September, 2008 and 1 April, 2009 treatment groups. 98

Figure 4.1 – Pre-existing Mechanisms Involved in Glycerol Biosynthesis. The processes of glycogenesis and glycogenolysis involve the following enzymes: glycogen phosphorylase (GP); triosephosphate isomerase (TPI); glycerol-3-phosphate dehydrogenase (G3PDH); glycerol kinase (GK); alcohol dehydrogenase (ADH); glycogen synthase (GS). The metabolism of lipids, specifically triglycerides, produces glycerol and occurs via triacylglycerol lipase (TAGL). Reducing equivalents required in the production of glycerol can be produced via the pentose phosphate pathway (PPP), involving the enzymes 6-phosphoglucolactonase (6-PGL) and glucose-6-phosphate dehydrogenase (G6PDH). The enzyme citrate synthase (CS) is involved in the citric acid cycle (CAC) and gluconeogenic enzymes include phosphoenolpyruvate carboxykinase (PEPCK) and fructose-1,6-bisphosphatase (FBP). Pyruvate kinase (PK) is an enzyme present within the lower-half of glycolysis. The following substrates are involved in the above processes: glucose-1-phosphate (G1P), glucose-6-phosphate (G6P), β-glucose-6-phosphate (β-G6P), glucono-1,5-lactone 6-phosphate (G-1,5-6P), fructose-6-phosphate (F6P), fructose-1,6-bisphosphtate (F16P), dihydroxyacetone phosphate (DHAP), glycerol-3-phosphate (G3P), glyceraldehyde-3-phosphate (GAP), glyceraldehyde (GA), phosphoenolpyruvate (PEP) and oxaloacetate (OAA). 106

Figure 4.2. Agarose gel (1.5%) run for 1 hour showing PCR product for succinate dehydrogenase (SuDH) optimized at three different magnesium chloride concentrations and two annealing temperatures. Note SuDH primers produced a single, amplicon-specific band of expected base pair size (~102bp) as determined by sequencing results (Table 4.1). 116

Figure 4.3. Standard curve produced for the glycogen synthase (GS) product by use of serial dilution. Concentration of pooled cDNA template was quantified by fluorometry and total cDNA input for RT-qPCR reactions calculated for each serial (1/5) dilution. Dilutions possessing standard deviations greater than 0.5 for technical replicates were eliminated from the standard curve (Applied Biosystems, 2008). 119

Figure 4.4 – Geometric mean fold change in *D. ponderosae* triacylglycerol lipase transcript accumulation relative to 19 September, 2008 and corresponding daily seasonal thermal data at the larval collection site for (A) fall 2008, and (B) spring 2009 study periods. Gene mRNA expression values were obtained from 4-8 *D. ponderosae* larval biological replicates, collected from two separate lodgepole pine trees, with 95% confidence intervals being displayed. One-way ANOVA were conducted for triacylglycerol lipase transcript accumulation data followed by Tukey's HSD *post-hoc* test for pair-wise multiple comparisons. Means found to be statistically different ($p<0.05$) are denoted with different lowercase letters. 122

Figure 4.5 – Geometric mean fold change in *D. ponderosae* glycogen phosphorylase transcript accumulation relative to 19 September, 2008 and corresponding daily seasonal thermal data at the larval collection site for (A) fall 2008, and (B) spring 2009 study periods. Gene transcript accumulation values were obtained from 4-8 *D. ponderosae* larval biological replicates, collected from two separate lodgepole pine trees, with 95% confidence intervals being displayed. One-way ANOVA were conducted for glycogen phosphorylase transcript accumulation data followed by Tukey's HSD *post-hoc* test for pair-wise multiple comparisons. Means found to be statistically different ($p<0.05$) are denoted with different lowercase letters. 125

Figure 4.6 – Geometric mean fold change in *D. ponderosae* phosphoenolpyruvate carboxykinase transcript accumulation relative to 19 September, 2008 and corresponding daily seasonal thermal data at the larval collection site for (A) fall 2008, and (B) spring 2009 study periods. Gene transcript accumulation values were obtained from 4-8 *D. ponderosae* larval biological replicates, collected from two separate lodgepole pine trees, with 95% confidence intervals being displayed. One-way ANOVA were conducted for phosphoenolpyruvate carboxykinase transcript accumulation data followed by Tukey's HSD *post-hoc* test for pair-wise multiple comparisons. Means found to be statistically different ($p<0.05$) are denoted with different lowercase letters. 128

Figure 4.7 – Geometric mean fold change in *D. ponderosae* fructose-1,6,-bisphosphatase transcript accumulation relative to 19 September, 2008 and corresponding daily seasonal thermal data at the larval collection site for (A) fall 2008, and (B) spring 2009 study periods. Gene transcript accumulation values were obtained from 4-8 *D. ponderosae* larval biological replicates, collected from two separate lodgepole pine trees, with 95% confidence intervals being displayed. One-way ANOVA were conducted for fructose-1,6,-bisphosphatase transcript accumulation data followed by Tukey's HSD *post-hoc* test for pair-wise multiple comparisons. Means found to be statistically different ($p<0.05$) are denoted with different lowercase letters. 131

Figure 4.8 – Geometric mean fold change in *D. ponderosae* glycogen synthase transcript accumulation relative to 19 September, 2008 and corresponding daily seasonal thermal data at the larval collection site for (A) fall 2008, and (B) spring 2009 study periods. Gene transcript accumulation values were obtained from 4-8 *D. ponderosae* larval biological replicates, collected from two separate lodgepole pine trees, with 95% confidence intervals being displayed. One-way ANOVA were conducted for glycogen synthase transcript accumulation data followed by Tukey's HSD *post-hoc* test for pair-wise multiple comparisons. Means found to be statistically different ($p<0.05$) are denoted with different lowercase letters. 134

Figure 4.9 – Geometric mean fold change in *D. ponderosae* alcohol dehydrogenase transcript accumulation relative to 19 September, 2008 and corresponding daily seasonal thermal data at the larval collection site for (A) fall 2008, and (B) spring 2009 study periods. Gene transcript accumulation values were obtained from 4-8 *D. ponderosae* larval biological replicates, collected from two separate lodgepole pine trees, with 95% confidence intervals being displayed. One-way ANOVA were conducted for alcohol dehydrogenase transcript accumulation data followed by Tukey's HSD *post-hoc* test for pair-wise multiple comparisons. Means found to be statistically different ($p<0.05$) are denoted with different lowercase letters. 136

Figure 4.10 – Geometric mean fold change in *D. ponderosae* triose-phosphate isomerase transcript accumulation relative to 19 September, 2008 and corresponding daily seasonal thermal data at the larval collection site for (A) fall 2008, and (B) spring 2009 study periods. Gene transcript accumulation values were obtained from 4-8 *D. ponderosae* larval biological replicates, collected from two separate lodgepole pine trees, with 95% confidence intervals being displayed. One-way ANOVA were conducted for triosephosphate isomerase transcript accumulation data followed by Tukey's HSD *post-hoc* test for pair-wise multiple comparisons. Means found to be statistically different ($p<0.05$) are denoted with different lowercase letters. 139

Figure 4.11 – Geometric mean fold change in *D. ponderosae* glycerol-3-phosphate dehydrogenase transcript accumulation relative to 19 September, 2008 and corresponding daily seasonal thermal data at the larval collection site for (A) fall 2008, and (B) spring 2009 study periods. Gene transcript accumulation values were obtained from 4-8 *D. ponderosae* larval biological replicates, collected from two separate lodgepole pine trees, with 95% confidence intervals being displayed. One-way ANOVA were conducted for glycerol-3-phosphate dehydrogenase transcript accumulation data followed by Tukey's HSD *post-hoc* test for pair-wise multiple comparisons. Means found to be statistically different ($p<0.05$) are denoted with different lowercase letters. 142

Figure 4.12 – Geometric mean fold change in *D. ponderosae* glycerol kinase transcript accumulation relative to 19 September, 2008 and corresponding daily seasonal thermal data at the larval collection site for (A) fall 2008, and (B) spring 2009 study periods. Gene transcript accumulation values were obtained from 4-8 *D. ponderosae* larval biological replicates, collected from two separate lodgepole pine trees, with 95% confidence intervals being displayed. One-way ANOVA were conducted for glycerol kinase transcript accumulation data followed by Tukey's HSD *post-hoc* test for pair-wise multiple comparisons. Means found to be statistically different ($p<0.05$) are denoted with different lowercase letters. 145

Figure 4.13 – Geometric mean fold change in *D. ponderosae* 6-phosphoglucolactonase transcript accumulation relative to 19 September, 2008 and corresponding daily seasonal thermal data at the larval collection site for (A) fall 2008, and (B) spring 2009 study periods. Gene transcript accumulation values were obtained from 4-8 *D. ponderosae* larval biological replicates, collected from two separate lodgepole pine trees, with 95% confidence intervals being displayed. One-way ANOVA were conducted for 6-phosphoglucolactonase transcript accumulation data followed by Tukey's HSD *post-hoc* test for pair-wise multiple comparisons. Means found to be statistically different ($p<0.05$) are denoted with different lowercase letters. 147

Figure 4.14 – Geometric mean fold change in *D. ponderosae* glucose-6-phosphate dehydrogenase transcript accumulation relative to 19 September, 2008 and corresponding daily seasonal thermal data at the larval collection site for (A) fall 2008, and (B) spring 2009 study periods. Gene transcript accumulation values were obtained from 4-8 *D. ponderosae* larval biological replicates, collected from two separate lodgepole pine trees, with 95% confidence intervals being displayed. One-way ANOVA were conducted for glucose-6-phosphate dehydrogenase transcript accumulation data followed by Tukey's HSD *post-hoc* test for pair-wise multiple comparisons. Means found to be statistically different ($p<0.05$) are denoted with different lowercase letters. 149

Figure 4.15 – Geometric mean fold change in *D. ponderosae* pyruvate kinase transcript accumulation relative to 19 September, 2008 and corresponding daily seasonal thermal data at the larval collection site for (A) fall 2008, and (B) spring 2009 study periods. Gene transcript accumulation values were obtained from 4-8 *D. ponderosae* larval biological replicates, collected from two separate lodgepole pine trees, with 95% confidence intervals being displayed. One-way ANOVA were conducted for pyruvate kinase transcript accumulation data followed by Tukey's HSD *post-hoc* test for pair-wise multiple comparisons. Means found to be statistically different ($p<0.05$) are denoted with different lowercase letters. 151

Figure 4.16 – Geometric mean fold change in *D. ponderosae* citrate synthase transcript accumulation relative to 19 September, 2008 and corresponding daily seasonal thermal data at the larval collection site for (A) fall 2008, and (B) spring 2009 study periods. Gene transcript accumulation values were obtained from 4-8 *D. ponderosae* larval biological replicates, collected from two separate lodgepole pine trees, with 95% confidence intervals being displayed. One-way ANOVA were conducted for citrate synthase transcript accumulation data followed by Tukey's HSD *post-hoc* test for pair-wise multiple comparisons. Means found to be statistically different ($p<0.05$) are denoted with different lowercase letters. 153

Dedication

I would like to begin by recognizing my family for their love and support over the years. Without them I would not be the person I am, nor would I have been able to get to this point.

I would like to specifically thank my mother, Leona, and my father, Donald, who have provided me with copious amounts of their time, effort and love. They have continuously encouraged me to find my own path in life, for which I am thankful for, but have continually reassured me that, " it's always okay to come home". My Auntie Sessie and Uncle Russ, have always modeled success humbly and have dispensed much valuable advice to me over the years. I've found much comfort in talking about the specifics of my project with my brother and good friend, Shane, with whom I can always count on for a compassionate perspective. I'd also like to thank all of these individuals for excusing my absence at Thanksgiving, Christmas and other family dinners while I pursued the completion this work.

If I were able to name, for recognition, all of the many other people who have brought me to this point in my life, this dedication would be at least as long as the rest of this thesis. I appreciate each one of them and dedicate this thesis to them.

Dad, I finally finished making a book.

Acknowledgements

I thank Janice Cooke and Ken Storey for agreeing to discuss both the specifics of RT-qPCR theory and insect cold tolerance early in the progression of this work. I express my gratitude to Chris Keeling for asking questions about my data presentation, which eventually precipitated into Chapter #2 of this thesis. I'd like to thank the many members of UNBC's Forest Research Interest Group (FIRG) who provided meaningful feedback on presentations of this work at several points in its progression. Thanks to those field assistants who put in several long days collecting field samples with me in the fall of 2008 & spring of 2009: Amy Thommasen, Lori-Ann Etchart, Travis Allen, Christopher Uy and Tiffany Clarke. Additional thanks to Tiffany Clarke for her work in the lab, specifically: for being so relentless/persistent in wanting to start "today", for her steady hand pipetting, for sharing her creative vision while making presentation images, for her laughter and good company during long field/lab days and for editing several versions of this work. I appreciate her as a fine colleague, and for also sharing Deep Thoughts & Important Things with me when I needed perspective. Thanks to Allison Fedorkiw and Fedorkiw family, for taking me into their home, for treating me like family and for teaching me the importance of celebration. I value the friendship I have had, and continue to have, with my good friend and roommate Eric Kopetski. I have learned much from his example as a superior scientist. I'd like to thank my committee members Stephen Rader, Stephen Dery and Geoff Payne for taking the time to review my work and to provide thoughtful feedback. I appreciate Ian Hartley for making the time to chair the oral defence, and for being supportive throughout the application process for graduate studies. I appreciate and would like to recognize all of the work

Eric Bayrd does on behalf of UNBC Chemstores. Several experiments were completed over holidays and on short timelines due solely to his diligence communicating with distributors. I'd like to thank Sarah Gray and members of the Gray lab for their patience and understanding as this work was in a perpetual state of near-completion. Specifically, I'd like to thank Alyssa Shaw for being an excellent sounding board while we both learned the intricacies of RT-qPCR thory. I feel extremely fortunate to have received the graduate supervision I have had from Dezene Huber. From consoling me when I returned back from Valemount my first full field day with only 9 beetles, to patiently providing me with enough room to make my own mistakes and allowing me the time and space to learn from them, to always supplying me with a strong role model to emulate. This work would not be possible without the contribution of these, and other unnamed, people. Thank all of you.

Introduction

1.1 Temperature and Mountain Pine Beetle Ecology

1.1.1 Mountain Pine Beetle Life Cycle

The majority of the life cycle of the mountain pine beetle, *Dendroctonus ponderosae* Hopkins, occurs beneath the bark of a host pine tree. While this phenomenon has proven to be a significant barrier to study this insect, four specific life stages have been identified: egg, larvae, pupae and adult.

Following aggregation on a susceptible tree and successful mating, female beetles deposit eggs in the phloem of their selected host (Safranyik & Carroll, 2006). Within one to two weeks, eggs hatch and larvae feed on host tree phloem forming their own larval galleries. While feeding actively from late summer to mid-fall, larvae progress through four stages termed instars. By mid-autumn, late instar larvae cease feeding and carve out an area called a pupal chamber. Within pupal chambers during winter, spring and mid-summer months, fourth instar larvae develop through a pupal life stage into teneral adults. Following a short period of further development and cuticular hardening under the bark, new adults emerge from host trees mid-summer and immediately disperse to forage for new hosts to colonize (Safranyik & Carroll, 2006).

1.1.2 Mountain Pine Beetle Development & Voltism

Both mountain pine beetle developmental timing and voltism are highly-temperature dependent. Mountain pine beetle populations occupying lower elevations or geographical latitudes experience higher annual temperatures than mountain pine beetle populations inhabiting higher elevations or geographical latitudes. In warmer environments, mountain pine beetles are normally univoltine, reproducing once per year.

Reid (1962) found a minimum of 833 degree-days must be achieved for a mountain pine beetle population to maintain univoltine behavior. However, in years with above average summer temperatures mountain pine beetles may display multivoltine behavior (Reid 1962).

When annual heat accumulation is insufficient for a complete cycle through development in one year, such is often the case at both higher elevations and geographical latitudes, slower development results in semivoltinism (Amman, 1973; Bentz *et al.,* 1991). A model produced by Logan & Powell (2001) showed that a warming of average annual temperature by just 2°C could result in shifting a semivoltine population to a synchronous univoltine population. As cold temperature is often cited as the most significant mortality factor mountain pine beetle populations experience (Safranyik 1978; Cole, 1981; Safranyik & Carroll, 2006; Stahl *et al.,* 2006; Aukema *et al.,* 2008), it is not surprising that semivoltine populations, in which each individual is exposed twice to the cold temperatures of winter, are characterized by producing fewer emerging adults (Amman, 1973; Safranyik, 1978). Mountain pine beetles employ physiological and biochemical adaptations that allow them to endure prolonged exposure to subzero temperatures, one of which is quiescence.

1.1.3 Mountain Pine Beetle Quiescence

Similar to diapause, quiescence occurs when temperatures fall below thermal thresholds required for an insect to maintain development at a uniform rate. Where diapause is distinguished by minimal development accompanied by depressed levels of metabolic activity (Danks, 2006), quiescence is characterized by a complete inhibition of developmental activity (Logan & Powell, 2005). Unique to quiescence is also the

relative ease at which the arrest of development is reversed. With diapause, developmental activity remains depressed even after developmentally favorable conditions return, whereas a state of quiescence is discontinued immediately following a restoration of developmentally favorable conditions (Danks, 2006). Mountain pine beetles oscillate between quiescence and ongoing developmental states on a daily basis, notably in late fall and early winter when thermal inputs fall below developmental threshold temperatures at night but exceed them at midday (Logan & Powell, 2005).

By employing the physiological adaptation of quiescence, overwintering mountain pine beetle larvae can reallocate limited stored energy reserves from use in maintaining development toward biochemical mechanisms that provide the insect with cold tolerant properties. Further discussion of mountain pine beetle-specific cold tolerance mechanisms is best prefaced by a detailed explanation of how cold tolerance is achieved within insects in general.

1.2 Mechanisms of Cold Tolerance in Insects

1.2.1 Freeze Tolerance and Freeze Avoidance

Cold tolerance refers to a range of biochemical and physiological mechanisms insects employ to endure subzero temperatures (Storey & Storey, 2004; pp473). Central any discussion regarding mechanisms by which insect cold tolerance is achieved is a working understanding of customary categories of freeze tolerance and freeze avoidance. Originally presented as alternative strategies by which insects survive low thermal environments (Salt, 1961), freeze tolerant and freeze avoidant categories have become a convenient framework in which to categorize cold tolerance compounds and mechanisms as they are discovered.

The primary distinction between freeze tolerant and freeze avoidant categories is made on the basis of whether or not ice formation results within bodily fluids (Danks, 2006). Freeze tolerant insects circumvent the damaging effects of intracellular ice formation by induced ice nucleation within extracellular spaces. This controlled induction at a high subzero temperature is a means to avoid intracellular freezing while maintaining adequate osmolarity within the cell.

Freeze avoidant insects are unable to survive the detrimental effects of internal ice formation, even within extracellular spaces. To evade cold mortality, freeze avoidant insects produce cryoprotectants that alter the freezing properties of their bodily fluids. Cryoprotectant-treated water can remain liquid well below the temperature where normal homogenous water crystallization occurs: a phenomenon known as 'supercooling'.

Freeze tolerant and freeze avoidant categories have provided a context which successive aspects of insect cold tolerance have been placed. Continued discoveries in the field of insect cold tolerance have resulted in the formation of new categories and the original nomenclature has evolved. Foremost authorities in the field of insect cold tolerance, Storey & Storey (2004, pp.474) categorize mechanisms by which ectotherms survive subzero temperatures into four main groups: anahydrobiosis, vitrification, freeze avoidance and freeze tolerance. These four groups will now be detailed and appropriate insect examples provided.

1.2.2 Anahydrobiosis

Anahydrobiosis is the elimination of free water within the cell and is a common freeze avoidant tactic. Homstrop & Somme (1998) observed a 91.6% drop in the water content of the *Onychiurus arcticus* at a temperature of -19.5°C. At subzero temperatures ice has a lower vapor pressure than liquid water (Danks, 2006). This property of water establishes a vapor pressure gradient between an insect's internal body water and the ice it contacts externally (Hawes & Bale, 2007). Initially the internal water loss increases the concentration of intracellular solutes, decreasing the internal liquid's supercooling point (SCP). The SCP of an insect's body fluid continues to decrease until insufficient water is left within the cell to nucleate. For *O. arcticus*, the minimum temperature at which all osmotically active water would be lost is -6.7°C (Worland *et al.,* 1998). At that point, freezing is less a concern than dehydration damage to cellular protein and membrane structure. Anatomical and physiological protection against desiccation is partially provided by the non-reducing sugar trehalose (Rudolf & Crow, 1985; Danks, 2006; Hawes & Bale, 2007). Over a three-week period at temperatures no less then -5.5°C Worland *et al.,* (1998) observed over a hundred-fold increase in trehalose concentration. The mechanism by which trehalose prevents membrane damage has yet to be confirmed. One hypothesis is that its trehalose's ability to hydrogen bond with polar regions of proteins and membrane phospholipids provides a stabilizing force (Rudolf & Crowe, 1985; Crowe *et al.,* 1998; Storey & Storey, 2004, pp.481; Storey, 1997).

1.2.3 Vitrification

An alternative cold tolerant mechanism utilizing trehalose is the process of vitrification. Vitrification is a cold tolerant mechanism in which intracellular water is transformed into a pseudo-solid amorphous glass (Hawes & Bale, 2007). Extreme increases in the viscosity of vitrified fluids result in liquids that exhibit molecular motion similar to crystalline solids. The accumulation of trehalose and other sugars in high concentration helps produce the unique properties of these highly viscous liquids due to their high glass transition temperatures (Storey & Storey, 2004, pp. 477). Unlike the production of crystalline solid water via heterogeneous freezing, vitrification does not place the cell under osmotic stress. When heterogeneous water freezes it expels all solutes from the crystal structure causing concentrations of solutes to increase in liquids surrounding the crystal structure. When an amorphous glass is produced via vitrification, the glass incorporates solutes (namely sugars) present within the intracellular fluid (Storey & Storey, 2004, pp. 476). While highly viscous, the lack of crystal structure and consequent absence of crystal rearrangement potential results in the amorphous glass not having the injurious effects on cellular structures that are a common result of crystallization. While infrequently observed within arthropods (Hawes & Bale, 2007), evidence of vitrification within *Eurosta solidaginis* (Wasylyk *et al.,* 1988) and *Cucujus clavipes* (Bennett *et al.,* 2005) has been previously documented.

1.2.4 Freeze Tolerance

Freeze tolerance in insects involves the presence of extracellular ice nucleating agents (INAs) (Duman, 2001). At high subzero temperatures close to their melting points, INAs initiate and target water crystallization to within extracellular spaces

instead of within cells. Upon supercooling, nucleation that initiates at lower subzero temperatures spreads rapidly and has a higher probability of spreading to intracellular fluids (Danks, 2006). INAs ensure that ice formation is slow, that crystal size is regulated and that location of ice formation is restricted to extracellular spaces (Storey & Storey, 2004, pp.477).

Extracellular ice formation acts to decrease the volume of free water on the extracellular side of the plasma membrane while increasing the concentration of solutes excluded from the crystal structure (Duman, 2001). Extracellular freezing creates an osmotic pressure imbalance causing transport of water out of the cell. This efflux of free water decreases the water to solute ratio within the cell, depressing the intracellular fluid SCP. The SCP of the extracellular space remains unchanged as the free water is added to the growing extracellular crystal structure (Duman, 2001). The size of extracellular ice crystals is regulated via production of high concentration solutes, such as polyols and sugars (Bale, 2002).

1.2.5 Freeze Avoidance

Freeze avoidant behavior and physiology are displayed by insects that cannot tolerate internal freezing. While freeze tolerant insects maintain extracellular INAs (Duman, 2001), freeze avoidant insects actively remove them. For body fluids to maintain a liquid state and supercool to subzero temperatures, freeze avoidant insects remove or inactivate exogenous INAs (Bale, 2002). Overwintering observations of the stag beetle, *Ceruchus piceus*, indicate that supercooling in this species involves the removal of hemolymph INAs (Neven *et al.,* 1986). Antifreeze proteins (AFPs), present within the hemolymph (Olsen & Duman, 1997a) and gut (Olsen & Duman, 1997b) of

Dendroides canadensis, were found to inhibit INA activity. AFPs lower the supercooling point of a fluid by absorbing into the surface of ice crystals (Bale, 2002). This absorption increases the surface free energy required for crystal growth, therefore demanding a lower temperature for crystallization to occur (Duman & Serianni, 2002). In a study of *D. canadensis*, the supercooling ability of AFPs was enhanced with increasing concentrations of either polyols or sugars (Li *et al.,* 1998). Of the solutes observed to enhance the function of AFPs, glycerol was found in the greatest abundance. The accumulation of glycerol – not coincidentally the most common cryoprotectant utilized by insects (Storey & Storey, 2004, pp.479) – can in part be explained by the relative ease in which it is produced and accumulated via pre-existing metabolic pathways, namely glycogenolysis.

In the freeze avoidant rice stem borer, *Chilo suppressalis*, metabolite transport data indicate glycol accumulation involves aquaglyceroporins (Izumni *et al.,* 2007). Aquaglyceroporins are membrane proteins that transport glycerol and water across the plasma membrane (Verkman, 2005). Inhibition of *C. suppressalis* aquaglycoporins with mercuric chloride was found to arrest water export and glycerol import within fat body cells (Izumni *et al.,* 2007). This inhibition was accompanied by serious freezing injuries of cellular tissue, indicating the significance of aquaglycoporins in freeze avoidant strategies.

1.2.6 Mechanism Cross-over

As was previously mentioned, freeze tolerance and freeze avoidance are two customary cold tolerance categories that provide a framework within which successive aspects of cold tolerance can be placed. This original cold tolerance classification

system can be accredited to Salt (1961), who initially referred to these categories as "freeze susceptible" and "freeze resistant". Several classification systems have since been advanced as alternative nomenclature to this first dichotomous grouping. Bale (1996) proposed grading insects into five cold tolerant categories, using cold exposure as a classification variable. Sinclair (1999) suggests a parallel organizational framework consisting of four cold tolerance categories based both on supercooling point and lower lethal temperatures. Both these classification systems assume that cold tolerant phenotypes are static properties. Modern discoveries in cryobiology have since expanded the field of cold tolerance, directly calling this assumption into question.

The discovery of active AFPs within freeze tolerant organisms seems somewhat of a paradox (Bale, 2002; Storey & Storey, 2004, pp.490). It appears counterintuitive that an organism that selects for INAs, which function at high supercooling points, would also select for AFPs, which depress the supercooling point (Lundheim, 2002). This paradox has been unraveled as insects have been identified that do not exclusively belong to one category, but rather have the ability to switch between strategies. Horwath & Duman (1984) report on a population of *D. canadensis* switching from freeze tolerant to freeze avoidant strategies. Similarly, Duman (1984) observed *Cucjus clavipes* using a freeze tolerant strategy in the winter of 1978-1979 followed by a freeze avoidant strategy in the winter of 1982-1983. Addressing these observations, Hawes & Bale (2007) have incorporated the concept of 'cryotype plasticity' into their system of cold tolerant classification. Grouping Storey & Storey's (2004, pp. 474) cold tolerant categories of vitrification and anahydrobiosis under a 'non-freezing' classification, Hawes & Bale (2007) add a novel 'mixed-strategy' group. This new grouping is interesting as it

challenges the conventional perspective in which cold tolerant mechanisms are classified, viewing them as a continuum of various cold tolerant strategies versus as a singular strategy. While heading in a more practical direction, Hawes & Bale's (2007) cold tolerance classification system is far from a final solution and further refining will be required, as the number of studies detailing the mechanisms by which insects achieve cold tolerance increase.

1.3 Mechanisms of Cold Tolerance in Mountain Pine Beetle

1.3.1 Indication of Cold Avoidance Mechanisms

While little work has been done to illuminate mechanisms by which mountain pine beetles achieve cold tolerance, findings from a study conducted by Bentz & Mullins (1999) suggest that the insects employ a freeze avoidant strategy. A supercooling point is defined as the temperature at which ice crystals begin to form within insect hemolymph. In the Bentz & Mullins (1999) study, larvae periodically sampled from four different geographic regions were gradually cooled to subzero-temperatures and had their supercooling points (SCP) individually assessed via a thermocouple system. Once the SCP of each larva was determined, larvae were allowed to equilibrate to room temperature. Of the larvae exposed to a temperature at their SCP, 100% experienced mortality. If mountain pine beetles were freeze tolerant insects, complete mortality would not have been experienced by larvae exposed to thermal treatment equal to their SCP. This result therefore fails to support the hypothesis that mountain pine beetle utilize freeze tolerant mechanisms of cold tolerance.

In the Bentz & Mullins (1999) study, while 100% mortality was observed for all larvae exposed to their SCP, a second sample of larvae exposed to thermal treatment

~4°C above the mean SCP displayed zero mortality. SCPs determined for larval samples were found to be positively related to seasonal phloem temperatures, decreasing in the fall/winter and increasing in the spring/summer. This observed suppression of SCP in coordination with thermal stress is characteristic of freeze avoidant behavior.

In addition to determining SCP, Bentz & Mullins (1999) conducted an assessment of polyol composition and seasonal quantity within mountain pine beetle hemolymph by both high-performance thin layer chromatography and gas chromatographic-mass spectroscopy methods. Of the polyols analyzed, glycerol was found to be the most abundant cryoprotectant accumulated by mountain pine beetle with sorbitol also being detected in minor amounts. Polyols are well known cryoprotectants, which are substances that depress the equilibrium freezing point of water (Storey, 2004; pp481). While significant seasonal differences in glycerol accumulation were not found for pooled larval samples exposed to different thermal treatments, small sample sizes and large associated experimental error terms provided a low probability of detecting statistically significant seasonal differences, should they have been present. Despite an absence of statistically significant results, Bentz & Mullins' (1999) data clearly identify glycerol as the most promising candidate for further cryoprotectant study within mountain pine beetle. Currently the mechanisms by which mountain pine beetle larvae produce glycerol are unknown. One powerful method that can be employed to determine glycerol's reaction mechanisms is through an assessment of gene expression via RT-qPCR.

1.4 Gene Expression & Methodology

1.4.1 Gene Expression

"Gene expression" is a term used to encompass the dual genetic processes of transcription and translation. Within the nucleus of a cell, genetic information stored within a gene is first converted, or more accurately "transcribed", into a complimentary intermediate genetic material called messenger RNA (mRNA). After incurring minor structural modifications mRNA is exported from the cell nucleus to the cytoplasm. Cytoplasmic mRNA serves as a genetic template from which functional gene products, namely proteins, are produced or "translated".

Functional gene products that catalyze the rates at which cellular reactions occur are referred to as enzymes. Enzymes convert cellular substrates into cellular products and often display substrate-specific behavior. A series of catalyzed reactions in which the products produced by an enzyme are the substrate for a succeeding enzyme are referred to as a mechanism pathway. To summarize, gene expression is the process from which cellular instructions stored within genes are converted into functional gene products in the form of proteins.

Each gene encodes for the material to assemble a specific enzyme, but at any given time within a cell, only some of these genes are expressed as proteins. When an organism experiences a stress, whether it be environmental, developmental or physiological, different proteins are synthesized in order to appropriately manage that stress. By evaluating and comparing how gene expression changes under different stressors, also known as treatments, researchers can make inferences related to the quantities of functional gene products present. By assaying genes that code for enzymes

of interest within a mechanism pathway, inferences about the amounts of cellular substrates and products present given a treatment can be made. One mean by which gene expression can be studied is via reverse transcription quantitative polymerase chain reaction (RT-qPCR) techniques.

1.4.2 Reverse Transcription Polymerase Chain Reaction (RT-qPCR)

Complimentary DNA (cDNA) is a DNA transcript that has been synthesized from an mRNA template through the process of reverse transcription (RT). From an RT reaction, each mRNA transcript present produces only one respective cDNA transcript. Being produced from an RT in a one-to-one ratio, the number of cDNA molecules produced is therefore proportional (and mainly equal) to the number of mRNA transcripts initially present in the sample. The number of mRNA transcripts, as indicated by cDNA quantification, relates to the number of functional gene products expressed within a sample; therefore, quantification of cDNA transcripts can serve as a proxy measure of gene expression. By comparing the quantities of cDNA produced within samples under different treatments, the relationship between treatments and gene expression can be deduced mathematically. This mathematical deduction stems from the exponential nature of polymerase chain reaction (PCR).

In theory, PCR produces copies of DNA or cDNA transcripts in an exponential fashion (Grinzinger, 2002). By repetitively cycling through temperatures compatible for PCR's three phases – denaturation, annealing, and extension, in the presence of chemical components required for DNA duplication – a theoretical doubling of PCR product can be achieved after each PCR cycle. Introducing fluorescent dye to a PCR reaction mixture provides a means by which the amplification of PCR products, referred to as

amplicons, can be monitored. The signal generated from either hydrolysis probes designed to bind to complimentary segments of amplicons (i.e. TaqMan® probes) or interchelating agents specific for DNA duplexes (i.e. SYBR® Green) can be quantified after each PCR cycle or in "real-time" versus at the end of a PCR amplification; this process is referred to as quantitative PCR (qPCR).

Within the exponential phase of PCR reaction, a linear relationship exists between PCR cycle number and the logarithm of the signal absorbance emitted by either a hydrolysis probe or interchelating agent. The PCR cycle at which a reaction achieves a given level of signal absorbance is termed the quantification cycle (Cq), previously referred to as the threshold cycle (Ct) (Bustin *et al.,* 2009). Gene expression values are achieved by first normalizing the Cq value obtained for a gene of interest (GOI) to the Cq value of a stably expressed reference gene (Vandesompele *et al.* 2002).

$$\Delta Cq = Cq_{GOI} - Cq_{Ref}$$

Relative or comparative gene expression values, reported as fold change, are obtained by comparing the ΔCq of a treatment sample to ΔCq of a control sample and relating this relationship back to the exponential nature of PCR (Livak & Schmittgen, 2001). This was initially referred to as the "delta-delta-Ct" (ΔΔCt) method of relative quantification.

$$\text{Relative expression} = 2^{-(\Delta Cq \text{ of treatment} - \Delta Cq \text{ of a control})}$$

The ΔΔCt method assumes that the PCR amplification efficiency (E) is equal for both the GOI and the reference gene. An accurate estimate of E is essential in order to calculate an initial cDNA input value via qPCR methods (Ruijter *et al.,* 2009). Small differences between expected and actual E values result in large over- or underestimates

of relative gene expression. A theoretical difference in E of only 5% (i.e. $1.95^{-\Delta\Delta Cq}$ or $2.05^{-\Delta\Delta Cq}$) can generate false fold change values of 242% with artificial fold changes reaching 1744% a difference in E of 10% (Pfaffl, 2006). Where it was initially common to assume a doubling of PCR product with each cycle for both target & reference genes (Livak & Schmittgen, 2001), this practice is no longer acceptable, at least by expected current publication standards (Bustin *et al.,* 2009). Gene specific E values are determined through data generated from standard dilution curves. When logarithmically transformed cDNA concentrations are plotted against their associated Cq values, the slope of the plot can be used to derive E (Pfaffl, 2001).

$$E = 10^{[-1/slope]}$$

Standard dilution curves serve a second utility in determining the dynamic linear range (DLR) for a GOI or reference gene. The DLR is the logarithmic cDNA input range over which a reaction holds a linear relationship to Cq (Bustin & Nolan, 2004). By ensuring that the initial cDNA input for a qPCR reaction falls within the DLR for both a GOI and its respective reference gene, E corrections can be incorporated into the ΔΔCt method for relative quantification (Pfaffl, 2001). This is referred to the amplification efficiency correction method of relative expression quantification.

$$\Delta Cq_{GOI} = GOI\ Cq_{Control} - GOI\ Cq_{Treatment}$$

$$\Delta Cq_{Ref} = Ref\ Cq_{Control} - Ref\ Cq_{Treatment}$$

$$\text{Relative Expression} = (E^{\Delta Cq\ GOI})/(E^{\Delta Cq\ Ref})$$

Taking gene specific E values into account, the efficiency correction method more accurately reflects differences in gene expression than the previous ΔΔCt method. The efficiency correction method however relies on the assumption that reference genes

are stably expressed in an unconditional manner. Considerable evidence however indicates that reference gene expression can vary between tissue types (Vandesompele *et al.,* 2002; Benn *et al.,* 2008; Thorrez *et al.,* 2008), treatments (Thellin *et al.,* 1999; Lee *et al.,* 2002; McCurley & Callard, 2008) or developmental stages (McCurley & Callard, 2008; Fernandes *et al.,* 2008; Van Hiel *et al.,* 2009; Garg *et al.*, 2010). An assessment of candidate reference gene stability is therefore necessary before normalization of GOI can be completed.

Vandesompelle *et al.* (2002) developed a software program, geNorm, which ranks candidate reference genes based on stability measures (M). Once identified, geNorm provides a geometric average of the most stable reference genes expression levels. This geometric average is referred to as a normalization factor (NF) and is a more stable measure to normalize GOI expression than any one single reference gene.

$$NF = [(E_{Ref1}{}^{\Delta Cq\ Ref1})*(E_{Ref2}{}^{\Delta Cq\ Ref2})*\ldots(E_{Refn}{}^{\Delta Cq\ Ref1})]^{(1/n)}$$

$$\text{Relative Expression} = (E^{\Delta Cq\ GOI})/NF;$$

In improving the original ΔΔCt method (Livak & Schmittgen, 2001) through the amplification efficiency correction method (Pfaffl, 2001) and subsequently into a method that geometrically averages multiple internal control genes (Vandesomepelle *et al.,* 2002), researchers have gained much more confidence in the GOI expression values they obtain via the RT-qPCR process.

While considerable attention has been, and will continue to be, focused on further refining the process in which gene expression values are obtained, the method developed by Vandesomepelle *et al.* (2002) provides the most theoretically sound approach to RT-qPCR that is currently available for application to our study objectives.

Having decreased the systematic error associated with differential amplification efficiencies and varying reference gene stability, the accuracy of gene expression measures obtained via this method is still highly conditional on initial levels of RNA integrity.

1.4.3 RNA Integrity & Gene Expression

Substantial evidence has amounted from artificial degradation studies indicating that RNA integrity can significantly influence gene expression results (Bustin *et al.,* 2009). Applying a thermal degradation time course methodology to samples of human liver carcinoma cell line HEPG2 origin and utilizing five reference genes, Gingrich *et al.* (2008) were able to artificially induce as much as a 1000-fold decrease in gene expression after seven hours of treatment. In a comprehensive human tissue panel where 414 RNA samples derived from 14 different human adult tissues and cell lines were analyzed, as much as a seven-fold difference in gene expression for three reference genes could be explained due to differences in RNA integrity (Imbeaud *et al.,* 2005). Several other studies have observed a positive relationship between decreases in RNA integrity and gene expression (Ho-Pun-Cheung *et al.,* 2009; Strand *et al.,* 2007; Schroeder *et al.,* 2006; Fleige *et al.,* 2006; Auer *et al.,* 2003; Bustin & Nolan, 2004; Fleige & Pfaffl, 2006). Bustin & Nolan (2004) note, "...there is little point in observing significant [gene expression] differences between samples if these differences are simply due to one sample being degraded". Consequently, considerable effort has been invested in developing methods by which RNA integrity levels can be assessed. Prior to surveying standard measures by which RNA integrity is currently assessed, a general understanding of the methods generating RNA integrity measures should be obtained.

Two main methods by which RNA integrity measures are obtained are via slab gel electrophoresis and microfluidic capillary electrophoresis.

1.4.4 Slab Gel Electrophoresis

For several decades, slab gel electrophoresis has been unparalleled with respect to nucleotide related analysis (Mueller *et al.,* 2000). This powerful technique uses the innate negative charge of nucleic acids – due to phosphate groups in the nucleic acid backbone – to conduct size separation. When the nucleic acids are loaded onto a slab gel and an electric current is supplied, nucleic acids will migrate to the positively charged anode electrode with the rate of nucleic acid migration being inversely proportional to logarithmic length (Wu *et al.,* 2008). In the last two decades, development of advanced genomic methodology and technology has placed significant demand pressures on this means of nucleotide related analysis. Necessity and consequent expectations for faster, more automated, higher throughput nucleotide related analysis have surpassed the structural limitations of slab gel electrophoresis (Muller *et al.,* 2000). It was in part these demand pressures and structural limitations inherent to slab gel electrophoresis that gave rise to microfluidic capillary electrophoresis (MCE).

1.4.5 Microfluidic Capillary Electrophoresis (MCE)

Microfluidic methods separate sometimes complex mixtures of molecular components in biological samples by using channels measuring from tens to hundreds of micrometers in diameter (Whitesides, 2006; Crevillen *et al.,* 2007). By combining the miniaturization of microfluidics technology with the well-established biochemical practice of electrophoresis, a more direct and convenient separation of nucleic acids can be achieved, termed microfluidics capillary electrophoresis (MCE) (Wu *et al.,* 2008).

At the center of MCE systems are so-called "chips" that are composed of sample wells adhered to a glass plate engraved with a system of microchannels. The MCE process begins with the addition of gel and stain solutions to the chip. A specialized instrument pressurizes the liquids within the chip forming a gel matrix so that the samples have a uniform media to migrate through. Samples and loading buffer are added to separate wells of the chip. Electrodes extending from an electrophoresis station lower and come into contact with the wells of the chip. By controlling the voltage and current applied to the chip, samples are directed from the loading channel to the separation channel of the chip. As the samples migrate through the chip's separation channels, the nucleic acid sample comes into contact with the gel stain. The stain intercalates with the nucleic acid molecule and as the sample passes a laser, the bound stain becomes excited and fluoresces. The amount of fluorescence emitted by a sample is recorded by a corresponding detector and is proportional to the size of the nucleic acids within the sample. Results of the MCE process can be expressed either in the form of a digital gel JPEG or as well specific electropheograms.

In addition to the decreased operational time and increased objectivity of results produced, MCE possesses many additional advantages when compared to slab gel electrophoresis (Mueller *et al.*, 2000). The detection sensitivity of MCE has been found to be far greater than that of slab gels employing ethidium bromide. Ahn *et al.* (1996) found that for a 10uL sample, the practical limits for DNA quantitation by ethidium bromide were 25-50ng compared to as little as 0.1ng from a 1uL sample for the Experion DNA 1K Analysis Kit. The decreases in volume input required for MCE is a second important advantage (Dolnik *et al.*, 2000). By only using a fraction of both

reagent and sample volume required for slab gel electrophoresis analysis, expenses associated with analysis reagents can be lowered and scarce samples can be conserved for downstream applications. Slab gel electrophoresis requires potential exposure to a cocktail of both mutagenic and carcinogenic substances (i.e UV light, formaldehyde, formalin, ethidium bromide, etc.). Chip technology minimizes potential contact with hazardous substances by encasing them all within a solid matrix and enclosed channels. It is for these mentioned advantages, among others, that MCE has become a preferred method to address clinical, environmental and food research questions (Crevillen *et al.,* 2007) involving various nucleotide analysis techniques. One such field that has significantly benefited by MCE is that of gene expression analyses, on which several measures of RNA integrity assessment rely.

1.4.6 28S/18S Measure of RNA Integrity

Historically, total RNA integrity was assessed via either native or denaturing slab gel electrophoresis (Schroeder *et al.,* 2006). Total RNA consists of some 80% rRNA (Alberts *et al.,* 2002; pp. 329), the majority of which is composed of either 18S or 28S rRNA subunits. When total RNA is separated on a slab gel, two distinct bands are generated corresponding to 18S and 28S subunits. With electrophoresis, the size of an RNA fragment on a slab gel is theoretically proportional to its band intensity. Being roughly twice as large as the 18S subunit, twice as many EtBr molecules bind the 28S subunit resulting in its band fluorescing at twice the intensity. Using 28S and 18S rRNA integrity as a proxy measure for mRNA integrity within total RNA, mRNA integrity is considered to be of high quality when the 28S/18S intensity ratio is approximately 2.0 (Denisov *et al.,* 2008).

While theoretically intuitive, the original source of the 28S/18S measure of assessing RNA integrity has proven elusive (Miller *et al.,* 2004) and more importantly, inconsistent in practice. In a study of marine bacteria, Kerhof (1997) found that ribosomal subunit mass was not accurately reflected via ethidium bromide fluorescence nor was a 28S/18S band intensity ratio of 2.0 found. While assessing RNA integrity for microarray analysis, Auer *et al.* (2003) found that while the intensity of 18S and 28S fluorescence decreased as RNA experienced increased levels of degradation, the 28S/18S ratio remained the same as intact RNA, providing an integrity false positive scenario. Conversely, a study evaluating the RNA integrity of postmortem human brain tissue found that adhering to 28S/18S threshold would have unnecessarily eliminated one-third of RNA samples of good integrity; an integrity false negative scenario (Miller *et al.,* 2004). A general dissatisfaction with the 28S/18S measure, coupled with the benefits provided by the advancing technology of MCE gave incentive to develop more reliable measures of RNA integrity.

1.4.7 MCE Measures of RNA Integrity

To date three main measures of RNA integrity generated via MCE exist: the degradometer (Auer *et al.,* 2003), the RNA quality indicator (RQI) (Denisov *et al.,* 2008) and the RNA integrity number (RIN) (Schroeder *et al.,* 2006). Each of these measures select multiple features, possessed within electropherograms generated via MCE, and incorporate them as parameters into specialized algorithms. The algorithms for the RQI and RIN methods were developed for commercial purposes whereas the degradometer was originally created as freeware. While the ways in which features are selected, measured and weighted differ between the three RNA integrity measures, one

commonality is that they all incorporate a 28S subunit peak parameter within their respective algorithms. The ribosomal 28S subunit of insect rRNA possesses a unique "hidden break" that cleaves under the denaturing conditions of MCE. Not having incorporated the nature of insect ribosomal 28S subunit into their mathematical algorithms, all current measures of RNA integrity have proven insufficient to assess RNA integrity of insect samples.

1.5 Objectives

I) To develop a measure of RNA integrity that accurately assesses RNA integrity within mountain pine beetle (and, likely, other insect) samples.

II) To identify reference genes for mountain pine beetle whose gene expression under cold treatment is most stable and therefore, most appropriate for further relative RT-qPCR analysis.

III) To assess changes in gene expression of genes of interest within the mountain pine beetle correlated to glycerol production within other insects, and to identify potential seasonal and/or thermal cues inducing any observed changes in gene expression.

1.6 Bibliography

Ahn, S.J., Costa, J., and Emanuel, J.R. (1996). PicoGreen quantitation of DNA: effective evaluation of samples pre- or post-PCR. *Nucleic Acids Research* 24(13): 2623-2625.

Alberts, B., Johnson, A., Lewis, J., Raff, M., Roberts, K., and Walter, P. (2002). *Molecular Biology of the Cell* (4th ed.). New York, New York: Garland Science, (pp. 329).

Amman, G.D. (1973). Population changes of the mountain pine beetle in relation to elevation. *Environmental Entomology* 2:541-547.

Auer, H., Lyianarachchi, S., Newsom D., Klisovic, M., Marucci, u., and Kornacker, K. (2003). Chipping away at the chip bias: RNA degradation in microarray analysis. *Nature Genetics* 35(4): 292-293.

Aukema, B.H., Carroll, A.L., Zheng, Y., Zhu, J., Raffa, K.F., Moore, R.D., Stahl, K., and Taylor, S.W. (2008). Movement of outbreak populations of mountain pine beetle: influences of spatiotemporal patterns and climate *Ecography* 31: 348-358.

Bale, J. S. (1996). Insect cold hardiness: a matter of life and death. *Eur. J. Entomol.* 93, 369-382.

Bale, J. S. (2002). Insects and low temperatures: from molecular biology to distributions and abundance. *Phil. Trans. R. Soc. Lond. B* 357: 849-862.

Benn, C., Fox, H., and Bates, G.P. (2008). Optimization of region-specific reference gene selection and relative gene expression analysis methods for pre-clinical trials of Huntington's disease. *Molecular Neurodegeneration*_17(3): 17.

Bennett, V.A., Sformo, T., Walters, K., Toien, O., Jeannet, K., Hochstrasser, R., Pan, Q., Serianni, A.S., Barnes, B.M. and Duman, J.G. (2005). Comparative overwintering physiology of Alaska and Indiana populations of the beetle *Cucujus clavipes* (Fabricius): roles of antifreeze proteins, polyols, dehydration and diapause. *J. Exp. Biol.* 208: 4467-4477.

Bentz, B.J., J.A. Logan, J.A., and Amman, G.D. (1991). Temperature-dependent development of the mountain pine beetle (Coleoptera: Scolytidae) and simulation of its penology. *Canadian Entomologist* 123(5): 1083-1094.

Bentz, B.J., Mullins, D.E. (1999). Ecology of mountain pine beetle (Coleoptera: Scolytidae) cold hardening in the intermountain West. *Environmental Entomology* 28: 577–587.

Bustin, S.A, and Nolan, T. (2004). Pitfalls of quantitative real-time reverse-transcription polymerase chain reaction. *Journal of Biomolecular Techniques* 15(3): 155-166.

Bustin, S.A., Benes, V., Garson, J.A, Hellemans, J., Hugget, J., Kubista, M., Mueller, R., Nolan, T., Pfaffl, M.W., Shipley G.L., Vandesompele, J., and Wittwer, C.T. (2009). The MIQE guidelines: minimum information for publication of quantitative real-time PCR experiments. *Clinical Chemistry* 55(4): 611-622.

Cole, W.E. (1981). Some risks and causes of mortality in mountain pine beetle populations: a long-term analysis. *Researches on Population Ecology* 23: 116-144.

Crevillen, A.G., Hervas, M., Lopez, M.A., Gonzalez, M.C., and Escarpa, A. (2007). Real sample analysis on microfluidic devices. *Talanta* 74: 342-357.

Crowe, J. H., Carpenter, J. F., and Crowe, L. M. (1998). The role of vitrification in anahydrobiosis. *Annu. Rev. Physiol.* 60: 73–103.

Danks, H.V. (2006). Insect adaptations to cold and changing environments *Can. Entomol.* 138: 1-23.

Denisov, V., Strong, W., Walder, M., Gingrich, J., and Wintz, H. (2008). Development and validation of RQI: an RNA quality indicator for the Experion™ automated electrophoresis system. *Bio-Rad Bulletin #5761(Rev B)* 1-6.

Dolnik, V., Liu, S., and Jovanovich, S. (2000). Capillary electrophoresis on microchip. *Electrophoresis* 21: 41-54.

Duman, J.G. (1984). Change in the overwintering mechanism in the Cucjus beetle *Cucjus clavipes. J. Insect Physiol.* 30: 235-239.

Duman, J.G. (2001). Antifreeze and ice nucleator proteins in terrestrial arthropods. *Annu. Rev. Physiol.* 63: 327-357.

Duman, J.G., and Serianni, A.S. (2002). The role of endogenous antifreeze protein enhancers in the hemolymph thermal hysteresis activity of the beetle *Dendroides canadensis. J. Insect Physiol.* 48: 103-111.

Fernandes, J.M.O., Mommens, M., Hagen, O., Babiak, I., and Solberg, C. (2008). Selection of suitable reference genes for real-time PCR studies of Atlantic halibut development. *Comparative Biochemistry and Physiology, Part B* 150: 23-32.

Fleige, S., and Pfaffl, M.W. (2006). RNA integrity and the effect on the real-time qRT-PCR performance. *Molecular Aspects of Medicine* 27: 126-139.

Fleige, S., Walf, V., Huch, S., Prgomet, C., Sehm, J., and Pfaffl, M.W. (2006). Comparison of relative mRNA quantification models and the impact of RNA integrity in quantitative real-time RT-PCR. *Biotechnology Letters* 28: 1601-1613.

Garg, R., Sahoo, A., Tyagi, A.K., and Jain, M. (2010). Validation of internal control genes for quantitative gene expression studies in chickpea (*Cicer arietinum* L.). *Biochemical and Biophysical Research Communications* 396: 283-288.

Gingrich, J., Rubio, T., and Karlak, C. (2008) Effect of RNA degradation on data quality in quantitative PCR and microarray experiments. *Bio-Rad Bulletin #5547(Rev A)*

Grinzinger, G. (2002). Gene quantification using real-time quantitative PCR: an emerging technology hits the mainstream. *Experimental Hematology* 30: 503-512.

Hawes, T.C., and Bale, J.S. (2007). Plasticity in arthropod cryotypes. *The Journal of Experimental Biology* 210: 2585-2592.

Holmstrup, M., and Sømme, L. (1998). Dehydration and cold hardiness in the Arctic collembolan *Onychiurus arcticus. J. Comp. Physiol. B* 168: 197-203.

Ho-Pun-Cheung, A., Bascoul-Mollevi, C., Assenat, E., Bossiere-Michot, F., Bibeau, F., Cellier, D., Ychou, M., and Lopez-Crapez, E. (2009). Reverse transcription-quantitative polymerase chain reaction: description of a RIN-based algorithm for accurate data normalization. *BMC Molecular Biology* 10: 31.

Horwath, K.L., and Duman, J.G. (1984). Yearly variations in the overwintering mechanisms of the cold-hardy beetle *Dendroides canadenis. Physio. Zool.* 57: 40-45.

Imbeaud, S., Graudens, E., Boulanger, V., Barlet, X., Zaborski, P., Eveno, E., Mueller, O., Schroeder, A., and Auffray, C. (2005). Towards standardization of RNA quality assessment using user-independent classifiers of microcapillary electrophoresis traces. *Nucleic Acids Research* 33(6): e56.

Izumi, Y., Sonoda, S., Yoshida, H., Danks, H.V., and Tsumuki, H. (2006). Role of membrane transport of water and glycerol in the freeze tolerance of the rice stem borer, *Chilo suppressalis* Walker (Lepidoptera: Pyralidae) *Journal of Insect Physiology* 52(2): 215-220.

Kerhof, L. (1997). Quantification of total RNA by ethidium bromide fluorescence may not accurately reflect the RNA mass. *Journal of Biochemical and Biophysical Methods* 34: 147-154.

Lee, P., Sladek, R., Greenwood, C.M.T, and Hudson, T.J. (2002). Control genes and variability: absence of ubiquitous reference transcripts in diverse mammalian expression studies. *Genome Research* 12: 292-297.

Li, N., Andorfer, C.A., and Duman, J.G. (1998). Enhancement of insect antifreeze protein activity by solutes of low molecular mass. *The Journal of Experimental Biology* 201: 2243–2251.

Livak, K.J., and Schmittgen, T.D. (2001). Analysis of relative gene expression data using real-time quantitative PCR and the $2^{-\Delta\Delta Ct}$ method. *Methods* 25: 402-408.

Logan, J.A., and Powell, J.A. (2001). Ghost forests, global warming, and the mountain pine beetle (Coleoptera: Scolytidae). *American Entomologist* 47(3): 160-172.

Lundheim, R. (2002). Physiology and ecological significance of biological ice nucleators. *Phil. Trans. R. Soc. Lond. B* 357:937-943

McCurley, A.T., and Callard, G.V. (2008). Characterization of housekeeping genes in zebrafish: male-female differences and effects of tissue type, developmental stage and chemical treatment. *BMC Molecular Biology* 9: 12.

Miller, C.L., Diglisic, S., Leister, F., Webster, M., and Yolken, R.H. (2004). Evaluating RNA status for RT-PCR in extracts of postmortem human brain tissue. *BioTechniques* 36: 628-633.

Mueller, O., Hahnenberger, K., Dittmann, M., Yee, H., Dubrow, R., Nagle, R., and Ilsley, D. (2000). A microfluidic system for high-speed reproducible DNA sizing and quantitation. *Electrophoresis* 21: 128-134.

Neven, L.G., Duman, J.G., Beals, J.M., and Castellino, F.J. (1986). Overwintering adaptations of the stag beetle, *Ceruchus piceus*: removal of ice nucleators in winter to promote supercooling . *J. Comp. Physiol.* 156: 707–716.

Olsen, T.M., and Duman, J.G. (1997a). Maintenance of the supercooled state in the gut of overwintering Pyrochroid larvae, *Dendroides canadensis*: role of gut ice nucleators and antifreeze proteins. *J. Comp. Physiol. B* 167: 114–122.

Olsen, T.M., and Duman, J.G. (1997b). Maintenance of the supercooled state in overwintering pyrochroid beetle larvae, *Dendroides canadensis*: role of hemolymph ice nucleators and antifreeze proteins. *J. Comp. Physiol. B* 167: 105–113.

Pfaffl, M.W. (2001). A new mathematical model for relative quantification in real-time RT-PCR. *Nucleic Acids Research* 29(9): 2000-2007.

Pfaffl, M.W. (2006). Chapter 3: Relative Quantification. In Dorak, M.T. (Ed.), *Real-time PCR* (pp.63-82). New York: Taylor & Francis Group

Powell, J.A., and Logan, J.A. (2005). Insect seasonality: circle map analysis of temperature-driven life cycles. *Theoretical Population Biology* 67:161-179.

Reid, R.W. (1962). Biology of the mountain pine beetle, *Dendroctonus ponderosae* Hopkins in the East Kootenay region of British Columbia. I. Life cycle, brood development and flight periods. *Canadian Entomologist* 95(5): 531-538.

Rudolfe, A.S., and Crowe, J.H. (1985). Membrane stabilization during freezing: the role of two natural cryoprotectant, trehalose and praline. *Cryobiology* 22: 367-377.

Ruijter, J.M., Ramakers, C., Hoogaars, W.M.H., Karlen, Y., Bakker, O., van den Hoff, M.J.B., and Moorman, A.F.M. (2009). Amplification efficiency: linking baseline and bias in the analysis of quantitative PCR data. *Nucleic Acids Research* 37(6): e45.

Safranyik, L. (1978). Effects of climate and weather on mountain pine beetle populations.(pp. 77-84) In Kibbee, D.L., Berryman, A.A., Amman, G.D., and Stark, R.W. (Eds.), *Theory and practice of mountain pine beetle management in lodgepole pine forests*. Symposium Proceedings, University of Idaho, Moscow, ID.

Safranyik, L., Carroll, A., (2006). The biology and epidemiology of the mountain pine beetle in lodgepole pine forests. (pp. 3-66) In: Safranyik, L., Wilson, B. (Eds.), *The mountain pine beetle, a synthesis of biology, management and impacts on lodgepole pine*. Natural Resources Canada, Canadian Forest Service, Pacific Forestry Centre, Victoria, BC.

Salt, R.W. (1961). Intracellular freezing in insects. *Nature* 193: 1207-1208.

Schroeder, A., Mueller, O., Stocker, S., Salowsky, R., Leiber, M., Gassmann, M., Lightfoot, S., Menzel, W., Granzow, M., and Ragg, T. (2006). The RIN: an RNA integrity number for assigning integrity values to RNA measurements. *BMC Molecular Biology* 7(3): 14.

Sinclair, B.J. (1999). Insect cold tolerance: how many kinds of frozen? *Eur. J. Entomol.* 96: 157–164.

Stahl, K., Moore, R.D., and McKendry, I.G. (2006) Climatology of winter cold spells in relation to mountain pine beetle mortality in British Columbia Canada *Climate Research* 32: 13-23.

Strand, C., Enell, J., Hedenfalk, I., Ferno, M. (2007). RNA quality in frozen breast cancer samples and the influence on gene expression analysis – a comparison of three evaluation methods using microcapillary electrophoresis traces. *BMC Molecular Biology* 8:38

Storey, K.B. (1997). Organic Solutes in Freezing Tolerance. *Comp. Biochem. Physiol.* 117A(3): 319-326

Storey, J.M. and Storey, K.B. (2004). *Cold hardiness and freeze tolerance.* In *Functional Metabolism: Regulation and Adaptation* (ed. K. B. Storey), pp. 473-503. New York: Wiley-Liss.

Thellin, O., Zorzi, W., Lakaye, B., De Borman, B., Coumans, B., Hennen, G., Grisar, T., Igout, A., and Heinen, E. (1999). Housekeeping genes as internal standards: use and limits. *Journal of Biotechnology* 75: 291-295.

Thorrez, L., Van Deun, K., Tranchevent, L.C., Van Lommel, L., Engelen, K., Marchal, K., Moreau, Y., Van Mechelen, I., and Schuit, F. (2008). Using ribosomal protein genes as reference: a tale of caution. *PLoS ONE* 3(3): e1854.

Vandesompele, J., De Preter, K., Pattyn, F., Poppe, B., Van Roy, N., De Paepe, A., and Speleman, F. (2002). Accurate normalization of real-time quantitative RT-PCR data by geometric averaging of multiple internal control genes. *Genome Biology* 3(7): research0034.I-0034.II.

Van Hiel, M.B., Wielendaele, P.V., Temmerman, L., Van Soest, S., Vuerinckx, K., Huybrechts, R., Vanden Broeck, J., and Simonet, G. (2009). Identification and validation of housekeeping genes in brains of the desert locust *Schistocerca gregaria* under different developmental conditions *BMC Molecular Biology* 10:56.

Verkman, A.S. (2005) More than just water channels: unexpected cellular roles of aquaporins. *Journal of Cell Science* 118: 3225-3232.

Wasylyck, J.M., and Baust, J.G. (1988). Partial glass formation: a novel mechanism of insect cryoprotection. *Cryobiology* 25: 451-458.

Whitesides, G.M. (2006). The origins and the future of microfluidics. *Nature* 442(27): 368-373.

Worland, M.R., Grubor-Lajsic, G., and Montiel, P.O. (1998). Partial desiccation induced by sub-zero temperatures as a component of the survival strategy of the Arctic collembolan *Onychiurus arcticus*. *J. Insect Physiol.* 44: 211-219.

Wu, D., Qin, J., and Lin, B. (2008). Electrophoretic separations on microfluidic chips *Journal of Chromatography A* 1184: 542-559.

RNA Integrity and Gene Expression in *Dendroctonus ponderosae*

2.1 Introduction

Gene expression is the process from which cellular instructions stored within genes are converted into proteins. Observed patterns of gene expression can be used to interpret the metabolic and physiological state of an organism under various conditions. Measurement of mRNA transcript levels, a proxy measure of gene expression, plays a vital role in gene expression research. Variable mRNA sample integrity has been found to cause inaccuracy within gene expression studies, with several sources observing a positive relationship between decreases in RNA integrity and gene expression (Ho-Pun-Cheung *et al.,* 2009; Strand *et al.,* 2007; Schroeder *et al.,* 2006; Fleige *et al.,* 2006; Auer *et al.,* 2003; Bustin and Nolan, 2004; Fleige and Pfaffl, 2006; Gingrich *et al.,* 2008). Bustin and Nolan (2004) state that "...there is little point in observing significant [gene expression] differences between samples if these differences are simply due to one sample being degraded". To address the variability that mRNA integrity can introduce to gene expression findings, considerable effort has been invested into developing methods by which mRNA integrity can be assessed.

Historically, total RNA integrity was assessed by either native or denaturing slab gel electrophoresis (Schroeder *et al.,* 2006). Using 28S and 18S rRNA integrity as a proxy measure for mRNA integrity within total RNA, mRNA integrity is considered to be of high quality when the 28S/18S intensity ratio is approximately 2.0 (Denisov *et al.,* 2008). While theoretically intuitive, this integrity measure has proven both inconsistent and unrepresentative of actual mRNA integrity in practice (Strand *et al.,* 2006; Copois *et al.*, 2007; Auer *et al.*, 2003; Imbeaud *et al.,* 2005; Miller *et al.,* 2004). In an assessment

of mRNA integrity for microarray analysis, Auer *et al.* (2003) observed the 28S/18S ratio for degraded total RNA remained the same as intact total RNA, providing an integrity false-positive scenario. Conversely, a study evaluating the total RNA integrity of postmortem human brain tissue for RT-qPCR found that adhering to 28S/18S threshold of 2.0 would have unnecessarily eliminated one-third of their tissue samples of good total RNA integrity (Miller *et al.,* 2004). An additional difficulty found in employing the 28S/18S intensity ratio, is the observed absence of a 28S rRNA subunit on denaturing slab gels for most insect (Ishiwaka and Newburgh, 1972; Davis and Mullersman., 1981; Hatton *et al.*, 2000; Basile-Borgia *et al.,* 2005; personal observation) and a few other non-insect species (Karlstedt *et al.,* 1992). A general dissatisfaction with the 28S/18S measure, coupled with the benefits provided by the advancing technology of microfluidics capillary electrophoresis (MCE) provided incentive to develop more reliable measures of RNA integrity.

MCE combines the miniaturization of microfluidics technology with the well-established biochemical practice of electrophoresis to achieve a more direct and convenient separation of nucleic acids than slab gel electrophoresis can provide (Wu *et al.,* 2008). To date the three main measures of RNA integrity generated via MCE are: the degradometer (Auer *et al.,* 2003), the RNA quality indicator (RQI) (Gingrich, 2008; Denisov *et al.,* 2008) and the RNA integrity number (RIN) (Schroeder *et al.,* 2006). Each of these measures select multiple features of electropherograms generated by MCE, and incorporate them as parameters into specialized algorithms. While the ways in which features are selected, measured and weighted differ between the three RNA integrity measures, one commonality is that they all incorporate a 28S subunit

electropherogram peak parameter within their respective algorithms. Similar to results produced by denaturing slab gel electrophoresis, MCE methods do not observe an intact 28S subunit when size separating insect RNA (Auer *et al.,* 2003; Tahoe *et al.,* 2004; Krupp, 2005). Without an intact 28S subunit to reference within their algorithms, all current RNA integrity measures fail to appropriately assess RNA integrity from insect samples. The unique behavior of a 28S rRNA and potential sources generating its novel nature exhibited on MCE apparatus, can be better understood following a review of the molecular mechanisms involved in post-transciptional insect rRNA processing.

Study of *Drosophila* 26S rRNA, analogous to 28S rRNA of other insects, has found that a post-transcriptional "hidden break" is introduced at the approximate center of the 26S polynucleotide chain prior to nuclear export (Jordan *et al.,* 1976). This 28S rRNA hidden break is almost exclusive to insect species and involves an incision event that removes a variable number of nucleotides, known as a "gap" (Ware *et al.,* 1985). Dissociation of two equally sized subunits, 28Sα and 28Sβ, previously adjoined by the gap sequence, occurs in the presence of denaturing agents such as heat, urea (Ishikawa and Newburgh, 1972) or dimethylsulfoxide (DMSO; Applebaum *et al.,* 1966). Buffers composed of high salt concentration have been found to prevent thermally induced dissociation of 28Sα and 28Sβ subunits, suggesting hydrogen-bonding involvement between subunits (Ishikawa and Newburgh, 1972). Further evidence of hydrogen bonding between 28Sα and 28Sβ has been observed while investigating the molecular mechanisms involved in introducing a hidden break within insect 28S rRNA. Primary sequence information and expected secondary structure of and around the gap have been compared in several insect species (*D. melanogaster* - Delanversin and Jacq, 1983;

Sciara coprophila - Ware *et al.,* 1985; *Bombyx mori* - Fujiwara and Ishikawa, 1986). Comparative research has identified the presence of three common 28S rRNA elements unique within most insect species: i) the presence of an "AU" rich stem-loop structure within the gap sequence, where hydrogen-bonds of the stem bind 28Sα and 28Sβ subunits together, ii) the presence of a specific "UAAU" sequence tract within the stem-loop structure of the gap sequence, and, iii) a conserved 5'-CGAAAGGG-3' sequence within the 28Sβ sequence, downstream of the stem-loop structure. The absence of both a "AU" rich stem-loop and "UAAU" tract within *Acyrthosiphon pisum* (Ogino *et al.,* 1990), the pea aphid, a unique insect species lacking a hidden break, further supports the involvement of these three characteristics in introducing a hidden break within insect 28S rRNA.

MCE of total RNA involves both 28S rRNA contact with the denaturing agent, DMSO, and thermal treatment to prevent secondary structure complications during RNA size separation. Either of these two denaturing conditions could be involved in the dissociation of 28Sα and 28Sβ subunits of insect rRNA, and consequently responsible in preventing the production of RNA integrity measures via MCE.

The aim of this study is to gain a better understanding as to what degree exposure to denaturing conditions, inherent to MCE, has on the behavior of insect 28S rRNA with the goal of using this information to design an RNA integrity measure for insect RNA. In designing an insect RNA integrity measure, this study compared different integrity measures generated from both native slab gel electrophoresis and MCE methods. Results from novel insect RNA integrity measures were assessed in relation to RT-qPCR generated mean-fold change mRNA apparent expression decreases for progressively

degraded samples. Results of this study indicate that this insect RNA integrity measure can reliably detect insect RNA samples of compromised RNA integrity.

2.2 Methods

2.2.1 Sample Collection and Preparation

On 20 May, 2009, multiple live *D. ponderosae* larvae of mixed instar and undetermined sex were manually removed from a single pine (*Pinus contorta*) tree located west of Tete Jaune Cache, British Columbia, Canada (N53° 3' 35.28" W119° 36' 52.74"). Larvae were individually deposited in 1.5mL microcentrifuge tubes, immediately placed in liquid nitrogen, transported back to UNBC laboratory facilities on dry ice where they were immediately stored at -80°C until genetic extractions were conducted.

2.2.2 Total RNA Extractions

Biological sample material allocated for each total RNA extraction was composed of a variable number of larvae sufficient to weigh in excess of 20mg (from 21-56mg). Prior to conducting total RNA extractions and while they were still frozen, larval samples were individually transferred into deep 96-well plates, containing a single stainless steel bead (4mm in diameter) and 200µL RNAlater®-ICE (Ambion, USA). Samples were soaked in solution for a minimum of 18 hours at -20°C. Prior to sample homogenization, residual RNAlater®-ICE was removed, 100µL of MagMax™-96 Kits lysis/binding solution (Ambion) was added to each sample well. Samples were completely homogenized by use of a GeneoGrinder 2000 (SpexCertiprep, USA) with six, 30-second intervals at 1500 strokes/minute, cooling on ice for 60 seconds between each interval. Sixty microlitres of 100% isopropanol were added to each lysate and homogenization plates were held at -20°C for 10 minutes.

2.2.3 Sample Assessment and Pooling of Total RNA Extractions

A total of 32 total RNA extractions were conducted with MagMax™-96 Kits (Ambion), using the animal tissue protocol with minor modifications. Estimates of extraction concentration and purity were obtained by use of a Nanodrop ND-1000 (Nanodrop Technologies, Inc., Wilmington, DE, USA), with sample 260/280 ratios ranging from 1.88-2.27. Thirty total RNA extractions of appropriate concentration and purity were selected and combined to produce ten samples of pooled total RNA. Total RNA concentration for the ten pooled samples were determined by use of a Qubit Quantification System (Invitrogen, USA) using 3μL of 1/10 diluted sample and 197μL of working solution. Estimates of pooled sample purity were obtained by use of a Nanodrop ND-1000 (Nanodrop Technologies, Inc.), with sample 260/280 ratios ranging from 1.98-2.07. The ten pooled sample concentrations were normalized to 100ng/uL and seven RNA aliquots of equal volumes were made from each sample.

2.2.4 Thermal Treatment of Pooled Sample Aliquots

RNA aliquots for the ten pooled total RNA samples were thermally treated in a thermocycler (MJ Mini, Biorad, USA) at 90°C for 0, 30, 60, 90, 180, 300 or 420 minutes. After thermal treatment, RNA aliquot purity was re-assessed by spectrophotometric methods (NanoDrop Technologies, Inc.).

A second thermal treatment assessment, referred to as the "thermal threshold sample," was conducted using an independent sample and methods described in section 2.2.1-2.2.3. From this pooled sample, six aliquots were produced which were thermally treated in a thermocycler (MJ Mini, Biorad) for two minutes at one of the following temperatures: 10°C, 20°C, 30°C, 40°C, 50°C or 60°C. Each thermal threshold aliquot

had its RNA integrity assessed via microfluidic capillary electrophoresis, as described in section 2.2.5.

2.2.5 Integrity Assessment of Thermally Treated Aliquots

The total RNA integrity of thermally treated aliquots was assessed by both slab gel electrophoresis and microfluidic capillary electrophoresis. Upon obtaining integrity information, RNA aliquots were stored at -80°C until reverse transcription reactions were conducted.

Slab gel electrophoresis was conducted using SYBR Green II Gel Stain (Invitrogen), where aliquots for each pooled sample were grouped onto the same gel. 800ng of each aliquot was run on a 1.5% agarose gel for 45 minutes at 120V. Gels were stained for 40 minutes with SYBR Green II RNA Gel Stain (Invitrogen) using a 1:10,000 dilution of stock reagent as per reagent manual. Gels were visualized on a transilluminator at 300nm with a specialized filter. An attempt was made to use densitometry software to obtain intensity values for 28S and 18S bands.

Microfluidic capillary electrophoresis methods employed Experion StdSens RNA Microchips (BioRad). A eukaryotic RNA standard and aliquots for each pooled sample were grouped onto the same chip, on which 100ng of each aliquot was run. Electropherograms produced for pooled samples were imported into Excel software (Microsoft Corp., Redmond, WA). Area under electropherogram curves were calculated for two defined intervals, referred to as the early phase and late phase, using a left endpoint method of estimation (Figure 2.1). The early phase was defined as the electropherogram interval starting after the 5S peak (~28-seconds) through to the beginning of the 18S peak (~41-seconds). Early phase area was selected for RNA

integrity investigation as it provides a region of the electropherogram that can be expected to produce a limited level of fluorescence (i.e. possesses few RNA fragments within this size range), resulting in a small early phase area. The late phase was defined as the electropherogram interval starting at the beginning of the 18S peak (~41-seconds) through to the end of the 18S peak (~42-seconds). Composed of the interval where the expected migration location of both the 18S and 28S fragments occur, the late phase area was selected for RNA integrity investigation as it provides a region of the electropherogram that can be expected to produce the majority (~70-85%) of the fluorescence detected from the whole electropherogram. Similar to a 28S/18S ratio, the ratio of late phase area to early phase area, referred to as an area quotient, can serve as a proxy measure of RNA integrity for samples of insect origin. Aliquots that failed to produce the distinct electropherogram landmarks that are required to ascertain early phase and late phase boundaries used the boundary points obtained for the untreated aliquot of that same sample.

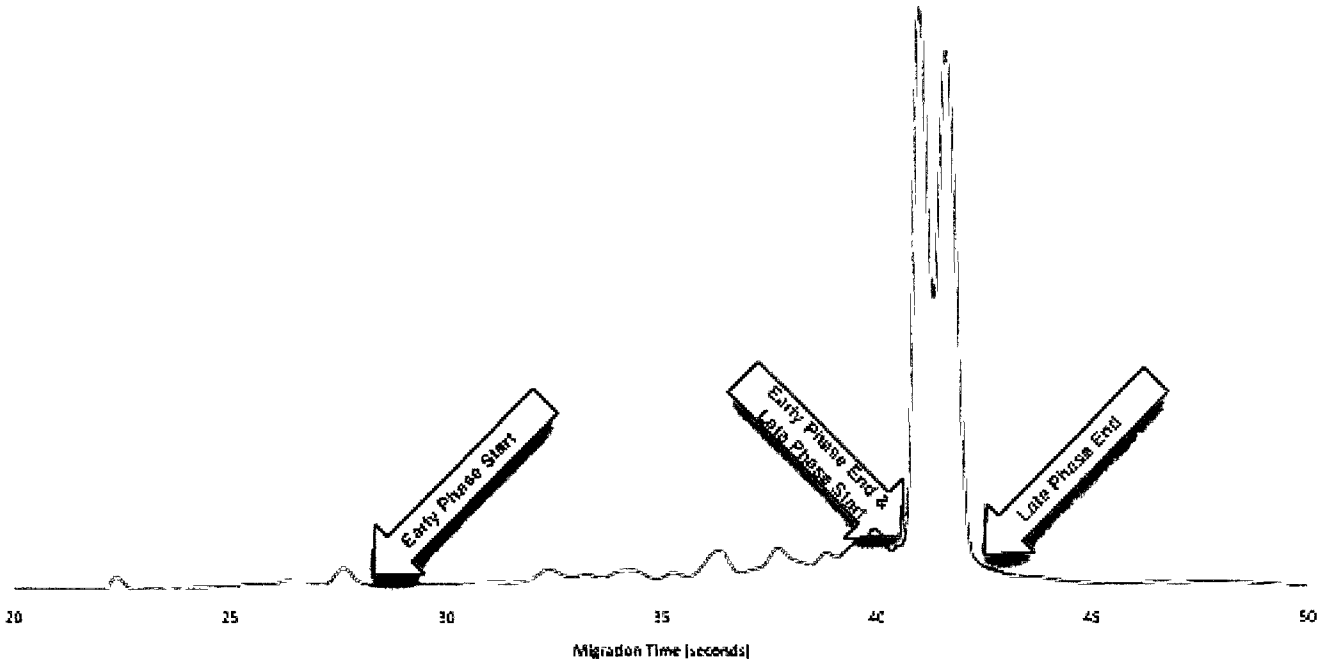

Figure 2.1 – Definition of early phase and late phase interval bounds. The early phase was defined as the electropherogram interval starting after the 5S peak (~28-seconds) through to the beginning of the 18S peak (~41-seconds). Early phase area was selected for RNA integrity investigation as it provides a region of the electropherogram that can be expected to produce limited fluorescence (i.e. possesses few RNA fragments within this size range), resulting in a small early phase area. The late phase was defined as the electropherogram interval starting at the beginning of the 18S peak (~41-seconds) through to the end of the 18S peak (~42-seconds). Composed of the interval where the expected migration location of both the 18S and 28S fragments occur, the late phase area was selected for RNA integrity investigation as it provides a region of the electropherogram that can be expected to produce the majority (~70-85%) of the fluorescence detected from the whole electropherogram. Similar to a 28S/18S ratio, the ratio of late phase area to early phase area, referred to as an area quotient, can serve as a proxy measure of RNA integrity for samples of insect origin.

2.2.6 Reverse Transcription Reactions

Each thermally treated aliquot contributed a total of 250ng total RNA to reverse transcription reactions with total reaction volumes equaling 20μL. Seven reverse transcription reactions, one for each thermal treatment, were conducted for each pooled sample in an MJ Mini Thermo Cycler (Biorad) with a High Capacity cDNA Reverse Transciption Kit (Invitrogen) using the manufacturer's procedure: 10 minutes at 25°C, 120 minutes at 37°C and 5 minutes at 85°C. The cDNA product of each reaction was quantified by use of a Qubit Quantification System (Invitrogen) using 1μL of sample and 199μL of working solution. Prior to conducting qPCR reactions, cDNA product was stored at -80°C.

2.2.7 Quantitative PCR & Fold Change Determination

An iQ5 (Biorad) real-time quantitative PCR (qPCR) machine was employed to quantify mRNA expression levels for thermally treated RNA aliquots for the following target genes: Glycogen phosphorylase (GP), Porphobilinogen deaminase (PBD) and TATA-box binding protein (TBP). Primer and probe sequences for the target genes can be located in Table 2.1 and Table 2.2.

Table 2.1. Primer sequence and properties of three target genes employed to evaluate how the integrity of seven thermally treated *D. ponderosae* total RNA aliquots influences mRNA quantification by RT-qPCR

Reference Gene	Sequence (5'-3')	[Primer] nM	% GC	T_A	Amplicon Size (bp)	E	DLR	R^2
GP Glycogen phosphorylase	TGGATCAAATGCAGAACGGATTC	600	43.4	63.6	107	94.9	5pg – 75ng	0.999
	GTAATCGGCCAGCAAGAAGAAC	600	50.0	63.6				
PBD Porphobilinogen deaminase	GGCTTCAATGTGTGTCCAGTG	900	52.3	56.07	135	100.1	5pg – 75ng	0.993
	CACCAAACCAACGAAAAGATGTTC	900	41.6	56.07				
TBP TATA-box binding protein	GCATCAGCCAGAAGAGGATCAAC	900	52.1	57.37	100	92.7	120pg – 75ng	0.998
	GGGAGCCAATGGAGGAACTTG	900	57.1	57.37				

Table 2.2. Hydrolysis probe sequences of three target genes employed to evaluate how the integrity of seven thermally treated *D. ponderosae* total RNA aliquots influences mRNA quantification by RT-qPCR

Gene	Probe sequence (5'-3')
GP Glycogen Phosphorylase	56-TAMN-CAGCAGATCCTCCGCCTTCCAACAA-3BHQ_2
PBD Porphobilinogen deaminase	56-JOEN-CGCCAATCTTATCACCGTTGCCG-3BHQ_1
TBP TATA-box binding protein	56-JOEN-CAACAACAACAGCAGCAGCAACAGC-3BHQ_1

Methods employed to obtain optimized RT-qPCR results for thermally treated aliquots for five of the ten pooled samples, using GS, PBD and TBP are described in sections 3.2.1-3.2.8 of chapter three.

Final mRNA quantification of RNA aliquots was performed using the comparative Ct (ΔΔCt; Livak and Schmittgen, 2001) method taking into account gene amplification efficiencies (E) (Pfaffl, 2002). Quantification of RNA aliquots is reported as relative transcription or the mean n-fold difference relative to a calibrator cDNA (i.e. transcript levels for 0-minute thermal treatment at 90°C).

Within each sample, ΔCq values for each RNA aliquot were obtained by subtracting the Cq values associated with each of the thermally treated RNA aliquots from the respective sample's calibrator (i.e. 0-minute thermal treatment) Cq value (Vandesompele *et al.,* 2002). Mean relative quantities (RQ) for each thermal treatment were calculated using the equation, $RQ = E^{(\Delta Cq)}$. Confidence intervals were calculated using the standard deviation of respective RQ values. All gene transcription levels were expressed as an n-fold difference relative to the calibrator by dividing the $RQ_{Calibrator}$ by $RQ_{Treatment}$ (Vandesompele *et al.,* 2002).

2.2.8 Statistical Analysis

For statistical analysis of each target gene, logarithmically transformed mRNA expression data for biological replicates were analyzed by R (Version 2.9.2; Ihaka and Gentleman, 1996). Analysis of Variance (ANOVA) assumptions of equal variance and normality were assessed for mRNA expression data. The presence of equal variance was assessed graphically by residual plots and statistically through use of Levene's test. The presence of normality was assessed graphically by histograms and quantile-quantile

plots, and statistically by use of the Sahpiro-Francia normality test. One-way ANOVAs were conducted for logarithmically transformed mRNA expression data and significant differences at the 0.05 and 0.01 alpha values denoted graphically.

2.3 Results

2.3.1 Integrity Assessment of Thermally Treated RNA Aliquots

Total RNA integrity of thermally treated aliquots was successfully assessed by both slab gel electrophoresis (Figure 2.2B) and microfluidic capillary electrophoresis (Figure 2.2A and 2.2C). Spectrophotometric 260/280 values for aliquots post-thermal treatment ranged from 2.01-2.13 and did not differ greatly from values obtained prior to thermal treatment, which ranged from 1.98-2.07.

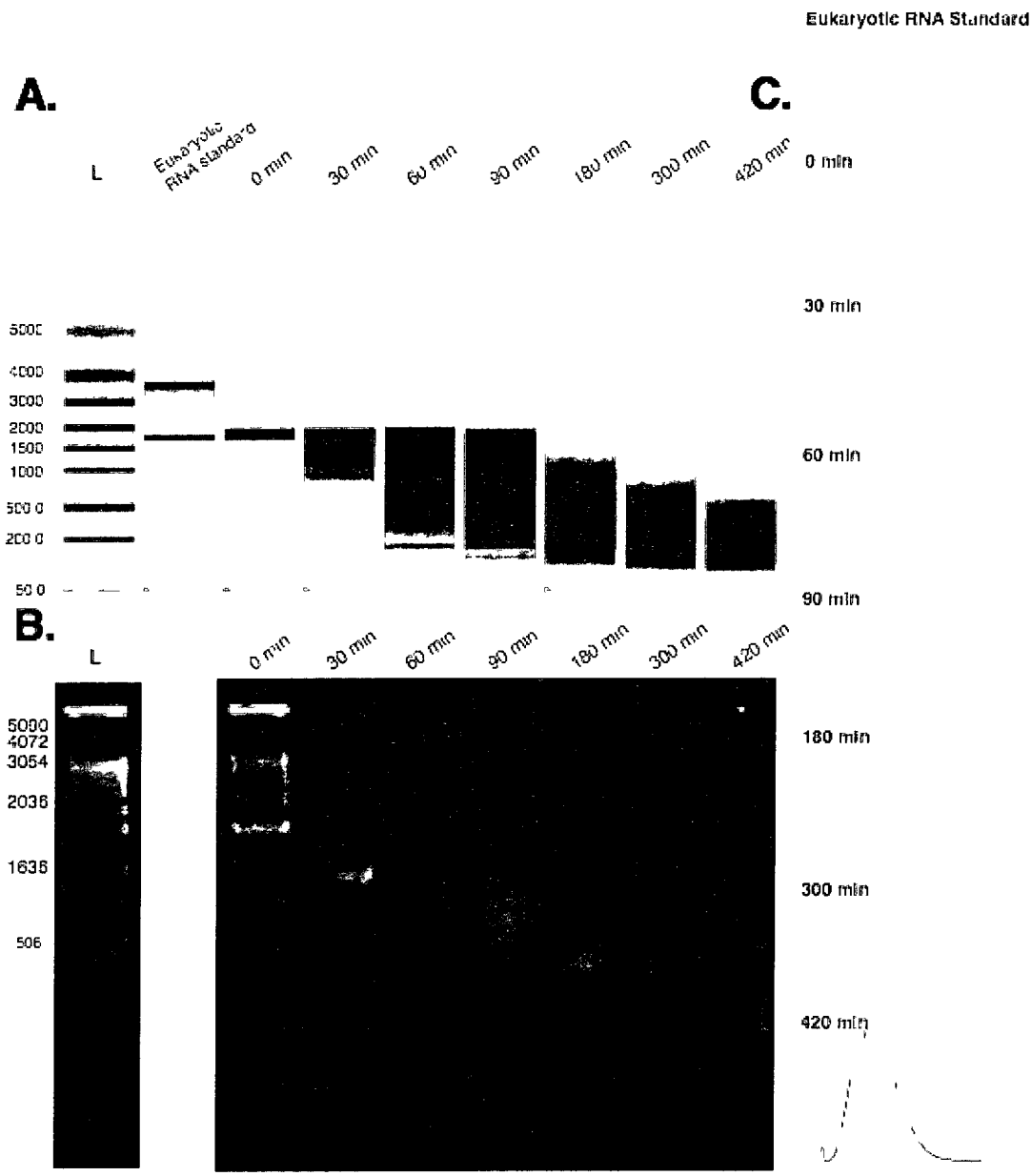
Eukaryotic RNA Standard
A.
C.
L
Eukaryotic RNA standard
0 min
30 min
60 min
90 min
180 min
300 min
420 min
5000
4000
3000
2000
1500
1000
500 0
200 0
50 0
B.
L
0 min
30 min
60 min
90 min
180 min
300 min
420 min
5090
4072
3054
2036
1636
506

Figure 2.2 – Assessment of total RNA integrity (for sample #9) by microfluidic capillary electrophoresis (MCE) and slab gel electrophoresis. Ten pooled *D. ponderosae* total RNA samples were thermally treated in a thermocycler (MJ Mini, Biorad) at 90°C for one of the following minute time intervals: 0, 30, 60, 90, 180, 300 or 420. (A) Digital microfluidic capillary electrophoresis RNA gel produced from loading 100ng of total RNA from each of the thermally treated aliquots for each pooled sample and a eukaryotic RNA standard onto a Experion StdSens RNA Microchip (BioRad, USA). (B) Agarose gel (1.5%, run for 45 minutes at 120V) produced from loading 800ng of each thermally treated RNA aliquot for a pooled sample and 75ng of 1kB DNA ladder (Invitrogen). Electrophoresized slab gels were stained for 40 minutes with SYBR Green II RNA Gel Stain (Invitrogen) using a 1:10,000 dilution of stock reagent as per reagent manual. Gels were visualized on a transilluminator at 300nm with a specialized filter. (C) Thermally treated RNA aliquot electropherograms produced by MEC methods. Electropherograms are displayed from 20 to 50 seconds and at variable fluorescence (RU) units.

2.3.1.1 Integrity Assessment by Slab Gel Electrophoresis

The untreated, 0-minute RNA aliquot produced several distinct bands on the slab gel, two of which, correspond to highly populous 28S and 18S rRNA subunits (Figure 2.2B). The first band of interest, corresponding to the expected size of a 28S rRNA subunit, is located somewhere between the 3054kB and 4072kB marks of the 1kB DNA ladder (Invitrogen). The second smaller and less intense band, corresponding to the expected size of a 18S rRNA subunit, is located just below the 2036kB mark of the ladder. The 2036kB band's intensity was too weak to be detected by densometry software and consequently, no 28S/18S intensity calculations could be made. Several other bands of larger size were detected in excess of 5090kB.

The 30-minute aliquot, and all other thermally treated aliquots, did not produce an observable band between the 3054kB and 4072kB marks of the 1kB DNA ladder. Similar to the untreated aliquot, the 30-minute aliquot produced a band that was detected <2036kB, but appeared to be of slightly larger size. Densometry software indicated that this band was of comparably higher fluorescence then that found for the 0-minute aliquot. A light smearing was visible below the distinct <2036kB band.

Both the 60- and 90-minute aliquots displayed one distinct band, <2036kB, at the same point as the 30-minute aliquot. This band was of a visibly larger size then that produced within the untreated aliquot. The relative intensity of the band showed a marked decrease within the 60-minute aliquot and even more so within the 90-minute aliquot. Increased smearing and intensity of products <1636kB was present in both samples, with the 90-minute aliquot producing more smearing and a high intensity of

fluorescence towards the bottom-half of the smear, relative to the level obtained for the 60-minute aliquot.

No distinct bands were visible from the 180-, 300-, and 420-minute aliquots. Progressively longer thermal treatments resulted in gradually increasing in production of shorter RNA products, as evidenced by an increased density of smearing further away from where samples were initially loaded onto the gel.

2.3.1.2 Integrity Assessment by Microfluidic Capillary Electrophoresis (MCE)

General banding patterns displayed using microfluidic capillary electrophoresis (MCE; Figure 2.2A), and the corresponding aliquot electropherograms (Figure 2.2C), reflected those observed using slab gel electrophoresis (Figure 2.2B).

A eukaryotic RNA standard produced two distinct bands, the first between 3000kB and 4000kB and the second between 1500kB and 2000kB. These bands produced peaks at 41-seconds and 47.25-seconds on the corresponding electropherogram and correspond to highly populous 28S and 18S rRNA subunits.

One notable banding pattern difference produced by MCE was that the untreated aliquot resulted in the production of only a single band. The larger band produced for both the eukaryotic RNA standard by MCE and the 0-minute aliquot produced by slab gel electrophoresis was absent within the 0-minute aliquot on the MCE digital gel. The shorter single band produced for 0-minute aliquot by MCE was also slightly larger in size than that produced for the eukaryotic standard. The electropherogram failed to display a peak in the 47-second range, but displayed a double-peak at 41.1- and 41.7-seconds respectively.

Electropherograms for all other thermally treated aliquots did not produce a peak in the 47-second retention time range. The 30-minute, 60-minute, and to a much less extent, the 90-minute thermally treated aliquots displayed the double-peak at the 41-second retention time range, as was detected within the untreated aliquot. The 180-, 300-, and 420-minute aliquots failed to produce a peak at the 41-second retention time range. Maximal fluorescence (RU) decreased and the relative number of peaks detected <41-seconds retention time increased with increasing thermal treatment.

2.3.2 Area Quotient Determination

As defined by Section 2.5, early phase and late phase area calculations were made and area quotients are shown below (Table 2.3).

Table 2.3 – Area quotients: average ratio of late phase area to early phase area for thermally treated RNA aliquots

Time	**n**	**Late Phase Area / Early Phase Area**	**95% - CI**
0 minutes	10	3.64	5.86×10^{-1}
30 minutes	9	3.08×10^{-1}	2.01×10^{-1}
60 minutes	9	3.11×10^{-2}	2.03×10^{-2}
90 minutes	8	2.91×10^{-2}	2.02×10^{-2}
180 minutes	9	1.37×10^{-2}	8.95×10^{-3}
300 minutes	10	2.55×10^{-3}	1.58×10^{-3}
420 minutes	7	3.07×10^{-3}	2.27×10^{-3}

Late phase area to early phase area ratios continually decreased, with increased thermal treatment duration time, from 3.64 for the 0-minute aliquot to 3.07×10^{-3} for the 420-minute aliquot.

2.3.3 Apparent mRNA n-Fold Expression Decrease

Cq values returned for both GP and PBD for the 0-minute aliquot were >35 and failed to return appropriate Cq values for all of the thermally treated aliquots in time series. mRNA n-fold apparent expression decrease calculations could not be made using either of these two primer pairs.

Cq values returned for TBP <35 for the entire time series and mean n-fold apparent expression decrease values were calculated (Figure 2.3).

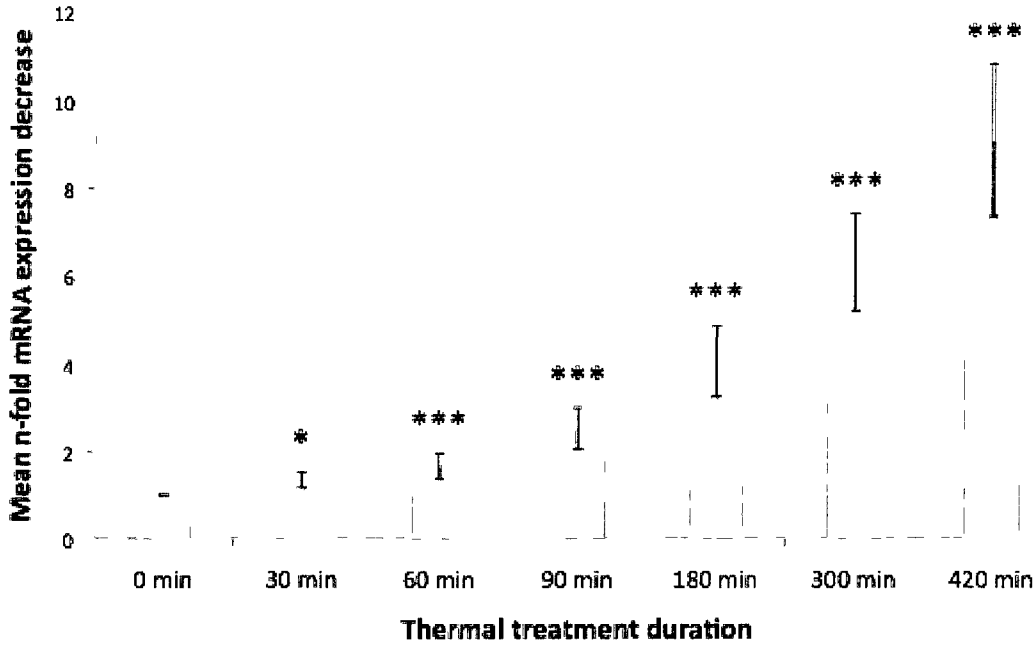

Figure 2.3 – Mean n-fold mRNA apparent expression decreases for thermally treated total RNA aliqots, relative to mRNA expression of an untreated aliquot, using TBP primers and probes. A one-way ANOVA was conducted with mean n-fold mRNA expression decreases significantly different from the mRNA expression for the untreated sample denoted (* = $p<0.05$; *** = $p<0.001$).

The mean n-fold mRNA apparent expression decrease for the total RNA aliquot thermally treated for 30-minutes was found to be significantly different ($p < 0.05$). All other thermally treated aliquots were found to have significantly different mean n-fold mRNA apparent expression decreases at a 0.001 alpha value. The mean mRNA apparent expression decrease reached a maximum of 9.08-fold for the 420-minute aliquot, registering slightly more than 11% of the mRNA expression quantified compared to the untreated aliquot, which was composed of the same pooled total RNA.

2.3.4 Thermal Threshold Determination

Thermal threshold results for 10°C, 20°C, 30°C treated aliquots produced two distinct bands (Figure 2.4A), equivalent to those displayed for the eukaryotic RNA standard thermally treated for an equal amount of time at 70°C (Figure 2.2A). Eletropherograms for these three aliquots produced two peaks, one at the 40- to 41-second retention time range, the other at the 45- to 46-second retention time range (Figure 2.4B). Maximum fluorescence intensity for these aliquots ranged from 4.00 – 7.29RU, which was achieved at the 45- to 46-second retention time range.

Thermal threshold results for 40°C, 50°C, 60°C treated aliquots produced only one distinct band (Figure 2.4A), equivalent to that displayed for the untreated aliquot from the previous thermal treatment assessment, which, as per MCE protocol instructions, was thermally treated for an equal amount of time at 70°C (Figure 2.2A). Eletropherograms for these three aliquots produced a single peak at the 40- to 41-second range (Figure 2.4B). The 30°C treated aliquot produced a very slight second peak at the 46.05-second mark that was of weak (i.e. 0.92RU) intensity. A twinning of the single peak was observed for the 50°C and 60°C treated aliquots. Maximum fluorescence

intensity for the 40°C, 50°C, 60°C treated aliquots ranged from 12.08 – 14.74RU, which was achieved at the 40- to 41-second retention time range.

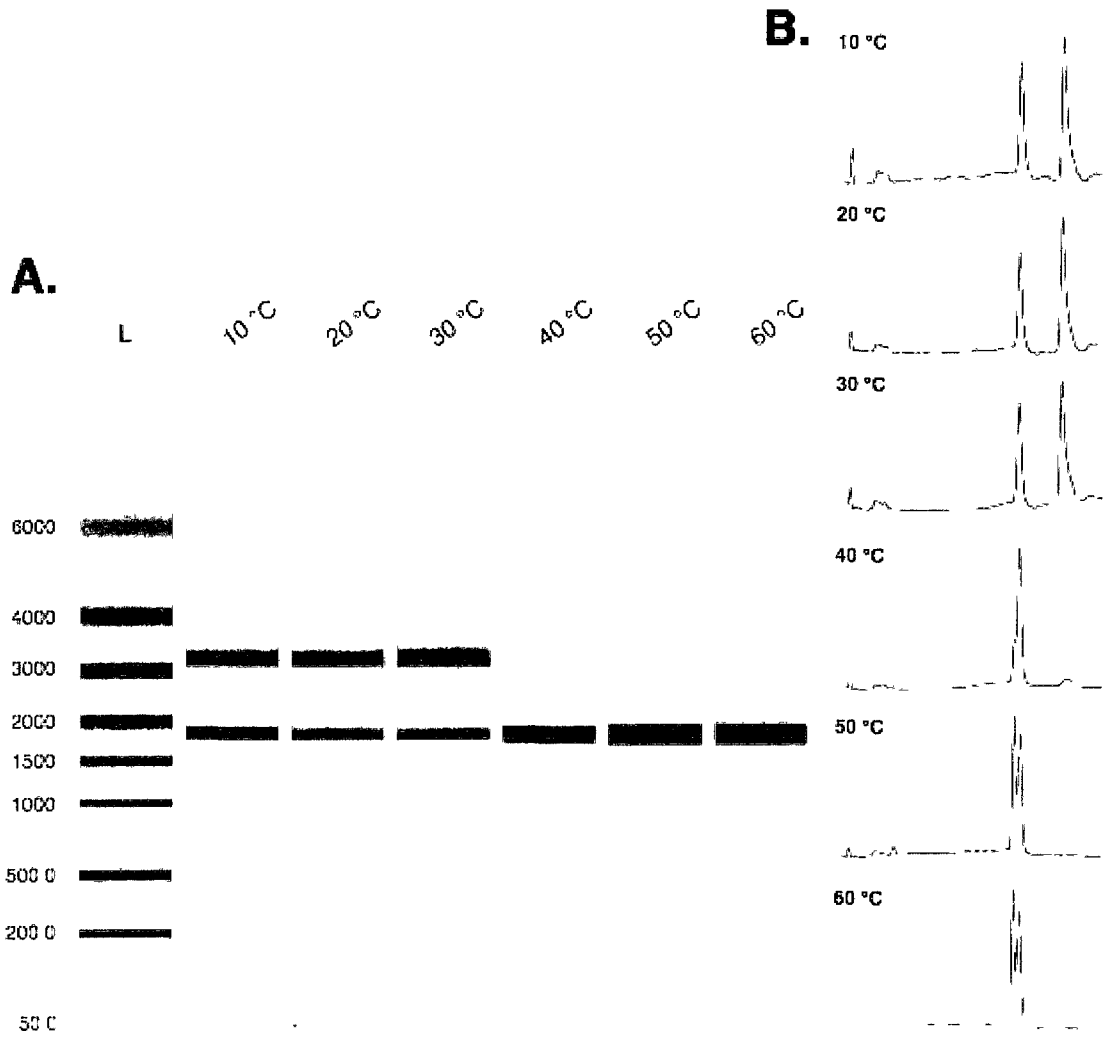

Figure 2.4 - Assessment of total RNA integrity by microfluidic capillary electrophoresis (MCE). A pooled 20 May, 2009 *D. ponderosae* total RNA sample was split into equal volume aliquots and thermally treated in a thermocycler (MJ Mini, Biorad, USA) for two minutes at one of the following temperatures: 10°C, 20°C, 30°C, 40°C, 50°C or 60°C. (A) Digital microfluidic capillary electrophoresis RNA gel produced from loading 100ng of total RNA from each of the thermally treated aliquots onto an Experion StdSens RNA Microchip (BioRad, USA). (B) Thermally treated RNA aliquot electropherograms produced by MEC methods. Electropherograms are displayed from 20 to 50 seconds and at variable fluorescence (RU) units.

2.4 Discussion

The time intervals chosen for thermal treatment did not allow for a 28S/18S intensity ratio to be calculated from native slab gels. Cleavage of 28S rRNA was witnessed for all thermally treated RNA aliquots, with the intensity of the 18S rRNA for untreated aliquots being too weak to quantify by densometry (Figure 2.2B). In a pilot experiment conducted prior to this study, 400ng of thermally treated RNA was stained with ethidium bromide and visualized on a transilluminator at 300nm (Appendix - Figure 7.1). Ethidium bromide is known to be less sensitive for RNA detection purposes than SYBR Green II, and yet, an equivalent amount of fluorescence intensity, as detected by densometry software, was observed during the pilot experiment as was for this study. Limited RNA sample material prevented the application of higher RNA quantities to native gels.

Area quotients and mRNA expression reveal that an area quotient threshold can be used to predict when significant apparent decreases in mRNA expression are occurring due to compromised RNA integrity versus other treatments investigated. All thermally treated aliquots returned mean n-fold mRNA apparent expression decreases that were significantly different from the mRNA expression for the untreated RNA aliquot (Figure 2.3); the least significantly different aliquot had been thermally treated for 30-minutes. When viewed in relation to area quotients, it can be predicted that a significant reduction of mRNA expression was caused due to a decrease in RNA integrity when area calculations were equal to or less than the area quotient of the 30-minute aliquot, or 0.3 (Table 2.3). This is not to say that RNA samples possessing area quotients in excess of 0.3 cannot also produce false mRNA expression decreases; just

that RNA samples possessing area quotients below 0.3 do not produce mRNA expression absent of false expression decreases.

To better determine the lowest area quotient present when significant decreases in mRNA expression are found to occur due to compromised RNA integrity, five thermally treated RNA aliquots were made at time intervals less than 30-minutes. Unfortunately due to technical difficulties results from this subsequent study were not obtained. A repeat of this subsequent study is recommended in intervals <30 minutes, however results from our thermal threshold experiment indicate that it would also be advantageous to decrease the thermal treatment from 90°C to ≤30°C to preserve an intact 28S rRNA (Figure 2.4).

Thermal threshold results were significant, as they indicated that thermal and not chemical (i.e. DMSO) denaturing conditions result in cleavage of the 28S rRNA in *D. ponderosae* during MCE processing. When exposed to a temperature of 40°C, sufficient energy is available to break hydrogen bonds between 28Sα and 28Sβ subunits, causing dissociation, which is displayed on MCE electropherograms. Ishikawa and Newburgh (1972) conducted several thermal treatment conditions involving total RNA isolated from *Galleria mellonella*, the greater wax moth. They observed that thermal treatment of total RNA for 15-minutes at 35°C resulted in 20% of 28S rRNA being cleaved. 28S rRNA cleavage increased to 90% when treated at 45°C for 5-minutes and 100% when treated for 15-minutes at 45°C. These results obtained by Ishikawa and Newburgh (1972) compare well to those obtained in this study. However there are advantages and disadvantages of thermal treatment prior to MCE that should be considered.

Thermal treatment of RNA prior to MCE is conducted in order to decrease the amount of secondary structure that can interfere with RNA size separation. The advantage thermal treatment provides in decreasing secondary structure of insect RNA must be compared against the potential cost of complicating the assessment of insect RNA integrity. While thermal treatment of $\leq 30°C$ provided the advantage of an intact insect 28S rRNA subunit, which could be used to generate standard RNA integrity measures, the amplitude of the electropherogram peaks were significantly decreased and resolution on the digital gel was decreased, assumed to be caused by increased RNA secondary structure. Thermal treatment of insect RNA should therefore be applied or avoided depending on how a researcher values the measurement of RNA integrity or size separation on a MCE digital gel.

RQI, a standard MCE RNA integrity measure, fails to be produced when a MCE chip ladder well incurs an IV failure or other well error. In addition to being compatible with assessing insect RNA integrity, one benefit of the area quotient shown here is that it does not require reference to the ladder size maker and can produce an integrity measure in absence of a successful ladder well run.

2.5 Conclusion

In this study, I observed as much as a 9-fold decrease in mRNA expression due solely to compromised RNA integrity. I identified that thermal and not chemical denaturing conditions, both inherent to MCE, resulted in cleavage of the 28S rRNA in *D. ponderosae*, but that thermal treatment ≤30°C resulted in maintaining an intact 28S rRNA. From results produced by varying levels of thermal treatment, an RNA integrity measure compatible with assessing insect RNA integrity was designed that can successfully predict when significant decreases in mRNA expression are occurring due to compromised RNA integrity versus other treatments investigated. Due to the conserved behavior of insect 28S rRNA under denaturing conditions, I expect that the novel RNA integrity measure developed here can be applied to RNA integrity assessment of other insect species.

2.6 Bibliography

Applebaum, S., Ebstein, R.P., and Wyatt, G.R. (1966). Dissociation of ribosomal ribonucleic acid from silkmoth pupae by heat and dimethylsulfoxide: evidence for specific cleavage points. *J. Mol. Biol.* 21(1): 29-41.

Auer, H., Lyianarachchi, S., Newsom D., Klisovic, M., Marucci, u., and Kornacker, K. (2003). Chipping away at the chip bias: RNA degradation in microarray analysis. *Nature Genetics* 35(4): 292-293.

Basile-Borgia, A.E., Dunbar, D.A. and Ware, V.C. (2005). Heterologous rRNA gene expression: internal fragmentation of *Sciara coprophila* 28S rRNA within microinjected *Xenopus laevis* oocytes. *Insect Molecular Biology* 14(5): 523-536.

Bustin, S.A, and Nolan, T. (2004). Pitfalls of quantitative real-time reverse-transcription polymerase chain reaction. *Journal of Biomolecular Techniques* 15(3): 155-166.

Copois, V., Bibeau, F., Bascoul-Mollevi, C., Salvetat, N., Chalbos, P., Bareil, C., Candeil L., Fraslon, C., Conseiller, E., Granci, V., Maziere, P., Kramar, A., Ychou, M., Pau, B., Martineau, P., Molina, F., and Del Rio, M. (2007). Impact of RNA degradation on gene expression profiles: Assessment of different methods to reliable determine RNA quality. *Journal of Biotechnology* 127: 549-559.

Davis, F.C., and Mullersman, R.W. (1981). Processing of the ribonucleic acid in the large ribosomal subunits of *Urechis caupot. Biochemistry* 20: 3554-3561.

DeLanversin, G., and Jacq, B. (1983). Sequence of the central break region of the precursor of *Drosophila* 26S ribosomal RNA. *C R Seances Acad Sci* 296: 1041–1044.

Denisov, V., Strong, W., Walder, M., Gingrich, J., and Wintz, H. (2008). Development and validation of RQI: an RNA quality indicator for the Experion™ automated electrophoresis system. *Bio-Rad Bulletin #5761(Rev B)* 1-6.

Fleige, S., and Pfaffl, M.W. (2006). RNA integrity and the effect on the real-time qRT-PCR performance. *Molecular Aspects of Medicine* 27: 126-139.

Fleige, S., Walf, V., Huch, S., Prgomet, C., Sehm, J., and Pfaffl, M.W. (2006). Comparison of relative mRNA quantification models and the impact of RNA integrity in quantitative real-time RT-PCR. *Biotechnology Letters* 28: 1601-1613.

Fujiwara, H., and Ishikawa, H. (1986). Molecular mechanism of introduction of the hidden break into the 28S rRNA of insects: implication based on structural studies. *Nucleic Acids Research* 14(16): 6393-6401.

Gingrich, J., Rubio, T., and Karlak, C. (2008) Effect of RNA degradation on data quality in quantitative PCR and microarray experiments. *Bio-Rad Bulletin #5547(Rev A)* 1-2.

Hatton, L.S., Eloranta, J.J., Figueiredo, L.M., Takagaki, Y., Manley, J.L., and O'Hare, K. (2000). The *Drosophila* homologue of the 64 kDa subunit of cleavage stimulation factor interacts with the 77 kDa subunit encoded by the suppressor of forked gene. *Nucleic Acids Research* 28(2): 520-526.

Ho-Pun-Cheung, A., Bascoul-Mollevi, C., Assenat, E., Bossiere-Michot, F., Bibeau, F., Cellier, D., Ychou, M., and Lopez-Crapez, E. (2009). Reverse transcription-quantitative polymerase chain reaction: description of a RIN-based algorithm for accurate data normalization. *BMC Molecular Biology* 10: 31.

Ihaka, R., and Gentleman, R. (1996). R: a language for data analysis and graphics. *Journal of Computational and Graphical Statistics* 5(3): 299-314.

Imbeaud, S., Graudens, E., Boulanger, V., Barlet, X., Zaborski, P., Eveno, E., Mueller, O., Schroeder, A., and Auffray, C. (2005). Towards standardization of RNA quality assessment using user-independent classifiers of microcapillary electrophoresis traces. *Nucleic Acids Research* 33(6): e56.

Ishiwaka, H., and Newburgh, R.W. (1972). Studies of the thermal conversion of 28S RNA of *Galleria mellonella* (L.) to an 18S product. *J. Mol. Biol.* 64: 135-144.

Jordan, B.R., Jourdan, R., and Jacq, B. (1976). Late steps in the maturation of *Drosophila* 26S ribosomal RNA: generation of 5.8S and 2S RNAs by cleavages occurring in the cytoplasm. *J. Mol. Biol.* 101: 85-105.

Karlstedt, K.A., Paatero, G.I.L., Makela, J., and Wikgren, B. (1992). A hidden break in the 28.0S rRNA from *Diphyllobothrium dendriticum. Journal of Helminthology* 66:193-197.

Krupp, G. (2005). Stringent RNA quality control using the Agilent 2100 bioanalyzer *Agilent Technologies Application Note 5989-1086EN* 1-8.

Livak, K.J., and Schmittgen, T.D. (2001). Analysis of relative gene expression data using real-time quantitative PCR and the $2^{-\Delta\Delta Ct}$ method. *Methods* 25: 402-408.

Miller, C.L., Diglisic, S., Leister, F., Webster, M., and Yolken, R.H. (2004). Evaluating RNA status for RT-PCR in extracts of postmortem human brain tissue. *BioTechniques* 36: 628-633.

Ogino, K., Eda-Fujiwara, H., Fujiwara, H., and Ishikawa, H. (1990). What causes the aphid 28S rRNA to lack the hidden break. *J Mol Evol* 30: 509-513.

Schroeder, A., Mueller, O., Stocker, S., Salowsky, R., Leiber, M., Gassmann, M., Lightfoot, S., Menzel, W., Granzow, M., and Ragg, T. (2006). The RIN: an RNA integrity number for assigning integrity values to RNA measurements. *BMC Molecular Biology* 7(3): 14.

Strand, C., Enell, J., Hedenfalk, I., Ferno, M. (2007). RNA quality in frozen breast cancer samples and the influence on gene expression analysis – a comparison of three evaluation methods using microcapillary electrophoresis traces. *BMC Molecular Biology* 8:38.

Tahoe, N.M.A., Mokhtarzadeh, A., and Curtsinger, J.W. (2004). Age-related RNA decline in adult *Drosophila melanogaster*. *J of Gerontology* 59A(9): 896-901.

Ware, V.C., Renkawitz, R., and Gerbi, S.A. (1985). rRNA processing: removal of only nineteen bases at the gap between 28Sα and 28Sβ rRNAs in *Sciara coprophila*. *Nucleic Acids Research* 13: 3581-3597.

Wu, D., Qin, J., and Lin, B. (2008). Electrophoretic separations on microfluidic chips *Journal of Chromatography A* 1184: 542-559.

2.7 Appendix

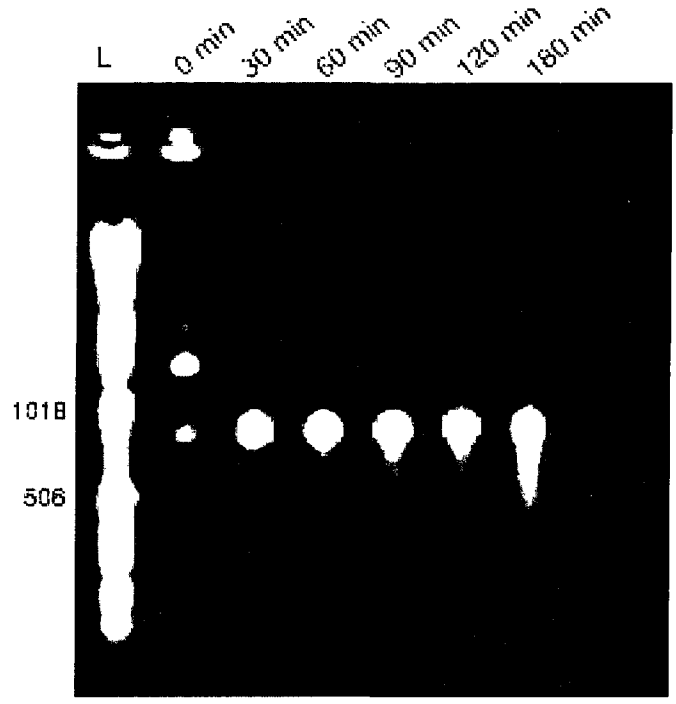

Figure 2.7.1 - 1.5% agarose gel (45 minutes at 120V) produced from loading 400ng of each thermally treated RNA aliquot for a pooled sample and 75ng of 1kB DNA ladder (Invitrogen) and visualized on a transilluminator at 300nm.

Evaluation of Reverse Transcription-Quantitative Polymerase Chain Reaction (RT-qPCR) Reference Genes for Seasonal Cold Tolerance Gene Expression Studies in *Dendroctonus ponderosae*

3.1 Introduction

Gene expression is the process by which cellular instructions stored within genes are converted into functional gene products in the form of proteins. Quantification of gene expression has become a powerful mean by which biological and ecological problems are investigated. By identifying how environmental, physiological, developmental or other treatments change transcription of a gene, researchers can better understand what function an associated gene product serves and the conditional parameters under which its production is regulated (Van Hiel *et al.,* 2009). When coupled with metabolomic information, knowledge of gene-specific function and regulation can provide a richer understanding of how cellular substrates of interest are accumulated and/or metabolized.

Reverse transcription quantitative PCR (RT-qPCR) is a powerful and economical methodology by which relationships between treatments and gene expression can be deduced mathematically. A quantitative relationship exists between the initial amount of cDNA used in a qPCR reaction and the amount of PCR product produced at any given cycle within the exponential phase of amplification (Gangisetty and Reddy, 2009). Within the exponential phase of a RT-qPCR reaction, a doubling of PCR product can be

assumed between each cycle, with a 10-fold increase in product occurring every 3.33 cycles (i.e. $2^{3.33} = 10$) (Grinzinger, 2002).

RT-qPCR quantification involves the relative normalization of gene of interest (GOI) expression levels to that of a stably expressed reference gene, formerly known as a housekeeping gene, for all tissues, treatments and developmental stages investigated. Considerable evidence indicates however that reference gene expression can vary between tissue types (Vandesomepele *et al.,* 2002; Benn *et al.,* 2008; Thorrez *et al.,* 2008), treatments (Thellin *et al.,* 1999; Lee *et al.,* 2002; McCurley and Callard, 2008) or developmental stages (McCurley and Callard, 2008; Fernandes *et al.,* 2008; Van Hiel *et al.,* 2009; Garg *et al.*, 2010). An assessment of candidate reference gene stability is therefore necessary before normalization of a GOI can occur (Bustin *et al.,* 2009).

Vandesompelle *et al.* (2002) developed a software program, geNorm, which ranks candidate reference genes based on expression stability measures. Once the most appropriate reference genes have been identified for a given treatment, geNorm provides a geometric average of the most stable reference genes' expression levels. This geometric average is referred to as a normalization factor and is a more stable measure to normalize GOI expression than any one single reference gene can provide.

After reviewing numerous gene expression studies, Suzuki *et al.* (2000) reported that over 90% used only a single reference gene. Evaluating reference gene expression in *Tribolium castaneum* after fungal challenge, Lord *et al.* (2010) state that with the exception of the honeybee, *Apis mellfiera*, no other insect species had had the expression stability of their reference genes appraised. While studies with *Bombyx mori* (Wang *et*

al., 2008), *Schistocerca gregaria* (Van Hiel *et al.,* 2009) and both *Folsomia candida* and *Orchesella cincta* (Boer *et al.,* 2009) have been conducted, it is fair to assume that very few insect gene expression studies justify the number and choice of their reference genes. Such a justification is deemed an essential piece of information required for publication as suggested within The Minimum Information for Publication of Quantitative Real-Time PCR Experiments Guidelines (MIQE; Bustin *et al.,* 2009).

The objective of this study is to address a significant and frequently neglected aspect of conducting gene expression research within *Dendroctonus ponderosae* and other insect species: the evaluation of reference gene expression stability across varied treatment groups. This study aims to identify the most appropriate number and choice of reference genes required to normalize expression of GOIs associated with seasonal cold tolerance in *D. ponderosae.*

3.2 Methods

3.2.1 Sample Collection and Preparation

Two pine (*Pinus contorta*) trees, freshly attacked by *D. ponderosae*, and located west of Tête Jaune Cache, British Columbia, Canada (N53° 3' 35.28" W119° 36' 52.74") were identified in late summer of 2008. Three temperature data loggers were affixed to each tree. They were located either at the base of the tree, at breast height on the north side of the tree and at breast height on the south side of the tree. Temperature data were recorded every 30 minutes throughout the study period. Multiple live *D. ponderosae* larvae of mixed instar and of undetermined sex were manually removed from trees on the following dates: 19 September, 2008, 3 October, 2008, 17 October, 2008, 31 October, 2008, 14 November, 2008, 18 March, 2009, 1 April, 2009, 14 April, 2009, 29 April, 2009 and 13 May, 2009. Larvae were individually deposited in 1.5mL microcentrifuge tubes, immediately placed in liquid nitrogen, transported back to UNBC laboratory facilities on dry ice where they were immediately stored at -80°C until genetic extractions were conducted.

3.2.2 Total RNA Extractions

Prior to conducting RNA extractions, larval samples were individually transferred into deep 96-well plates, one larva per well, containing a single stainless steel bead (4mm in diameter) and 200µL RNAlater®-ICE (Ambion, USA). Samples were soaked in solution for a minimum of 18 hours at -20°C. Prior to sample homogenization, residual RNAlater®-ICE was removed, 100µL of MagMax™-96 Kits lysis/binding solution (Ambion) was added to each sample well. Samples were

completely homogenized by use of a GeneoGrinder 2000 (SpexCertiprep, USA) with six, 30-second intervals at 1500 strokes/minute, cooling on ice for 60 seconds between each interval. Sixty microlitres of 100% isopropanol were added to each lysate and homogenization plates were held at -20°C for 10 minutes.

A total of 201 RNA extractions were conducted with MagMax™-96 Kits (Ambion), using the animal tissue protocol with minor modifications. All extractions were conducted between 22 May and 3 June, 2010. RNA concentration was acquired by use of a Qubit Quantification System (Invitrogen, USA) using 3μL of sample and 197μL of working solution. Estimates of sample purity were obtained by use of a Nanodrop ND-1000 (Nanodrop Technologies, Inc., USA), with sample 260/280 ratios ranging from 1.8-2.2. Sample integrity was assessed via Experion StdSens (BioRad, USA) microfluidics chips with sample electropherograms visually inspected for evidence of RNA degradation. RNA extractions were stored at -80°C until reverse transcription reactions were conducted.

3.2.3 Reverse Transcription Reactions

3.2.3.1 Pooled cDNA

Twenty total RNA extraction aliquots – one from each of the two trees sampled at each of the 10 collection weeks - were pooled together prior to conducting reverse transcription reactions. Each RNA aliquot contributed a total of 400ng total RNA with total pooled volume equaling 400μL. Fifty microliter aliquots of the pooled RNA (~1mg total RNA/RT-reaction) were combined with an equal volume of a High Capacity cDNA Reverse Transciption Kit (Invitrogen) Master Mix to produce a total reaction volume of

100μL. Eight reverse transcription reactions were conducted in an MJ Mini Thermo Cycler (Biorad) with a High Capacity cDNA Reverse Transciption Kit (Invitrogen) using the manufacturer's procedure: 10 minutes at 25°C, 120 minutes at 37°C and 5 minutes at 85°C. The cDNA product of each reaction was quantified by use of a Qubit Quantification System (Invitrogen, USA) using 2μL of sample and 198μL of working solution. During the time that optimal qPCR reaction conditions were being determined, unused cDNA product was stored at -80°C.

3.2.3.2 Dataset Samples

Eight total RNA extractions from each respective sampling week were selected for reverse transcription with a High Capacity cDNA Reverse Transciption Kit (Invitrogen) using the previously stated manufacturer's procedure. In each RT-reaction, 800ng of total RNA was reverse transcribed in a total reaction volume of 40μL. A 20μL no-amplification control was also included by replacing RNA template with nuclease-free water. While it is understood that selecting samples with high total RNA yields for further processing may result in potential sample bias, for our high-throughput purposes, no other selection method could be employed without project downscaling. Of the eight RNA extractions selected from each week, the two sampling trees contributed an equal number of samples (i.e. 4 larvae), with the exception of two weeks where 5 and 3 larvae were contributed from the respective trees due to low RNA yields; 19 September, 2008 and 31 October, 2008. Each cDNA product was quantified by use of a Qubit Quantification System (Invitrogen, USA) using 2μL of sample and 198μL of working solution. Dataset sample cDNA was diluted 1:9 with nuclease-free water, 25μL aliquots

made and cDNA products stored at -80°C until optimal qPCR reaction conditions were determined.

3.2.4 Bioinformatics and Primer and Probe Design

Sequence information for seven reference genes – RNA polymerase II (RPII), porphobilinogen deaminase (PBD), actin (ACT), α-tubulin (TUB), TATA-box binding protein (TBP), tyrosine 3-monooxygenase (YWHAZ) and succinate dehydrogenase (SuDH) - was acquired from the TRIA Project's Expressed Sequence Tag (EST) database. Reference gene identification and selection was based on a literature search of endogenous control stability studies using both insect and non-insect species (Scharlaken *et al.,* 2008; Van Hiel *et al.,* 2009; Wang *et al.,* 2008). Appropriate sequence information, in the form of EST contigs, was obtained using one of two methods: 1) keyword searches using a database utility and, 2) performing database tBLASTn searches by entering sequence information acquired from NCBI for closely related species (e.g. *Tribolium castaneum*, *Bombyx mori*, *Ips typographus*, etc.). All six possible translated reading frames for resulting EST contigs were produced via an ExPASy protein translation utility (www.expasy.org/tools). While it does not indicate functionality, the reading frame producing the longest continuous amino acid sequence with fewest stop codons was selected for further analysis. The potential protein-coding region for a contig was determined by locating the start and stop codons abutting the longest continuous amino acid sequence. This protein-coding region was evaluated by performing tBLASTx and pBLAST searches on NCBI (ww.ncbi.nlm.nih.gov/) databases and confirming that the reference genes of interest resulted for insect species possessing the lowest expectation values.

Having identified both the reading frame and the position of protein coding region, contigs were then assessed by aligning all available reads for a respective reference gene. Reference genes' contig consensus sequences were cleaned by deleting all nucleotides that: 1) situated outside of the determined protein coding region, 2) that appeared in less than three contig reads, or 3) contained apparent single nucleotide polymorphisms (SNPs). Nucleotide sequences were translated into their respective amino acid sequences and tBLASTn searches were conducted to further evaluate cleaned contig sequences. Obtaining the lowest expectation values for insect species and for the reference gene of interest provided confidence that the original reference gene contig selected was an appropriate choice.

Cleaned contig sequence information was employed to design primers and hydrolysis probes for subsequent RT-qPCR experiments. Primers and hydrolysis probes were designed utilizing Beacon Designer 7.0 software (Premier Biosoft, USA). Reference gene-specific hydrolysis primers and probes (Table 3.1. and 3.2) were produced using multiplex default settings and purchased from Integrated DNA Technologies Inc. RT-qPCR experiments involving SuDH, TUB and YWHAZ reference genes used SYBR Green chemistry versus hydrolysis probes as a reporter dye.

3.3.2.5 *Primer Specificity and PCR Reaction Optimization*

Initial validation of primer specificity was performed via sequencing of PCR conventional amplicons. For each 25μL PCR reaction the following component volumes were used: 2.5μL forward primer (5μM), 2.5μL reverse primer (5μM), 2.5μL dNTPs (2mM each), 0.5μL Taq DNA polymerase (5U/μL), 2.5μL reaction buffer (10X) and

4μL of cDNA template from pooled samples (25-50ng/μL). In order to obtain varied $MgCl_2$ concentrations (1mM, 2mM, 3mM, 4mM, 5mM and 6mM) the following volumes of $MgCl_2$ (50mM) were added respectively: 0.5μL, 1.0μL, 1.5μL, 2.0μL, 2.5μL, and 3.0μL. An appropriate amount of nuclease-free water (Ambion) was added to obtain a total PCR reaction volume of 25μL.

For each of the six magnesium chloride concentrations, primer-specific annealing temperatures were produced through use of a thermal gradient. Reactions were thermally optimized by assessment of the following eight annealing temperatures: 55.0°C, 55.5°C, 56.3°C, 57.4°C, 58.7°C, 59.8°C, 60.6°C, and 61.0°C. Thermocycling protocols were run with a 5 minute initial denaturing step at 95°C, followed by 35 cycles of: 30 seconds at 95°C, 30 seconds at one of the various aforementioned annealing temperatures and 60 seconds at 72°C in an MJ Mini Thermo Cycler (BioRad).

For sequencing purposes, optimum annealing temperatures were assessed via production of a single PCR product band of expected amplicon size on a 1.5% agarose.

Prior to sequencing, selected PCR products were cleaned via a PCR Purification Kit (Qiagen, USA). Sequencing reactions were prepared by adding two to six nanograms of PCR product to 10pmol of either forward or reverse primer and the total reaction volume was brought to 15μL with nuclease-free water. Two sequencing reactions per gene were prepared. Samples were processed at the University of British Columbia – Okanagan Campus, Fragment Analysis & DNA Sequencing Services lab, Kelowna, Canada on a 3130XL DNA Analyzer (Applied Biosystems, USA) by a trained technician.

3.2.6 qPCR Reaction Optimization

3.2.6.1 Annealing Temperature Optimization

The iQ5 (Biorad) real-time quantitative PCR machine was employed to optimize primer pair-specific annealing temperatures for qPCR reactions, a further refinement to previous estimates of annealing temperatures obtained by conventional PCR. A thermal gradient feature was applied to iQ5 protocols in which each row of the reaction block assumed a different annealing temperature when incorporated within a cycle. The gradient of annealing temperatures had a range of 10°C with the lowest annealing temperature for each gene starting one degree lower than previous annealing temperature estimates determined by conventional PCR. qPCR protocols consisted of an initial denaturation step at 95°C for 3 minutes followed by 40 cycles of 10 seconds at 95°C and 30 seconds at a respective annealing temperature. qPCR optical fluorescence data was acquired during the annealing phase of the reaction. Melt curves were produced for the three reference genes using SYBR Green chemistry - SuDH, TUB and YWHAZ - to assess for non-specific amplification.

Well factors are used by the iQ5 to optimize the quality of fluorescence data in order to compensate for system irregularities and pipetting error. Dynamic well factors – those collected directly from the reaction wells of the experimental plate prior to a qPCR protocol being initiated – were used in the optimization of annealing temperatures for RPII, PBD and ACT respectively. Due to different fluorophores being present on the same qPCR plate, persistent well factors – those collected from a separate plate prior to

the experimental plate being run - were required to quantify annealing temperature optimization reactions for: TUB, TBP, YWHAZ, and SuDH.

All qPCR annealing temperature optimizations were conducted using 96-well plates (iQ 96-well PCR Plates, Biorad) sealed with adhesive strips (Biorad). Prior to qPCR reactions being performed, the following calibrations were exercised on the iQ5 as suggested by the manufacturer: mask alignment, background calibration, persistent well factor generation and pure dye calibration (IQ dye calibrator solution set, Biorad).

A 1/10 dilution of pooled cDNA was used as template for reactions with each annealing temperature being tested in duplicate. For reference genes employing hydrolysis probe chemistry (i.e. RPII, PBD, ACT and TBP) reactions of 25µL total volume consisting of the following component volumes were conducted: 2.5µL forward primer (9µM), 2.5µL reverse primer (9µM), 2.5µL Probe (2.5µM), 2.5µL pooled cDNA template (3.07ng/µL), 2.5µL nuclease-free H_2O and 12.5µL iQ Supermix (2X; Biorad). For reference genes using SYBR Green chemistry (i.e. SuDH, TUB and YWHAZ), total reaction volumes of 25µL were used with similar reaction components. The only notable difference is that no probe volume was required and 5µL of nuclease-free water was added to make up a 25µL total reaction volume and iQ SYBR Green Supermix (Biorad) was used in place of iQ Supermix.

3.2.6.2 Primer Concentration Optimization

With the utilization of optimized annealing temperatures and the same reaction components as were employed for the annealing temperature optimization, primer concentration optimization reactions were conducted for reference genes. A 1/10

dilution of pooled cDNA (2.87ng/μL) was used as template for all primer concentration optimization reactions that were run in triplicate for each of the following forward and reverse primer pair concentration combinations (F/R): 3μM/6μM, 3μM/9μM, 6μM/3μM, 6μM/6μM, 6μM/9μM, 9μM/3μM, 9μM/6μM and 9μM/9μM.

3.2.6.3 Dynamic Linear Range (DLR) and Reference Gene Amplification Efficiency Determination (E)

Standard curves covering just less than five orders of magnitude were produced from a series of seven serial dilutions and used to determine reference gene-specific dynamic linear ranges (DLR) and amplification efficiency (E)-values.

Pooled cDNA of a known concentration (30.0ng/μL) was serially diluted 1:4 with nuclease-free water producing the following cDNA template dilutions: 1/5, 1/25, 1/125, 1/625, 1/3125, 1/15625 and 1/78125. Optimal annealing temperatures and primer concentrations were used in addition to the previously detailed qPCR protocol and qPCR reaction components. Standard curves were run in triplicate. Logarithmically transformed cDNA concentrations were plotted against their associated Cq (cycle of quantification) values. R^2 of the plot and the standard deviation for dilution replicates were assessed and appropriate replicates and/or dilutions were excluded from the standard curve. No standard dilution was retained within the dilution series where a more concentrated standard had been excluded or whose technical replicate standard deviation exceeded 0.5, a threshold recommended by Nolan *et al.,* (2006). All Cq values for the DLR were between 10-35 and R^2 values were no less than 0.990. The DLR was

determined to be all cDNA input amounts that remained within the standard curve after assessment criteria were applied.

When logarithmically transformed cDNA concentrations are plotted against their associated Cq values, the slope of the plot holds the following relationship to a gene's amplification efficiency (E): $E = 10^{[-1/slope]}$ (Pfaffl, 2001). All reference gene E-values were calculated by applying the above equation to standard curves after assessment criteria were applied. As suggested within the MIQE guidelines, accepted E-values were those between 90-105% (Bustin *et al.,* 2009).

3.2.7 qPCR Dataset Reactions and Sample Analysis

Optimal annealing temperatures and primer concentrations were utilized, in addition to previously stated qPCR protocols and reaction components, to assess the gene expression of a total of eighty biological replicates - eight biological replicates from 10 sampling weeks (i.e. treatments). Each biological replicate had two associated technical replicates. Biological replicates whose technical replicate standard deviation exceeded 0.5 (Nolan *et al.,* 2006), were excluded from the dataset. Biological replicates for each reference gene were spread across two plates and in addition, each plate contained no less than three no-template control replicates and six inter-plate calibrator replicates. Pooled reverse transcription no-amplification controls were run in duplicate. After both plates for a respective reference gene had been run, a gene study file was created using iQ5 software (Biorad).

Due to minute differences in plate plastics, run ramp times or run temperatures, a comparison of Cq values obtained from multiple runs should not occur without plate

calibration. iQ5 software (Biorad) makes use of a specialized algorithm that inputs Cq values associated with a sample present on multiple plates, known as an inter-plate calibrator, to merge multiple plate output files into one file. This one file, or gene study, possesses calibrated Cq values for all samples from all plates as though they had all been collected from the same run.

3.2.8 Assessment of Genomic DNA (gDNA) Contamination

To assess genomic DNA (gDNA) contamination within dataset sample total RNA extractions, and to limit any gDNA contamination contributing to the gene expression values obtained, 1/10 dilutions of these RNA extractions were run on the iQ5. The protocol, annealing temperatures, primer concentrations, reaction components and plate composition used for qPCR of the eighty dataset samples were identical, with the exception of dataset sample RNA serving as a nucleic acid template, versus dataset sample cDNA. Primers and probes designed for actin (ACT) were used and a gene study composed of two ACT runs for dataset sample cDNA and two ACT runs for dataset sample RNA were made. Cq values were compared within biological replicates between RNA and cDNA runs. As suggested elsewhere, biological replicates with ΔCq values less than 5 – corresponding to a gDNA composition within RNA extractions of more than 3.125% - were eliminated from the study (Nolan *et al.,* 2006).

3.2.9 Reference Gene Expression Stability Determination

In order to assess reference gene expression stability, Cq values for biological replicates were converted into relative quantities (Q). For each reference gene, Cq values for respective biological replicates were subtracted from the minimum Cq value

obtained for all treatments within that reference gene, producing a ΔCq value. Using previously determined E-values, relative quantities were obtained from the following formula: $Q = E_{Ref}^{\Delta Cq}$. Biological replicates that did not possess Cq values for all seven reference genes evaluated were excluded from the study. Relative quantities were entered into geNorm with the suggested pair-wise variation cut-off of 0.15 being employed (Vandesompelle *et al.,* 2002). geNorm analysis was conducted determining both overall treatment and within treatments reference gene expression stability rankings.

3.3 Results

3.3.1 Primer Design and Specificity Validation

Primers and hydrolysis probes for seven commonly used reference genes (Scharlaken *et al.,* 2008; Van Hiel *et al.,* 2009; Wang *et al.,* 2008) were designed (Table 3.1 and 3.2) and validated prior to gene expression evaluation via RT-qPCR methods.

Table 3.1. Primer sequence and properties used in evaluation of seven candidate RT-qPCR reference genes employed to investigate seasonal cold tolerance in *D. ponderosae*.

Reference Gene		Sequence (5'-3')	% GC	T_A	Amplicon Size (bp)	E	DLR	R^2
RPII	RNA polymerase II	GACGTTGGAGCAGTTCAAAGAG	50	57.9	125	103.9	24pg – 75ng	0.997
		GGAAGAACACGAACATCTGGTC	50	57.9				
PBD	Porphobilinogen deaminase	GGCTTCAATGTGTGTCCAGTG	52.3	56.07	135	100.1	5pg – 75ng	0.993
		CACCAAACCAACGAAAAGATGTTC	41.6	56.07				
ACT	Actin	AAATTTTAACCGAACGTGGATATTC	32	56.07	110	92.8	0.96ng – 75ng	0.998
		CATCTCCTGTTCAAAGTCCAGAG	47.8	56.07				
TUB *	α-Tubulin	ACAATGAGGCTATTTACGATA	33.3	59.77	103	103.4	0.96ng – 75ng	0.999
		GTGATTGACGAGACGATT	44.4	59.77				
TBP	TATA-box binding protein	GCATCAGCCAGAAGAGGATCAAC	52.1	57.37	100	92.7	120pg – 75ng	0.998
		GGGAGCCAATGGAGGAACTTG	57.1	57.37				
YWHAZ *	Tyrosine 3-monooxygenase	GATGATGCCATTGCTGAG	50	59.77	108	102.0	5pg – 75ng	0.999
		TGTATCACTGGTCCATAACG	45	59.77				
SuDH *	Succinate dehydrogenase	AGAGCCAATTCCAGTAAT	38.8	56.12	102	99.0	5pg – 75ng	0.995
		ACTTTGTCTTCGTTGTTG	38.8	56.12				

*Quantification conducted using SYBR Green Chemistry

Table 3.2. Hydrolysis probe sequence used in evaluation of four candidate RT-qPCR reference genes employed to investigate seasonal cold tolerance in *D. ponderosae*.

Gene		Probe sequence (5'-3')
RPII	RNA polymerase II	56-JOEN-CGGCAAACCCAGCGAGAAGAGGC-3BHQ_1
PBD	Porphobilinogen deaminase	56-JOEN-CGCCAATCTTATCACCGTTGCCG-3BHQ_1
ACT	Actin	56-JOEN-TCACCACCACTGCCGAAAGGGAA-3BHQ_1
TBP	TATA-box binding protein	56-JOEN-CAACAACAACAGCAGCAGCAACAGC-3BHQ_1

Specificity of each primer pair was first assessed via agarose gel visualization (Figure 3.1 is an example of such a gel for succinate dehydrogenase). For all primer pairs used in reference gene evaluation via RT-qPCR, a single band of expected amplicon size was obtained. Amplicon composition was confirmed via sequencing. Where single bands were produced by multiple reaction conditions (i.e. $MgCl_2$ or annealing temperature) the reaction conditions producing the most intense amplicon band was selected as optimal for sequencing. Sequencing results for amplicons were compared to sequence information for contigs identified from TRIA EST database as potential reference gene sequences. Primers were assumed to be specific for a particular gene when sequencing results for the product matched expected contig segments for that gene. Complementarity of hydrolysis probes was also assessed through similar sequence comparisons.

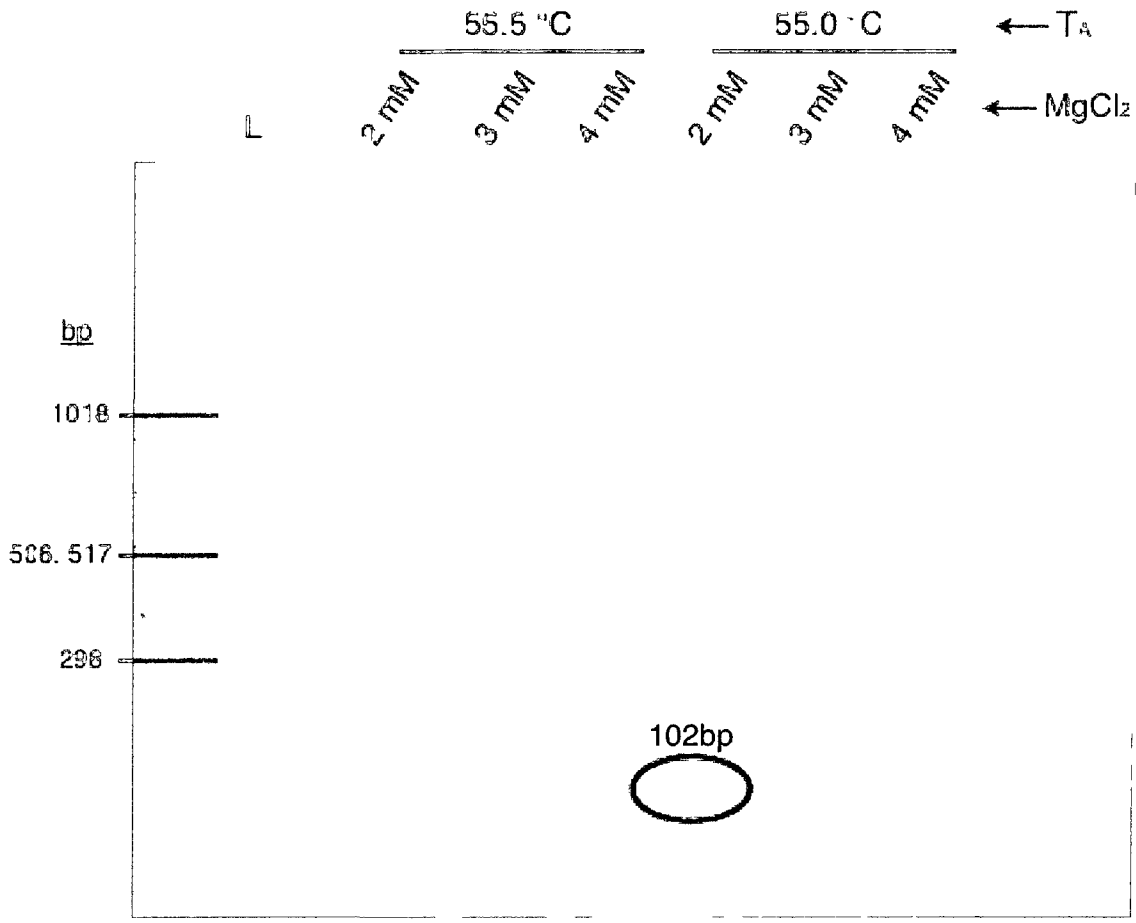

Figure 3.1. Agarose gel (1.5%) run for 1 hour showing PCR product for succinate dehydrogenase (SuDH) optimized at three different magnesium chloride concentrations and two annealing temperatures. Note SuDH primers produced a single, amplicon-specific band of expected base pair size as determined by sequencing results (Table 3.1).

3.3.2 RT-qPCR Reaction Optimization

Optimal annealing temperatures (Table 3.1) were determined to be the highest gradient temperatures found to produce the lowest, most consistent Cq values, as indicated by low technical replicate standard deviation. For reference genes utilizing SYBR Green chemistry, melt curves exhibited no evidence of non-specific binding or primer dimers at optimal primer concentrations. Optimal annealing temperatures ranged from 56.07°C for PBD and ACT to 59.77°C for YWHAZ and TUB (Table 3.1). Optimal annealing temperatures as determined using RT-qPCR with a thermal gradient option were found to be consistently different from those determined by conventional PCR methods, differing as much as 2.5°C in the case of RPII's primer set (data not shown).

Optimal primer concentrations were determined to be the lowest concentrations found to produce the lowest, most consistent Cq values, as indicated by low technical replicate standard deviation. All primer concentrations were determined to be optimal at 9μM with the exception of TUB's reverse primer, which was found to perform optimally at 6μM (data not shown).

3.3.3 Dynamic Linear Range (DLR) and Reference Gene Amplification Efficiency Determination (E)

Standard curves successfully spanned no less than 2.80 log concentrations to a maximum of 4.89 log concentrations, corresponding to DLRs of between 0.96pg and 75ng of cDNA template (Table 3.1). In the case of ACT, the DLR for RT-qPCR purposes was found to be sensitive at as little as 0.96pg of cDNA template (Figure 3.2). Coefficient of determination (R^2) values for standard curves ranged from 0.993 to 0.999

(Table 3.1) and gene amplification efficiency (E)-values varied from 92.8% to 103.9%. No E-value or DLR differentiation was apparent between genes when using hydrolysis probes versus using SYBR Green chemistry (Table 3.1).

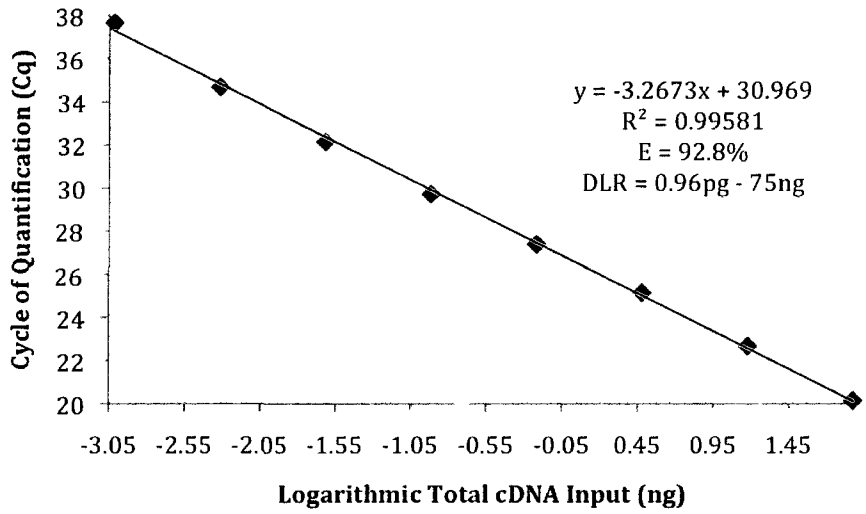

Figure 3.2. Standard curve produced for Actin (ACT) by use of serial dilution. Concentration of pooled cDNA template was quantified by fluorometry and total cDNA input for RT-qPCR reactions calculated for each serial (1/5) dilution. Dilutions possessing standard deviations greater than 0.5 for technical replicates were eliminated from the standard curve (Applied Biosystems, 2008).

3.3.4 geNorm Input and Output

RT-qPCR methods were applied to 80 *D. ponderosae* biological replicates, of which 62 were determined appropriate for further geNorm analysis. Five *D. ponderosae* biological replicates, four collected in the fall of 2008 and one collected in the spring of 2009, were excluded when results for RNA extracts differed by less than five Cq values from their respective cDNA values, possibly indicating gDNA contamination, assessed via RT-qPCR with ACT primers. An additional, thirteen *D. ponderosae* biological replicates, five collected in the fall of 2008 and eight collected in the spring of 2009, were excluded due to standard deviations for technical replicates being greater than 0.5. Treatment groups were composed of five to eight *D. ponderosae* biological replicates, with the exception of the 14 November, 2008 treatment group, which consisted of three *D. ponderosae* biological replicates.

Considerable variation between treatment groups was found via geNorm analysis with respect to reference gene stability ranks (Table 3.3 and Table 3.4). All candidate reference genes occupied one of the top two stability rank positions for a least one treatment group, with the exception of TUB, which was consistently found to be the least stable reference gene evaluated for all treatment groups. For most treatment groups ACT, YWHAZ, RPII, and PBD, regularly clustered among the top four stability ranks, with SuDH, TBP, and TUB, frequently clustered among the bottom three stability ranks. These two expression stability clade designations are consistent with results returned for the rankings found for the dataset composed of biological replicates from all treatment groups

Table 3.3. Candidate reference genes for normalization of GOIs associated with seasonal cold tolerance in *D. ponderosae* listed according to their respective stability as determined by geNorm. An overall stability ranking including all study treatments was produced. Rankings were further differentiated by treatment, as defined by the collection date during Fall 2008 period of study. Bold-faced type indicates the number of reference genes required to achieve a pair-wise variation just below or closest to 0.15 and the number of *D. ponderosae* biological replicates composing a treatment group are reported.

Stability Rank	19 Sept, 2008 – 13 May, 2009	19 Sept., 2008	3 Oct., 2008	17 Oct., 2008	31 Oct., 2008	14 Nov., 2008
1/2	**ACT/ YWHAZ**	**RPII/ SuDH**	**TBP/ YWHAZ**	**ACT/ YWHAZ**	**RPII/ PBD**	**RPII/ YWHAZ**
3	**RPII**	PBD	RPII	RPII	YWHAZ	**ACT**
4	**PBD**	ACT	PBD	SuDH	TBP	PBD
5	SuDH	YWHAZ	ACT	TBP	ACT	TBP
6	TBP	TBP	SuDH	PBD	SuDH	SuDH
7	TUB	TUB	TUB	TUB	TUB	TUB
Number of biological replicates (n)	62	6	7	5	5	3

Table 3.4. Candidate reference genes for normalization of GOIs associated with seasonal cold tolerance in *D. ponderosae* listed according to their respective stability as determined by geNorm. Rankings differentiated by treatment, as defined by the collection date during Spring 2009 period of study. Bold-faced type indicates the number of reference genes required to achieve a pair-wise variation just below or closest to 0.15 and the number of *D. ponderosae* biological replicates composing a treatment group are reported.

Stability Rank	18 March, 2009	1 April, 2009	14 April, 2009	29 April, 2009	13 May, 2009
1/2	**SuDH/ YWHAZ**	**SuDH / TBP**	**RPII/ TBP**	**ACT/ YWHAZ**	**ACT/ YWHAZ**
3	PBD	PBD	YWHAZ	RPII	**RPII**
4	RPII	ACT	PBD	PBD	**PBD**
5	TBP	YWHAZ	SuDH	TBP	**SuDH**
6	ACT	RPII	ACT	SuDH	TBP
7	TUB	TUB	TUB	TUB	TUB
Number of biological replicates (n)	7	6	7	7	7

Within most treatments, the number of reference genes required to achieve a pair-wise variation just below or closest to 0.15 (Vandesompele *et al.,* 2002) was two, as indicated by bold-faced type in Table 3.3 and 3.4. geNorm analysis indicated that the 14 November, 2008 treatment group was most stable with the addition of a third reference gene, where five reference genes were returned for the 13 May, 2009 treatment group. Overall, for the dataset composed of biological replicates from all treatment groups, four reference genes were required to achieve a pair-wise variation below 0.15 (Figure 3.3).

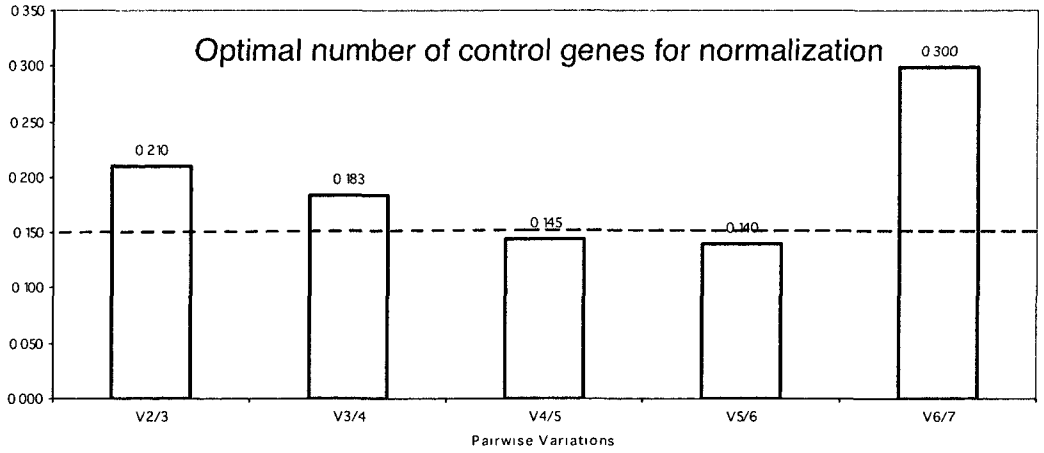

Figure 3.3. geNorm pair-wise variation analysis using forward addition to determine the optimal number of reference genes required to contribute to a normalization factor. For the dataset composed of *D. ponderosae* biological replicates from all treatment groups (n=62), four reference genes were required to achieve a pair-wise variation below 0.15. Accurate normalization of GOIs associated with seasonal cold tolerance in *D. ponderosae* is therefore best achieved from a normalization factor made up of ACT, YWHAZ, RPII, and PBD expression data (Table 3.2).

3.4 Discussion

Reference genes are used to account for sample-to-sample variation of GOI expression levels determined via RT-qPCR (Scharlaken *et al.,* 2008). While it is exceedingly common to use a single reference gene for normalization purposes (Suzuki *et al.,* 2000), a growing body of evidence indicates that universally applicable reference genes for all tissue and treatment types do not exist (Vandesomepelle *et al.,* 2002). Furthermore, studies show that GOI expression results can produce statistically significant differences when normalized to a single reference gene versus a combination of stably expressed reference genes (Piehler *et al.,* 2010). Inappropriate reference gene selection is therefore a significant liability for expression studies and warrants a thoughtful selection, evaluation, and justification of reference genes employed prior to submission for publication (Bustin *et al.,* 2009).

In this study, I evaluated the expression stability of seven candidate reference genes – ACT, PBD, RPII, SuDH, TBP, TUB and YWHAZ - to determine the optimal number and choice of reference genes required to accurately normalize expression of GOIs associated with seasonal cold tolerance in *D. ponderosae.*

In advance of obtaining expression data for candidate reference genes, considerable time and effort was expended optimizing RT-qPCR reaction conditions, specifically annealing temperatures, primer concentrations and gene amplification efficiency (E). An assessment of optimization efforts reveals that experiments involving the optimization of annealing temperatures and determination of gene specific E-values were wisely invested. However, experiments in which optimal primer concentrations

were assessed appeared to produce negligible improvements on RT-qPCR results obtained to achieve study objectives.

Optimal annealing temperatures as determined using RT-qPCR with a thermal gradient option were found to be consistently different from those determined by conventional PCR methods, differing as much as 2.5°C in the case of RPII's primer set (data not shown). Annealing temperature optimization experiments via both RT-qPCR and conventional PCR methods failed to produce amplicons at several temperatures exceeding optimal annealing temperatures whereas non-specific amplification and primer-dimer formation occurred at temperatures below optimal annealing temperatures (data not shown). Some annealing temperatures tested via conventional PCR methods, that failed to produce amplicons, were found to be the most optimal when assessed via RT-qPCR, indicating evidence of machine-specific amplification protocols. Lack of amplicon production due to annealing temperatures being too high for adequate primer annealing would under-represent reference gene expression levels and misrepresent expression stability relative to other reference genes. Primer-dimer formation or non-specific amplification due to depressed annealing temperatures would over-represent reference gene expression levels also misrepresenting relative expression stability. Because I took steps to address these potential pit-falls, it is possible to have more confidence in the gene expression stability results this study has produced for *D. ponderosae* under the treatments investigated.

By use of standard curves, reference gene-specific E-values were found to range from 92.7% for TBP to 103.9%, for RPII, an 11.2% difference, with coefficient of determination (R^2) values varying from 0.995 to 0.999 (Table 3.1). A theoretical

difference in an E-value of only 5% (i.e. $1.95^{-\Delta\Delta Cq}$ or $2.05^{-\Delta\Delta Cq}$) can generate GOI false fold change values of 242% when using a classical delta-delta-Ct (ΔΔCt) method (Livak and Schmittgen, 2001) of RT-qPCR analysis; artificial fold changes reach 1744% for a difference in an E-value of 10% (Pfaffl, 2006). When comparing GOI expression values normalized to TBP versus RPII using a single reference gene method, expression fold change values could differ in excess of three orders of magnitude using ΔΔCt method of analysis. By determining each reference gene's E-value and applying it within an efficiency correction method of analysis that geometrically averages multiple internal control genes (Vandesomepelle *et al.,* 2002), GOI gene expression values obtained via RT-qPCR can significantly limit both Type I and II error within measured fold changes. Using standard curves to obtain DLRs assured that determined E-values could be used to explain the quantitative relationship between the amount of input cDNA a qPCR reaction initiates with and the amount of PCR product produced at any given cycle within the exponential phase of a PCR reaction (Nolan *et al.*, 2006). Using the DLR, scarce amounts of biological replicate genetic material could be conserved over thousands of reactions. From a simple analysis of the Cq values produced from standard curves, it was determined that all RNA extractions corresponding to biological replicates for all treatment groups could be diluted tenfold, effectively increasing the number of GOIs potentially investigated by an order of magnitude. One can conclude that this study's yields were increased significantly though the determination of E and DLR.

Where considerable effort was applied to optimize primer concentrations for each reference gene, negligible improvements on RT-qPCR results were produced. All primer concentrations were determined to be optimal at the highest primer concentration,

9μM, with the exception of TUB's reverse primer, which was found to perform optimally at 6μM (data not shown). Furthermore, the Cq value produced for TUB at a reverse primer concentration of 9μM was marginally higher than that tested at 6μM, providing little justification to use the more dilute primer concentration. It would therefore be advisable to exclude unnecessary experiments designed to optimize primer concentration for investigation of GOIs associated with seasonal cold tolerance in *D. ponderosae*. TUB, a frequently used reference gene for RT-qPCR normalization, was consistently found to possess the least stable expression level for all treatment groups. While considerable variation was found between treatment groups with respect to reference gene stability ranks (Table 3.3 and Table 3.4), two general stability clades were identified. For most treatment groups ACT, YWHAZ, RPII and PBD - the most stable clade and not coincidentally genes identified as most appropriate to normalize expression studies composed of biological replicates from all treatments - regularly clustered among the top four stability ranks. SuDH, TBP and TUB - the least stable clade - frequently clustered among the bottom three stability ranks. Only the September 19, 2008 and April 01, 2009 treatment groups returned geNorm results where ACT and YWHAZ, the two highest ranked reference genes found for the dataset composed of biological replicates from all treatment groups, were absent from the top three ranks; a proxy measure of increased expression stability rank variation. These results could in part be explained by differences in developmental-specific reference gene expression stability.

Synchrony refers to a coordination of development and sexual maturation within a population over a similar time period (Powell and Logan, 2005). Within an

evolutionary context, decreased fecundity associated with asynchrony is a selective pressure for adaptations or mechanisms that cause cohorts to remain within coincident life stages. When measuring *D. ponderosae* development at seven different constant temperatures Amman and Cole (1983) distinguished individual developmental rates among larval instars. It was observed that at lower temperatures, first and second instars were able to develop at a "moderately fast" rate compared to third and fourth instars. It was concluded that progressively higher temperature thresholds were required for successive instar development to occur. In similar controlled constant-temperature rearing experiments using eleven temperatures regimes Bentz *et al.* (1991) produced results indicating that late developmental stages of *D. ponderosae* had higher temperature thresholds than did early developmental stages. The findings of these two studies indicate a potential thermal mechanism by which *D. ponderosae* achieve life stage synchrony.

The treatment groups for this study were composed of *D. ponderosae* biological replicates of undetermined instar. Temperature data collected at the sample site (data not shown) indicate a substantial decrease in mean daily temperatures initiated in early October of 2008, after biological replicates for the 19 September, 2008 treatment were obtained but prior to the 3 October, 2008 treatment collection date (Figure 3.4). During the spring of 2009, the only mean daily temperature recorded below 0°C coincided with the 18 March, 2008 treatment group biological replicate collection date. All subsequent treatment group collection dates occurred while mean temperatures were above 0°C. Seasonal variation in temperature provides a natural thermal cline for *D. ponderosae* development. When this *in vivo* thermal cline is applied to the progressive system of

developmental thresholds found for *D. ponderosae* (Amman and Cole, 1983; Bentz *et al.*, 1991), specifically between 19 September and 3 October, 2008, a movement away from developmental variation towards a state of synchrony occurs (Figure 3.4).

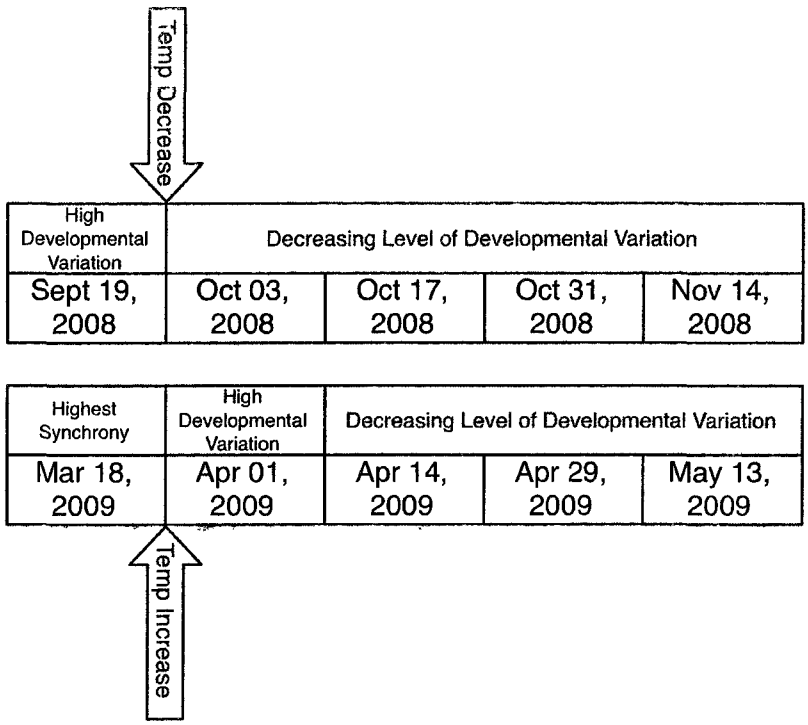

Figure 3.4 Developmental variation illustrated as a mechanism explaining expression stability rank variation for 19 September, 2008 and 1 April, 2009 treatment groups.

Conversely, when thermal clines are removed, specifically between 18 March, 2009 and 1 April, 2009, the developmental gradient shifts from a point of general synchrony towards increased developmental variation, which would decrease as more individuals become sexually mature over time. Within the context of a developmental gradient, the points of highest expected developmental variation would occur on 19 September, 2008 and 1 April, 2009. These two treatment groups contained the greatest amount of variation in expression stability rank, which would be understandable if the biological replicates making up each of those respective treatments contained a greater range of larval instars (i.e. developmental variation). Considerable evidence indicates that reference gene expression can vary between developmental stages (McCurley and Callard, 2008; Fernandes *et al.,* 2008; Van Hiel *et al.,* 2009; Garg *et al.*, 2010).

3.5 Conclusion

While considerable treatment-to-treatment variation was detected, this study's results indicate accurate normalization of GOIs associated with seasonal cold tolerance in *D. ponderosae* is best achieved from a normalization factor made up of ACT, YWHAZ, RPII and PBD expression data. Periods of synchrony and of increased development were used to explain treatments returning the greatest amount of expression stability rank variation. This study serves as an informational resource for future RT-qPCR studies, within the field of entomology and beyond, proving the necessity of evaluating reference genes prior to normalization of GOI expression.

3.6 Bibliography

Amman, G.,D., and Cole, W.E. (1983). Mountain pine beetle dynamics in lodgepole pine forests. Part II: population dynamics. USDA Forest Service, Intermountain Forest and Range Experiment Station, General Technical Report INT-145. pp. 20.

Applied Biosystems. (2008). Real-time PCR: understanding CT. Application Note (136AP01-01), pp. 1-6.

Benn, C., Fox, H., and Bates, G.P. (2008). Optimization of region-specific reference gene selection and relative gene expression analysis methods for pre-clinical trials of Huntington's disease. *Molecular Neurodegeneration*_17(3): 17.

Bentz, B.J., Logan, J.A., and Amman, G.D. (1991). Temperature-dependent development of the mountain pine beetle (Coleoptera: Scolytidae) and simulation of its penology. *Canadian Entomologist* 123(5): 1083-1094.

Bustin, S.A., Benes, V., Garson, J.A, Hellemans, J., Hugget, J., Kubista, M., Mueller, R., Nolan, T., Pfaffl, M.W., Shipley G.L., Vandesompele, J., and Wittwer, C.T. (2009). The MIQE guidelines: minimum information for publication of quantitative real-time PCR experiments. *Clinical Chemistry* 55(4): 611-622.

de Boer, M.E., de Boer, T.E., Marien, J., Timmermans, M.J.T.N., Nota, B., van Straalen, N.M., Ellers, J., and Roelofs, D. (2009). Reference genes for QRT-PCR tested under various stress conditions in *Folsomia candida* and *Orchesella cincta* (Insecta, Collembola). *BMC Molecular Biology* 10:54

Fernandes, J.M.O., Mommens, M., Hagen, O., Babiak, I., and Solberg, C. (2008). Selection of suitable reference genes for real-time PCR studies of Atlantic halibut development. *Comparative Biochemistry and Physiology, Part B* 150: 23-32.

Garg, R., Sahoo, A., Tyagi, A.K., and Jain, M. (2010). Validation of internal control genes for quantitative gene expression studies in chickpea (*Cicer arietinum* L.). *Biochemical and Biophysical Research Communications* 396: 283-288.

Grinzinger, G. (2002). Gene quantification using real-time quantitative PCR: an emerging technology hits the mainstream. *Experimental Hematology* 30: 503-512.

Kubista, M., Andrade, J.M., Bengtsson, M., Forootan, A., Jonak, J., Lind, K., Sindelka, R., Sjoback, R., Sjogreen, B., Strombom, L., Stahlberg, A., and Zoric, N. (2006). The real-time polymerase chain reaction *Molecular Aspects of Medicine* 27:95-125.

Lee, P., Sladek, R., Greenwood, C.M.T, and Hudson, T.J. (2002). Control genes and variability: absence of ubiquitous reference transcripts in diverse mammalian expression studies. *Genome Research* 12: 292-297.

Livak, K.J., and Schmittgen, T.D. (2001). Analysis of relative gene expression data using real-time quantitative PCR and the $2^{-\Delta\Delta Ct}$ method. *Methods* 25: 402-408.

Lord, J.C., Hartzer, K., Toutges, M., and Oppert, B. (2010). Evaluation of quantitative PCR reference genes for gene expression studies in *Tribolium castaneum* after fungal challenge. *Journal of Microbiological Methods* 80: 219-221.

McCurley, A.T., and Callard, G.V. (2008). Characterization of housekeeping genes in zebrafish: male-female differences and effects of tissue type, developmental stage and chemical treatment. *BMC Molecular Biology* 9: 12.

Nolan, T., Hands, R.E., and Bustin, S.A. (2006). Quantification of mRNA using real-time RT-PCR. *Nature Protocols* 1(3): 1559-1582.

Pfaffl, M.W. (2001). A new mathematical model for relative quantification in real-time RT-PCR. *Nucleic Acids Research* 29(9): 2000-2007.

Piehler A.P., Grimholt, R.M., Ovstebo, R., and Berg, J.P. (2010). Gene expression results in lipopolysaccharide-stimulated monocytes depend significantly on the choice of reference genes. *BMC Immunology* 11: 21.

Powell, J.A., and Logan, J.A. (2005). Insect seasonality: circle map analysis of temperature-driven life cycles. *Theoretical Population Biology* 67:161-179.

Scharlaken, B., de Graaf, D.C., Goossens, K., Brunain, M., Peelman, L.J., and Jacobs, F.J. (2008). Reference gene selection for insect expression studies using quantitative real-time PCR: the head of the honeybee, *Apis mellifera,* after a bacterial challenge. *Journal of Insect Science* 8(33):10.

Suzuki, T., Higgins, P.J., and Crawford, D.R. (2000). Control selection for RNA quantitation. *Biotechniques* 29: 332-337.

Thellin, O., Zorzi, W., Lakaye, B., De Borman, B., Coumans, B., Hennen, G., Grisar, T., Igout, A., and Heinen, E. (1999). Housekeeping genes as internal standards: use and limits. *Journal of Biotechnology* 75: 291-295.

Thorrez, L., Van Deun, K., Tranchevent, L.C., Van Lommel, L., Engelen, K., Marchal, K., Moreau, Y., Van Mechelen, I., and Schuit, F. (2008). Using ribosomal protein genes as reference: a tale of caution. *PLoS ONE* 3(3): e1854.

Vandesompele, J., De Preter, K., Pattyn, F., Poppe, B., Van Roy, N., De Paepe, A., and Speleman, F. (2002). Accuarate normalization of real-time quantitative RT-PCR data by geometric averaging of multiple internal control genes. *Genome Biology* 3(7): research0034.I-0034.II.

Van Hiel, M.B., Wielendaele, P.V., Temmerman, L., Van Soest, S., Vuerinckx, K., Huybrechts, R., Vanden Broeck, J., and Simonet, G. (2009). Identification and validation of housekeeping genes in brains of the desert locust *Schistocerca gregaria* under different developmental conditions *BMC Molecular Biology* 10:56.

Wang, G., Xia, Q., Cheng, D., Duan, J., Zhao, P., Chen, J., and Zhu, Li. (2008). Reference genes identified in the silkworm *Bombyx mori* during metamorphism based on oligonucleotide microarray and confirmed by qRT-PCR. *Insect Science* 15(5):405-413.

Seasonal Transcript Accumulation of Glycerol Biosynthetic Genes in *Dendroctonus ponderosae*

4.1 Introduction

During the winter months in the BC Interior, *Dendroctonus ponderosae* Hopkins, the mountain pine beetle, must endure prolonged exposure to sub-zero temperatures. Within host trees, these cold temperatures are often cited as the largest single source of mountain pine beetle mortality (Safranyik 1978; Cole 1981; Safranyik and Carroll, 2002; Stahl *et al.,* 2006; Aukema *et al.,* 2008). While fall and winter temperatures regularly reach far below the equilibrium freezing point of mountain pine beetle bodily fluids, damaging effects of ice formation within biological tissues of the mountain pine beetle are routinely circumvented. By employing the physiological adaptation of quiescence (Powell and Logan, 2005), well documented in other insects, overwintering mountain pine beetle larvae can reallocate limited stored energy reserves from use in maintaining development and basal metabolism toward biochemical mechanisms that provide the insect with an ability to potentially survive very cold winter temperatures (Li *et al.,* 2002; Joanisse and Storey, 1994b).

Cold tolerance refers to a range of biochemical and physiological mechanisms insects employ to endure temperatures below the equilibrium freezing point of their bodily fluids (Storey, 2004; pp473). The primary distinction between two major categories of cold tolerance - freeze tolerance and freeze avoidance - is made on the basis of whether or not ice formation results within intracellular bodily fluids (Danks, 2006). Freeze tolerant insects maintain adequate cell osmolarity and prevent the damaging effects of intracellular ice formation by inducing controlled ice nucleation

within extracellular spaces (Duman, 2001). Freeze avoidant insects evade cold mortality by producing cryoprotectants, often polyols, that alter the freezing properties of their bodily fluids (Bale, 2002; Baust, 1983), and in some documented cases, enhance the supercooling ability of antifreeze proteins (Li *et al.,* 1998).

Glycerol is the most common cryoprotectant used by insects to achieve states of freeze avoidance (Storey, 2004; pp 481). The production of glycerol as cryoprotectant can in part be explained by the relative ease and diverse ways in which it can be produced and accumulated via pre-existing metabolic pathways (Figure 4.1).

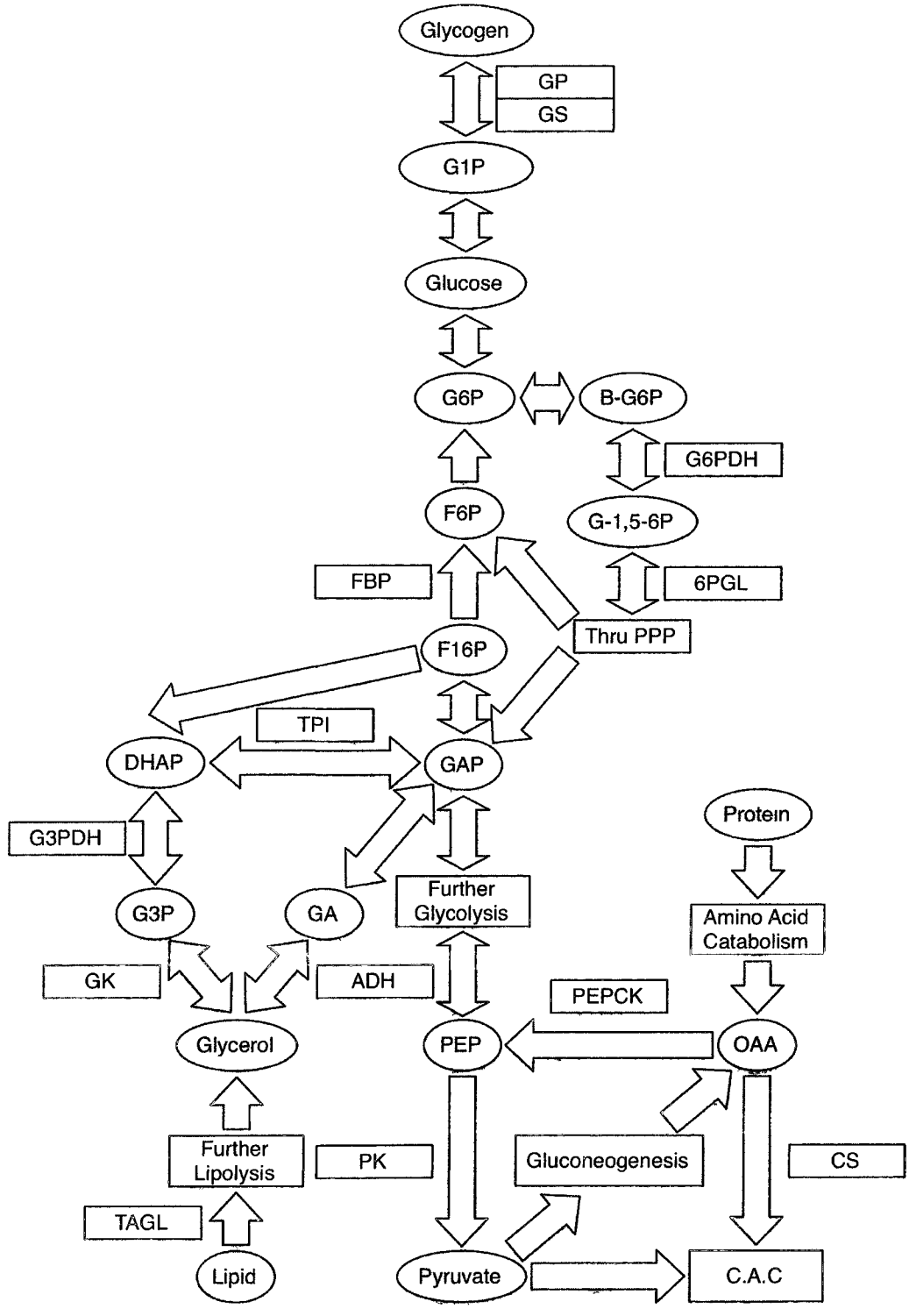
Glycogen
GP
GS
G1P
Glucose
G6P
B-G6P
G6PDH
F6P
G-1,5-6P
FBP
6PGL
Thru PPP
F16P
TPI
DHAP
GAP
G3PDH
Protein
Amino Acid Catabolism
Further Glycolysis
G3P
GA
GK
ADH
PEPCK
Glycerol
PEP
OAA
Further Lipolysis
PK
Gluconeogenesis
CS
TAGL
Lipid
Pyruvate
C.A.C

Figure 4.1 – Pre-existing Mechanisms Involved in Glycerol Biosynthesis. The processes of glycogenesis, glycogenolysis, and the production of glycerol involve the following enzymes: glycogen phosphorylase (GP); triosephosphate isomerase (TPI); glycerol-3-phosphate dehydrogenase (G3PDH); glycerol kinase (GK); alcohol dehydrogenase (ADH); glycogen synthase (GS). The metabolism of lipids, specifically triglycerides, produces glycerol and occurs via triacylglycerol lipase (TAGL). Reducing equivalents required in the production of glycerol can be produced via the pentose phosphate pathway (PPP), involving the enzymes 6-phosphoglucolactonase (6-PGL) and glucose-6-phosphate dehydrogenase (G6PDH). The enzyme citrate synthase (CS) is involved in the citric acid cycle (CAC) and gluconeogenic enzymes include phosphoenolpyruvate carboxykinase (PEPCK) and fructose-1,6-bisphosphatase (FBP). Pyruvate kinase (PK) is an enzyme present within the lower-half of glycolysis. The following substrates are involved in the above processes: glucose-1-phosphate (G1P), glucose-6-phosphate (G6P), β-glucose-6-phosphate (β-G6P), glucono-1,5-lactone 6-phosphate (G-1,5-6P), fructose-6-phosphate (F6P), fructose-1,6-bisphosphtate (F16P), dihydroxyacetone phosphate (DHAP), glycerol-3-phosphate (G3P), glyceraldehyde-3-phosphate (GAP), glyceraldehyde (GA), phosphoenolpyruvate (PEP) and oxaloacetate (OAA).

When exposed to seasonally cold temperatures, mountain pine beetle larvae cease feeding and void their gut to remove potential ice nucleating agents (Regniere and Bentz, 2007). While existing in a state of hypo-nutrition and quiescence during the winter, the mountain pine beetle must balance the allocation of limited energetic storage molecules between development, basal metabolism and mechanisms that provide the insect with cold tolerant properties. As temporal changes in basal metabolism, the onset of quiescence, and production of glycerol for cryoprotectant purposes are all reflected within the same, or similar, metabolic pathways, it is difficult to attribute changes in mRNA expression within these pathways to a singular source (Delinger and Lee, 1998; Delinger, 2002; Danks, 2006). Despite this complication, the search for the substrate by which glycerol is produced can be narrowed to three major energetic storage molecules: glycogen, lipids and proteins. To understand both the scale and the scope of seasonal glycerol accumulation within the mountain pine beetle via the metabolism of these three substrates, appropriate investigation of the following inter-related processes should also be included within a comprehensive mRNA expression study: lipolysis, amino acid catabolism, gluconeogenesis and the pentose phosphate pathway.

While little work has been done to illuminate mechanisms by which the mountain pine beetle achieves a state of cold tolerance, findings from a study conducted by Bentz and Mullins (1999) suggest that *D. ponderosae* employ a freeze avoidant strategy. An assessment of polyol composition and seasonal quantity within mountain pine beetle hemolymph indicated glycerol is the most abundant cryoprotectant accumulated by overwintering larvae. Despite an absence of statistically significant seasonal differences

in glycerol accumulation, Bentz and Mullins' (1999) data clearly identify glycerol as the most promising candidate for further cryoprotectant study within mountain pine beetle.

Currently the mechanisms by which mountain pine beetle larvae produce glycerol are unknown. Because glycerol is important with respect to cold tolerance physiology in the mountain pine beetle, a better understanding of how glycerol biosynthesis is both seasonally and temporally regulated is therefore of significant ecological importance. One powerful method that can be employed to determine glycerol's reaction mechanisms is through an assessment of mRNA expression via reverse transcription quantitative PCR (RT-qPCR). Gene expression is the process by which cellular instructions stored within cells are converted into functional gene products. By assessing relative changes in an enzyme's mRNA expression, one can make inferences as to the amounts of substrate and product present at given points in time.

The objective of this study was to elucidate mechanisms by which mountain pine beetle seasonally metabolize the cryoprotectant glycerol. By assessing changes in mRNA expression of genes of interest (GOI) within the mountain pine beetle, correlated to glycerol production within other insects, this study aimed to determine: i) which major energetic storage molecule glycerol is metabolized from within the mountain pine beetle; ii) if glycerol is reconverted to the major energetic storage molecule glycogen in the spring; iii) the intermediate substrates involved in glycerol metabolism; iv) how mRNA expression of GOIs within gluconeogenesis, the citric acid cycle and the pentose pathway are augmented while periods of glycerol accumulation occur; and v) potential seasonal and/or thermal cues inducing observed changes in GOI mRNA expression.

4.2 Methods

4.2.1 RT-qPCR and Temperature

Methods used to obtain temperature and optimized RT-qPCR results from seasonally treated biological replicates for the following genes of interest (GOI) are detailed in sections 3.2.1-3.2.8 of Chapter 3: Pyruvate kinase (PK), glycogen phosphorylase (GP), citrate synthase (CS), 6-phosphoglucolactonase (6-PGL), glucose-6-phosphate dehydrogenase (G6PDH), glycerol-3-phosphate dehydrogenase (G3PDH), fructose-1,6-bisphosphatase (FBP), alcohol dehydrogenase (ADH), triosephosphate isomerase (TPI), phosphoenolpyruvate carboxykinase (PEPCK), glycerol kinase (GK), glycogen synthase (GS) and triacylglycerol lipase (TAGL). Primer sequences and gene-specific properties determined are shown in Table 4.1 and all GOIs used hydrolysis probes using TAMARA, ROX or FAM fluorophores (Table 4.2.).

Table 4 1 Primer sequence and properties used in evaluation of fourteen RT-qPCR genes of interest (GOI) employed to investigate seasonal cold tolerance in *D ponderosae*

	Reference Gene	Sequence (5'-3')	[Primer] nM	% GC	T_A	Amplicon Size (bp)	DLR	E	R^2
PK	Pyruvate Kinase	CTTATCCTTTGGCTATTGCTTTGG	600	41 6	62 5	123	24pg – 75ng	91 5	0 996
		ATCTGTGGTCAGCTTAATAGTATCG	300	40	62 5				
GP	Glycogen phosphorylase	TGGATCAAATGCAGAACGGATTC	600	43 4	63 6	107	5pg – 75ng	94 9	0 999
		GTAATCGGCCAGCAAGAAGAAC	600	50 0	63 6				
CS	Citrate Synthase	GACTTCGATTTGTGACGAGAGAG	600	47 8	63 0	142	12pg – 75ng	93 9	0 999
		CAGACGTATGGAGGCAAACATC	300	50	63 0				
6-PGL	6-phosphoglucolactonase	CCGATTTGATCTACTGCTGCTG	600	50	53 8	108	12pg – 75ng	98 9	0 997
		GTGATTGGAGCCACCCATTTG	900	52 3	53 8				
G6PDH	Glucose-6-phosphate Dehydrogenase	GCAGAAGTAAGAATTCAGTTTGAGG	900	40	62 5	137	5pg – 75ng	100 1	0 995
		GCCATACCAGGAGTTTTCACC	900	52 3	62 5				
G3PDH	Glycerol-3-phosphate Dehydrogenase	TGTTCTGCGAAACCACCATTG	900	47 6	53	126	24pg – 75ng	95 5	0 999
		CGCCGCAAACTTCCACAG	300	61 1	53				
FBP	Fructose-1,6-bisphosphatase	CACAGCTACCGGAGAACTCAC	300	57 1	63 3	139	24pg – 75ng	96 9	0 999
		CACTTCTTCGCCCTGTACATTTG	900	47 8	63 3				
ADH	Alcohol Dehydrogenase	ATCCTCTACACGGCGGTTTG	900	55	63 3	147	12pg – 75ng	90	0 996
		ATCACCTGGCTTCACACTGG	300	55	63 3				
TPI	Triosephosphate Isomerase	ACGCCCCAGCAAGCTCAG	900	66 6	63 3	106	24pg – 75ng	96 3	0 998
		CCGAACCGCCGTATTGGATTC	900	57 1	63 3				
PEPCK	Phosphoenolpyruvate Carboxykinase	GGCATCGAACTCACTGACTCC	600	57 1	63 0	129	5pg 75ng	100	0 995
		GGTGCCGACCGAGTGGAG	300	72 2	63 0				
GK	Glycerol Kinase	GCTATCGACGAGGGTACATCC	900	57 1	62 5	106	24pg – 75ng	93 8	0 993
		CTTGAGGGCATATTTGGGAAAGG	900	47 8	62 5				
GS	Glycogen Synthase	GAACGACCCGGTGCTCAG	300	66 6	57 8	125	24pg – 75ng	92 9	0 996
		CGTAGTCCAGCCCGAAGAG	600	63 1	57 8				
TAGL	Triacylglycerol Lipase	TCTACGTGTATACCTCTCAGAATCG	300	44	63 0	100	24pg – 75ng	92 8	0 999
		GTGTCTCTGTTAGCAGCGAATC	600	50	63 0				

Table 4.2. Hydrolysis probe sequence used in evaluation of fourteen RT-qPCR genes of interest (GOI) employed to investigate seasonal cold tolerance in *D. ponderosae*.

Gene		Probe sequence (5'-3')
PK	Pyruvate kinase	56-TAMN-CAGCAGATCCTCCGCCTTCCAACAA-3BHQ_2
GP	Glycogen phosphorylase	56-ROXN-CAGCCCAAGCAATCCAGACGAGTTC-3BHQ_2
CS	Citrate synthase	56-FAM-CCACAGCAACGAAATAACACCACCA-3BHQ_1
6-PGL	6-phosphoglucolactonase	56-TAMN-ACACCTGCTCTCTGTTTCCTGGACA-3BHQ_2
G6PDH	Glucose-6-phosphate dehydrogenase	56-ROXN-AGCCTCGCCTGGTTGAACTCTAATC-3BHQ_2
G3PDH	Glycerol-3-phosphate Dehydrogenase	56-TAMN-TCATCGTCCACCACCACCACTCG-3BHQ_2
FBP	Fructose-1,6-bisphosphatase	56-ROXN-AGCTACTCAATGCCATCCAGACTGC-3BHQ_2
ADH	Alcohol Dehydrogenase	56-FAM-TCCAACACTCTCGACCACTCCAGC-3BHQ_1
TPI	Triosephosphate Isomerase	56-TAMN-AAGTCCATCAGTCGCTACGCCAGTG-3BHQ_2
PEPCK	Phosphoenolpyruvate Carboxykinase	56-ROXN-TTGACGAACTCCTCCGCCTCTTGC-3BHQ_2
GK	Glycerol Kinase	56-FAM-ACAACCTCTGTAGTGCCAGCCTTGA-3BHQ_1
GS	Glycogen Synthase	56-TAMN-TCTTCAACACCGCCGAGGACCG-3BHQ_2
TAGL	Triacylglycerol Lipase	56-ROXN-ACCCAAATAAGAGCCAGTGACGCCA-3BHQ_2

Three temperature data loggers (iButton, Thermochron) were affixed to each tree from which biological samples were extracted. Data loggers were located either at the base of the tree, at breast height on the north side of the tree and at breast height on the south side of the tree. Temperature data were recorded every 30 minutes throughout the study period. Daily minimum, mean and maximum temperatures were determined and plotted over time in Excel. Due to technical difficulties, seventeen hours of temperature data were lost between 9:36 a.m., 1 April, 2009 and 2:36 a.m., 2 April, 2009. Daily minimum, mean and maximum temperatures for 1 April, 2009 were estimated by averaging daily minimum, mean and maximum temperatures for 31 March, 2009 and 2 April, 2009.

4.2.2 GOI mRNA Expression Determination

GOI transcript accumulation normalization for each biological replicate was achieved from a normalization factor made up of ACT, YWHAZ, RPII and PBD reference gene transcript accumulation data. These four reference genes were previously determined by geNorm analysis in Chapter 3 to be most appropriate for GOI transcript accumulation normalization consisting of biological replicates from all treatment groups.

4.2.3. Graphical and Statistical Analysis

For statistical analysis of each GOI, logarithmically transformed normalized mRNA expression data for biological replicates were analyzed in R (Version 2.9.2). Analysis of variance (ANOVA) assumptions of equal variance and normality were assessed for mRNA expression data. The presence of equal variance was assessed graphically via residual plots and statistically by Levene's test. The presence of normality was assessed graphically by histograms and quantile-quantile plots, and

statistically by the Sahpiro-Francia normality test. One-way ANOVA were conducted for mRNA expression data followed by Tukey's HSD *post-hoc* test for pair-wise multiple comparisons.

For graphical analysis, data normalization was performed as in Willems *et al.* (2008). Geometric mean fold changes for each treatment were set relative to 19 September, 2008 mean mRNA expression level. Relative fold changes and their respective 95% confidence intervals were plotted via Microsoft Excel with statistically significant differences being denoted.

4.3 Results

4.3.1 Primer Design and Specificity Validation

Primers and hydrolysis probes for seven commonly used reference genes were designed (Table 4.1 and 4.2) and validated prior to GOI mRNA expression evaluation via RT-qPCR.

Specificity of each primer pair was first assessed by agarose gel visualization (Figure 4.2 is an example of such a gel for the succinate dehydrogenase product). For all primer pairs used in reference gene evaluation by RT-qPCR, a single band of expected amplicon size was obtained. Amplicon composition was confirmed by sequencing. Where single bands were produced by multiple reaction conditions (i.e. [$MgCl_2$] or annealing temperature) the reaction conditions producing the most intense amplicon band were selected as optimal for sequencing. Sequencing results for amplicons were compared to sequence information for contigs identified from a mountain pine beetle EST database as potential reference gene sequences. Primers were assumed to be specific for a particular gene when sequencing results for the product matched expected contig segments for that gene. Complementarity of hydrolysis probes were also assessed though similar sequence comparisons.

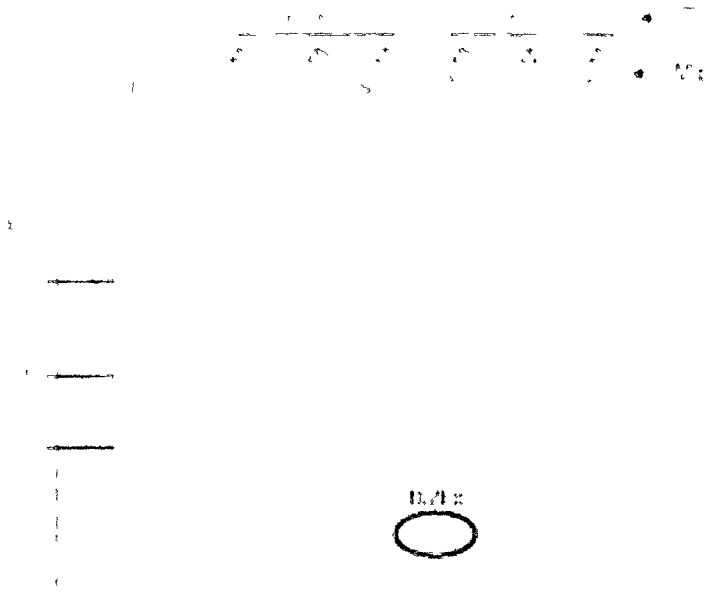

Figure 4.2. Agarose gel (1.5%) run for 1 hour showing PCR product for succinate dehydrogenase (SuDH) optimized at three different magnesium chloride concentrations and two annealing temperatures. Note SuDH primers produced a single, amplicon-specific band of expected base pair size (~102bp) as determined by sequencing results (Table 4.1).

4.3.2 RT-qPCR Reaction Optimization

Optimal annealing temperatures (Table 4.1) were determined to be the highest gradient temperatures found to produce the lowest and most consistent Cq values, as indicated by low technical replicate standard deviation. Optimal annealing temperatures ranged from 53.0°C for G3PDH to 63.6°C for GP (Table 4.1). Optimal annealing temperatures, as determined using RT-qPCR with a thermal gradient option, were found to be consistently different from those determined by conventional PCR methods. Optimal annealing temperatures were found to be underestimated by standard PCR methods by as much as 7.5°C in the case of PK, G6PDH, PEPCK, GK and TAGL primer sets and overestimated by 3.3°C in the case of G3PDH (data not shown).

Optimal primer concentrations were determined to be the lowest concentrations found to produce the lowest, most consistent Cq values, as indicated by low technical replicate standard deviation. Optimal forward and reverse primer concentrations for GOIs were found to vary from 300nM to 900nM with no discernable trend (Table 4.1).

4.3.3 Dynamic Linear Range (DLR) and GOI Amplification Efficiency Determination (E)

Standard curves successfully spanned no less than 2.80 log concentrations to a maximum of 4.19 log concentrations, corresponding to DLRs of between 5pg and 75ng of cDNA template (Table 4.1). In the case of GS, the DLR for RT-qPCR purposes was found to be sensitive at as little as 5pg of cDNA template (Figure 4.3). Coefficient of determination (R^2) values for standard curves ranged from 0.993 to 0.999 (Table 4.1) and gene amplification efficiency (E)-values varied from 90.0% to 100.1%. No E-value

or DLR differentiation was apparent between genes when using hydrolysis probes versus using SYBR Green chemistry (Table 4.1).

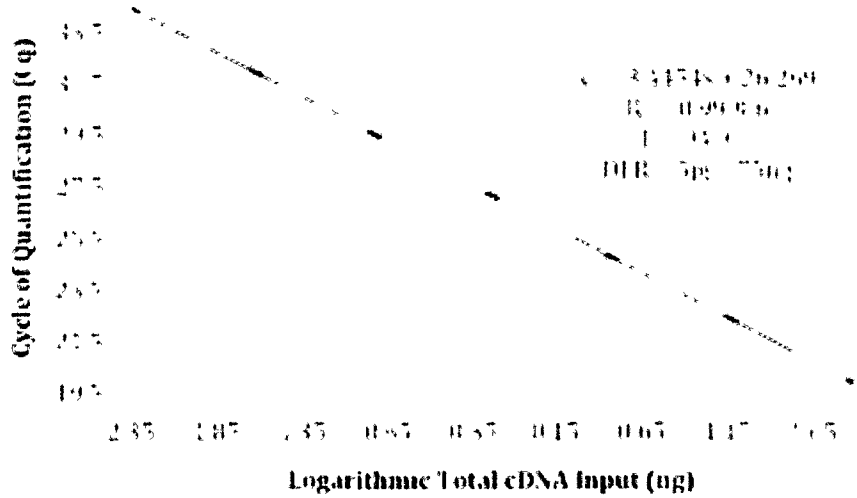

Figure 4.3. Standard curve produced for the glycogen synthase (GS) product by use of serial dilution. Concentration of pooled cDNA template was quantified by fluorometry and total cDNA input for RT-qPCR reactions calculated for each serial (1/5) dilution. Dilutions possessing standard deviations greater than 0.5 for technical replicates were eliminated from the standard curve (Applied Biosystems, 2008).

4.3.5 Temperature Data

4.3.5.1 Fall 2008

Temperature data for the fall 2008 study period indicated that a maximum daily temperature high of 30.0°C was reached twice: on both 29 September and 1 October, 2008 (Figure 4.4A). A maximum daily temperature low of -1.5°C was documented on 14 November, 2008. Mean daily temperature was at its highest point, 15.3°C, on 19 September, 2008 and reached its lowest point of -2.0°C on 14 November, 2008. From a high of 10.5°C on 8 October, 2008, minimum daily temperatures first reached below 0°C on 8 October, 2008 and fell as low as -4.5°C on 19 October, 2008.

4.3.5.2 Spring 2009

The lowest maximum, mean and minimum daily temperatures recorded at the study sample site occurred within three weeks prior to the first biological sample collection for the spring 2009 dataset (Figure 4.4B). The lowest maximum daily temperature of -8.0°C was recorded on 25 February, 2009. The lowest mean daily temperature of -16.7°C and lowest maximum daily temperature of -27.5°C were both recorded on 10 March, 2009. The first sample collection of spring 2009 occurred on 18 March, 2009 and corresponded to the last day recording a subzero mean daily temperature. After that point in time, temperatures generally increased, reaching maximum, mean and minimum daily highs of 29.5°C, 12.4°C and 5.0°C on 2 May, 12 May and 2 May, 2009 respectively.

4.3.6 GOI mRNA Expression Results

As noted previously, all geometric mean-fold changes for both fall 2008 and spring 2009 treatment groups for all GOI were set relative to 19 September, 2008 transcript accumulation levels.

4.3.6.1 GOI Associated with Major Energetic Storage Molecule Metabolism

4.3.6.1.1 Triacylglycerol Lipase (TAGL)

Triacylglycerol lipase (TAGL) exhibited constant transcript accumulation throughout the fall 2008 (Figure 4.4A) and spring 2009 (Figure 4.4B) study periods.

Geometric mean-fold change values did not show significant differences both within and among the 2008 and 2009 study periods. While a low of a 0.49-fold change was reached for the 14 November, 2008 treatment group, all other treatment groups for the fall 2008 study period returned non-significant increases in TAGL transcript accumulation. All spring 2009 treatment groups returned non-significant decreases in TAGL transcript accumulation, ranging from a low of 0.58-fold change on 29 April, 2009 to a high of 0.89-fold change on 18 March, 2009.

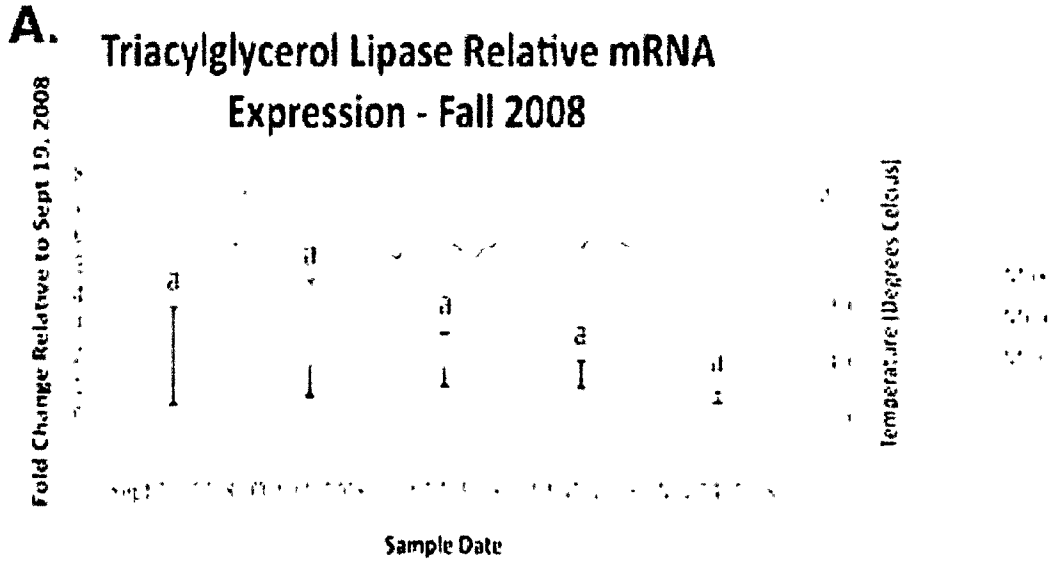

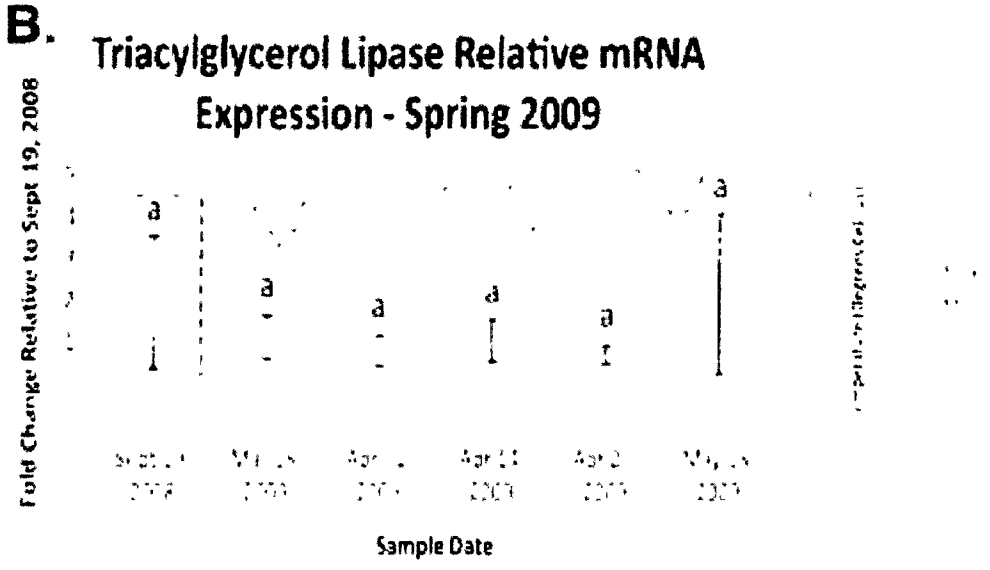

Figure 4.4 – Geometric mean fold change in *D. ponderosae* triacylglycerol lipase transcript accumulation relative to 19 September, 2008 and corresponding daily seasonal thermal data at the larval collection site for (A) fall 2008, and (B) spring 2009 study periods. Gene mRNA expression values were obtained from 4-8 *D. ponderosae* larval biological replicates, collected from two separate lodgepole pine trees, with 95% confidence intervals being displayed. One-way ANOVA were conducted for triacylglycerol lipase transcript accumulation data followed by Tukey's HSD *post-hoc* test for pair-wise multiple comparisons. Means found to be statistically different ($p<0.05$) are denoted with different lowercase letters.

4.3.6.1.2 Glycogen Phosphorylase (GP)

Seasonal glycogen phosphorylase (GP) transcript accumulation trends exhibited throughout the fall 2008 study period (Figure 4.5A) were found to be different from those found for GP transcript accumulation for spring 2009 study period (Figure 4.5B).

A statistically significant increase in GP transcript accumulation was found for the fall 2008 study period (Figure 4.5A). A 1.80-fold increase in GP transcript accumulation was obtained for the 3 October, 2008 treatment group, which was not significantly different than the 19 September, control group's transcript accumulation level. The geometric mean-fold change for 17 October, 2008 GP transcript accumulation was found to be a 5.08-fold increase and significantly different from the control group. GP transcript accumulation reached an observed maximum transcript accumulation level in the 31 October, 2008 treatment group with a 5.71-fold increase over the control group. The geometric mean-fold change in GP transcript accumulation for 31 October, 2008 was found to be significantly different from both the 19 September, and 03 October, 2008 treatment groups but not significantly different from the 17 October, and 14 November, 2008 treatment groups.

A statistically significant decrease in GP transcript accumulation was found for the spring 2009 study period (Figure 4.5B). Geometric mean-fold changes for GP transcript accumulation, compared to the control group, started at a maximum of 7.65-fold increase for the 18 March, 2009 treatment group and reached a minimum of 0.82-fold change for the 13 May, 2009 treatment group. The geometric mean-fold change for 18 March, 2009 GP transcript accumulation was found to be significantly different from both the control and all other spring 2009 treatment groups. Decreasing from 18 March,

2009 levels, the geometric mean fold change for 1 April 2009 GP transcript accumulation was found to be 3.03-fold increase and significantly different from all subsequent spring 2009 treatment groups. GP transcript accumulation levels observed in 14 April and 29 April, 2009 treatment groups were found to be a 0.86-fold change and 1.1-fold increase relative to the control group. These transcript accumulation values were not found to be significantly different from one another, the control group or the 13 May treatment groups but were found to be significantly different from the 18 March and 1 April, 2009 treatment groups.

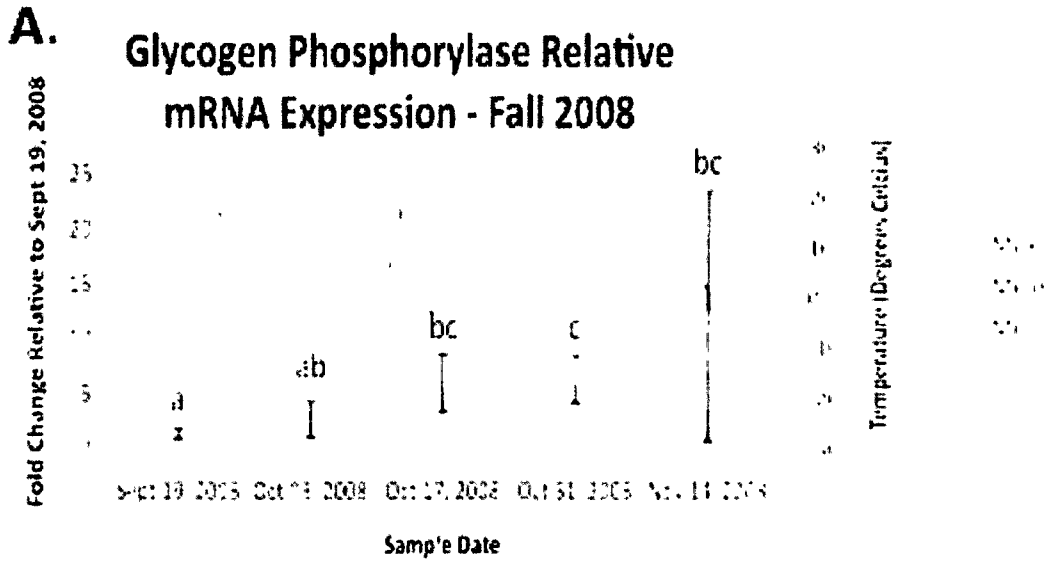

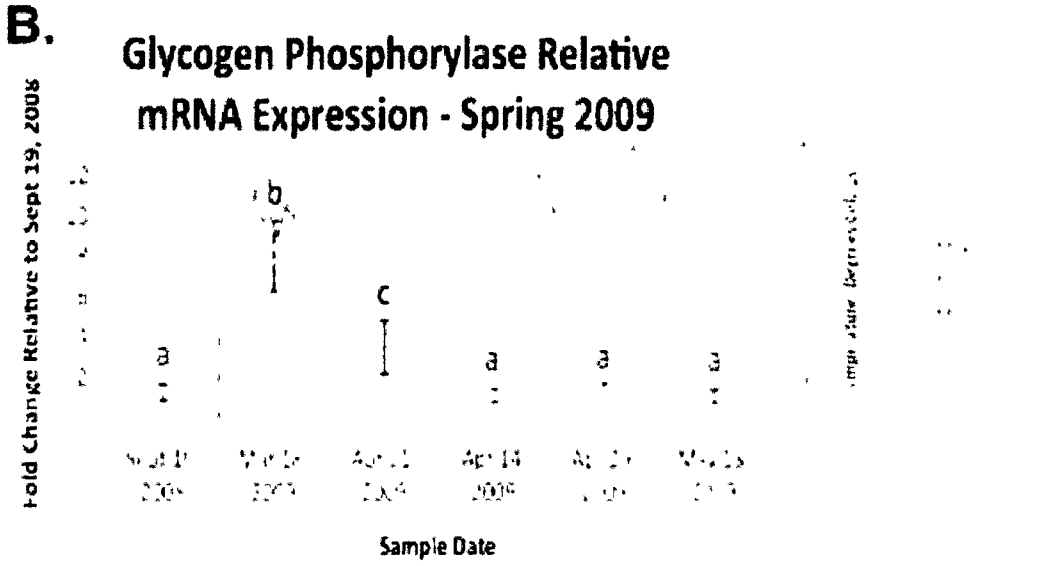

Figure 4.5 – Geometric mean fold change in *D. ponderosae* glycogen phosphorylase transcript accumulation relative to 19 September, 2008 and corresponding daily seasonal thermal data at the larval collection site for (A) fall 2008, and (B) spring 2009 study periods. Gene transcript accumulation values were obtained from 4-8 *D. ponderosae* larval biological replicates, collected from two separate lodgepole pine trees, with 95% confidence intervals being displayed. One-way ANOVA were conducted for glycogen phosphorylase transcript accumulation data followed by Tukey's HSD *post-hoc* test for pair-wise multiple comparisons. Means found to be statistically different ($p<0.05$) are denoted with different lowercase letters.

4.3.6.2 GOI Associated with the Gluconeogenesis

4.3.6.2.1 Phosphoenolpyruvate Carboxykinase (PEPCK)

Seasonal phosphoenolpyruvate carboxykinase (PEPCK) transcript accumulation trends exhibited throughout the fall 2008 study period (Figure 4.6A) were found to be different from those found for PEPCK transcript accumulation for the spring 2009 study period (Figure 4.6B).

A significant increase in PEPCK transcript accumulation was found across the fall 2008 study period (Figure 4.6A). A 2.67-fold increase in PEPCK transcript accumulation was obtained for the 3 October, 2008 treatment group, which was not significantly different than the 19 September transcript accumulation level. The geometric mean-fold change for 17 October, 2008 PEPCK transcript accumulation was found to be a 24.54-fold increase and significantly different from the control and 3 October, 2008 treatment groups. From 17 October, 2008, PEPCK did not return statistically different transcript accumulation results, with the observed maximum transcript accumulation level reaching a 34.54-fold increase for the 31 October, 2008 treatment group and a 17.61-fold increase for the 14 November, 2008 treatment group.

A statistically significant decrease in PEPCK transcript accumulation was found for the spring 2009 study period (Figure 4.6B). Geometric mean-fold changes for PEPCK transcript accumulation, compared to the control group, started at a maximum of a 58.64-fold increase for the 18 March, 2009 treatment group and reached a minimum of a 1.01-fold increase for the 14 April, 2009 treatment group. With exception of the 1 April, 2009 treatment group, the geometric mean-fold change for 18 March, 2009

PEPCK transcript accumulation was found to be significantly different from all other spring 2009 treatment groups. Decreasing from 18 March, 2009 levels, the geometric mean fold change for 1 April, 2009 PEPCK transcript accumulation was found to be a 5.37-fold increase and significantly different from all subsequent spring 2009 treatment groups. PEPCK transcript accumulation levels observed for the 29 April and 13 May 2009 treatment groups were found to be 1.19-fold and 1.25-fold increases respective to the control group. These transcript accumulation values were not found to be significantly different from one another, the 19 September, 2008 control, or the 11 April treatment groups but were found to be significantly different from the 18 March and 1 April, 2009 treatment groups.

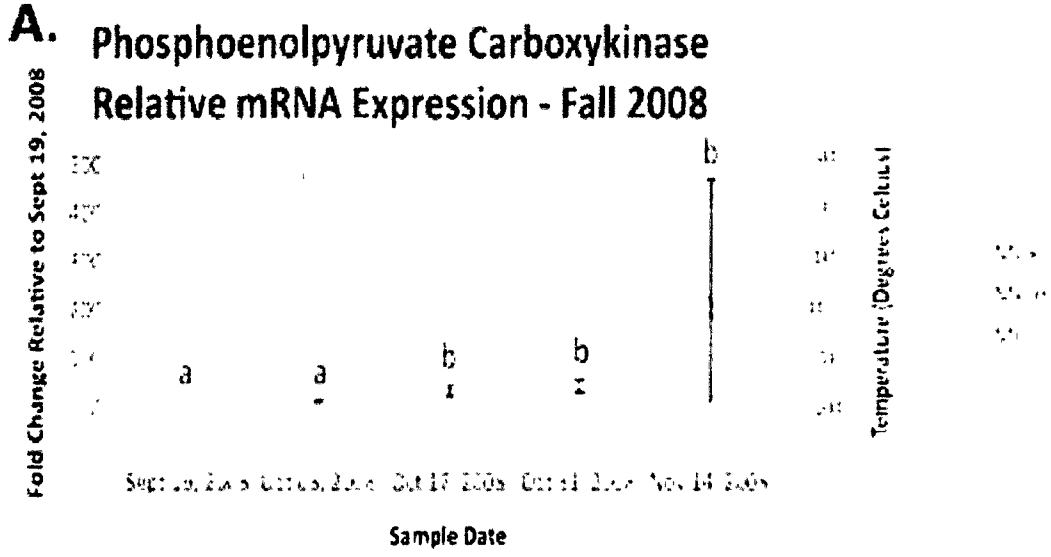

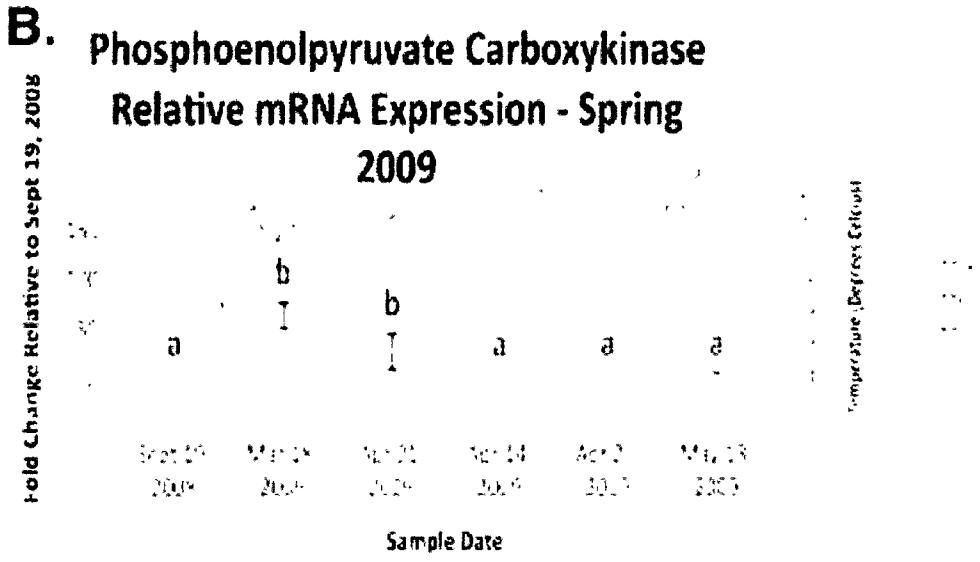

Figure 4.6 – Geometric mean fold change in *D. ponderosae* phosphoenolpyruvate carboxykinase transcript accumulation relative to 19 September, 2008 and corresponding daily seasonal thermal data at the larval collection site for (A) fall 2008, and (B) spring 2009 study periods. Gene transcript accumulation values were obtained from 4-8 *D. ponderosae* larval biological replicates, collected from two separate lodgepole pine trees, with 95% confidence intervals being displayed. One-way ANOVA were conducted for phosphoenolpyruvate carboxykinase transcript accumulation data followed by Tukey's HSD *post-hoc* test for pair-wise multiple comparisons. Means found to be statistically different ($p<0.05$) are denoted with different lowercase letters.

4.3.6.2.2 Fructose-1,6-bisphosphatase (FBP)

Seasonal fructose-1,6-bisphosphatase (FBP) transcript accumulation trends exhibited throughout the fall 2008 study period (Figure 4.7A) were found to be different from those found for FBP transcript accumulation for the spring 2009 study period (Figure 4.7B).

A significant increase in FBP transcript accumulation was found across the fall 2008 study period (Figure 4.7A). A 1.45-fold increase in FBP transcript accumulation was obtained for the 3 October, 2008 treatment group, which was not significantly different than the 19 September transcript accumulation level. The geometric mean-fold change for 17 October, 2008 FBP transcript accumulation was found to be a 6.88-fold increase and significantly different from the control and 3 October, 2008 treatment groups. From 17 October, 2008, FBP did not to return statistically different transcript accumulation results, with the observed maximum transcript accumulation level reaching a 8.72-fold increase for the 31 October, 2008 treatment group and a 5.73-fold increase for the 14 November, 2008 treatment group.

A statistically significant decrease in FBP transcript accumulation was found for the spring 2009 study period (Figure 4.7B). Geometric mean-fold changes for FBP transcript accumulation, compared to the control group, started at a maximum of a 13.47-fold increase for the 18 March, 2009 treatment group and reached a minimum of a 0.61-fold change for the 13 May, 2009 treatment group. With exception of the 1 April, 2009 treatment group, the geometric mean-fold change for 18 March, 2009 FBP transcript accumulation was found to be significantly different from all other spring 2009 treatment groups. Decreasing from 18 March, 2009 levels, the geometric mean fold

change for 1 April, 2009 FBP transcript accumulation was found to be a 5.37-fold increase and significantly different from all subsequent spring 2009 treatment groups. FBP transcript accumulation levels observed for the 14 April and 29 April, 2009 treatment groups were found to be 1.07-fold and 1.19-fold increase respective to the control group. These transcript accumulation values were not found to be significantly different from one another, the 19 September, 2008 control, or the 13 May treatment groups but were found to be significantly different from the 18 March and 1 April, 2009 treatment groups.

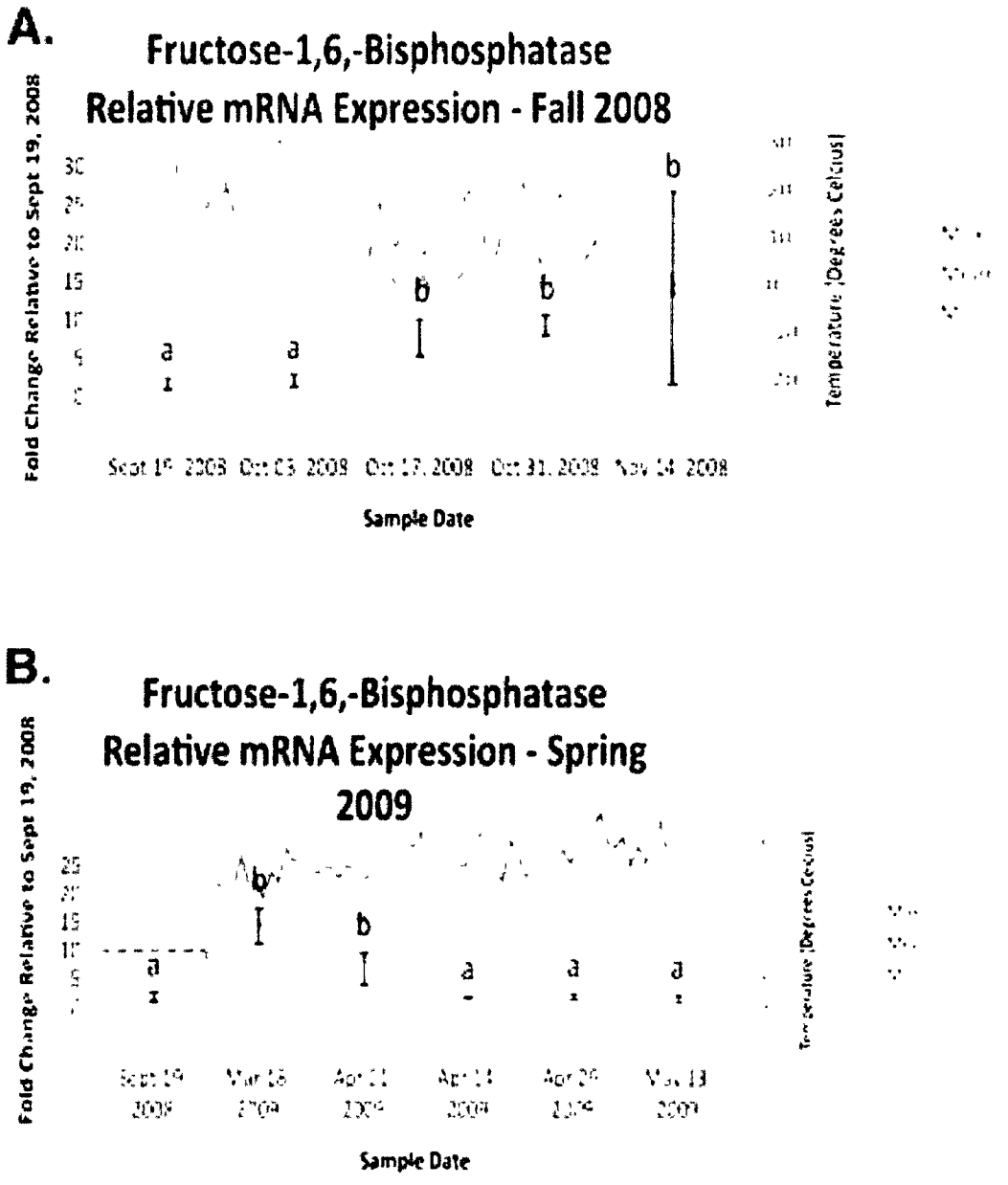

Figure 4.7 – Geometric mean fold change in *D. ponderosae* fructose-1,6,-bisphosphatase transcript accumulation relative to 19 September, 2008 and corresponding daily seasonal thermal data at the larval collection site for (A) fall 2008, and (B) spring 2009 study periods. Gene transcript accumulation values were obtained from 4-8 *D. ponderosae* larval biological replicates, collected from two separate lodgepole pine trees, with 95% confidence intervals being displayed. One-way ANOVA were conducted for fructose-1,6,-bisphosphatase transcript accumulation data followed by Tukey's HSD *post-hoc* test for pair-wise multiple comparisons. Means found to be statistically different ($p<0.05$) are denoted with different lowercase letters.

4.3.6.3 GOI Involved in Glycogenesis

4.3.6.3.1 Glycogen Synthase (GS)

Seasonal glycogen synthase (GS) transcript accumulation trends exhibited throughout the fall 2008 study period (Figure 4.8A) were found to be different from those found for GS transcript accumulation for spring 2009 study period (Figure 4.8B).

A small but significant increase in GS transcript accumulation was found across the fall 2008 study period (Figure 4.8A). A 1.54-fold increase in GS transcript accumulation was obtained for the 3 October, 2008 treatment group, which was not significantly different than the 19 September transcript accumulation level. The geometric mean-fold change for 17 October, 2008 GS transcript accumulation was found to be a 1.86-fold increase and significantly different from the 19 September, 2008 control group. From 17 October, 2008, GS did not return statistically different transcript accumulation results, with the observed maximum transcript accumulation level reaching a 2.02-fold increase for the 14 November, 2008 treatment group.

A significant decrease in GS transcript accumulation was found for the spring 2009 study period (Figure 4.8B). Geometric mean-fold changes for GS transcript accumulation, compared to the control group, started at a maximum of a 3.07-fold increase for the 18 March, 2009 treatment group and reached a minimum of a 0.95-fold change for the 29 April, 2009 treatment group. With the exception of the 1 April, 2009 treatment group, the geometric mean-fold change for 18 March, 2009 GS transcript accumulation was found to be significantly different from all other spring 2009 treatment groups. Decreasing from 18 March, 2009 levels, the geometric mean fold change for 1 April, 2009 GS transcript accumulation was found to be a 1.94-fold increase and

significantly different from the 29 April and 13 May, 2009 treatment groups. GS transcript accumulation levels observed in 14 April and 13 May, 2009 treatment groups were found to be a 0.95-fold change and a 1.02-fold increase respective to the control group. These transcript accumulation values were not found to be significantly different from one or from either the control group or the 29 April, 2009 treatment groups.

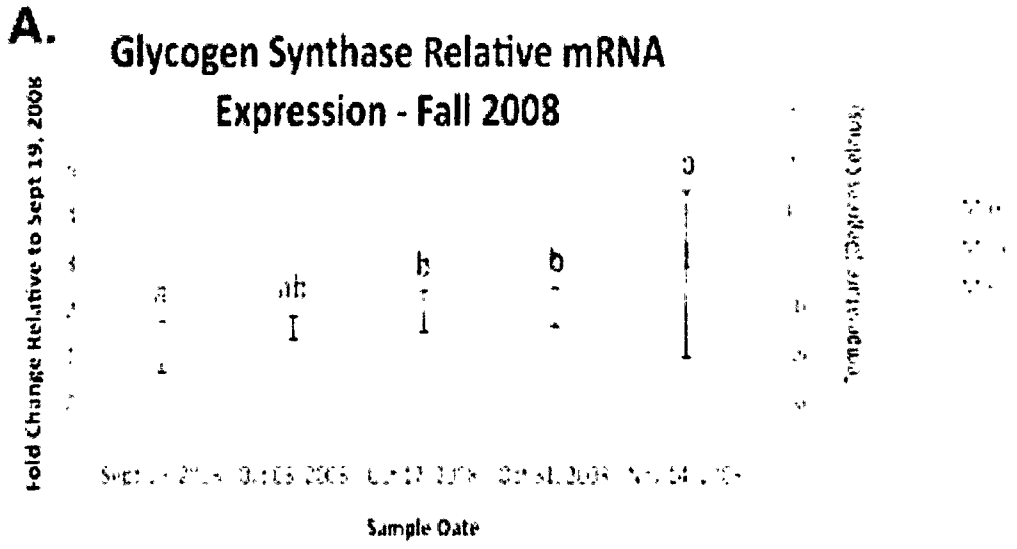

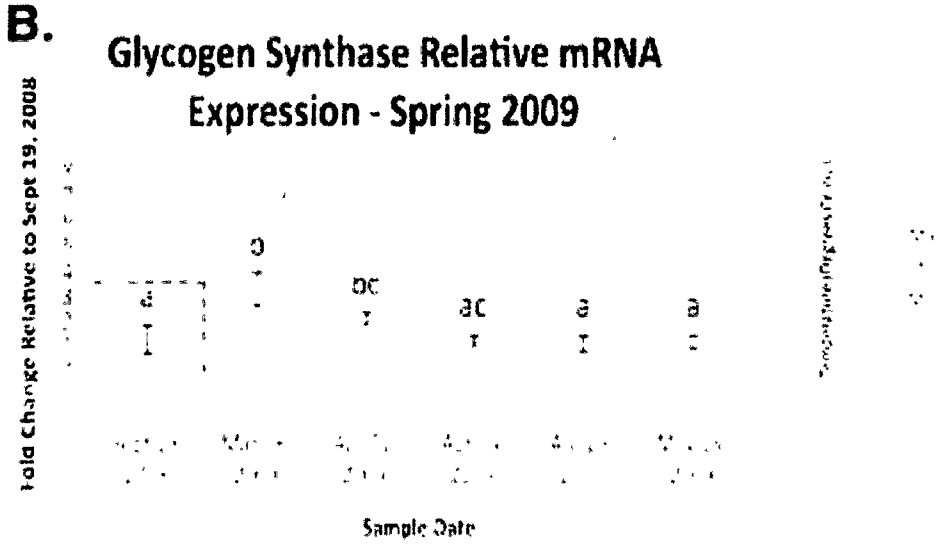

Figure 4.8 – Geometric mean fold change in *D. ponderosae* glycogen synthase transcript accumulation relative to 19 September, 2008 and corresponding daily seasonal thermal data at the larval collection site for (A) fall 2008, and (B) spring 2009 study periods. Gene transcript accumulation values were obtained from 4-8 *D. ponderosae* larval biological replicates, collected from two separate lodgepole pine trees, with 95% confidence intervals being displayed. One-way ANOVA were conducted for glycogen synthase transcript accumulation data followed by Tukey's HSD *post-hoc* test for pair-wise multiple comparisons. Means found to be statistically different ($p<0.05$) are denoted with different lowercase letters.

4.3.6.4 GOI Associated with Substrate Intermediates Involved in Glycerol Metabolism

4.3.6.4.1 Alcohol Dehydrogenase (ADH)

Alcohol dehydrogenase (ADH) exhibited constant transcript accumulation throughout the fall 2008 (Figure 4.9A) and spring 2009 (Figure 4.9B) study periods. Geometric mean-fold change values for ADH did not produce significant differences within 2008 and 2009 study periods. Significant differences were returned among 2008 and 2009 study periods.

For the fall 2008 study period, non-significant relative increases were obtained, with fold changes ranging from 1.05 for 17 October, 2008 to 1.37 for 14 November, 2008.

For the spring 2009 study period, all treatment groups were found to be significantly different from the 19 September, 2008 control group, but not from one another. The 18 March, 1 April and 14 April, 2009 treatment groups returned transcript accumulation increases of 3.95-fold, 3.62-fold and 3.76-fold respectively. The 29 April and 13 May, 2009 treatment groups returned transcript accumulation increases of 2.50-fold and 3.43-fold.

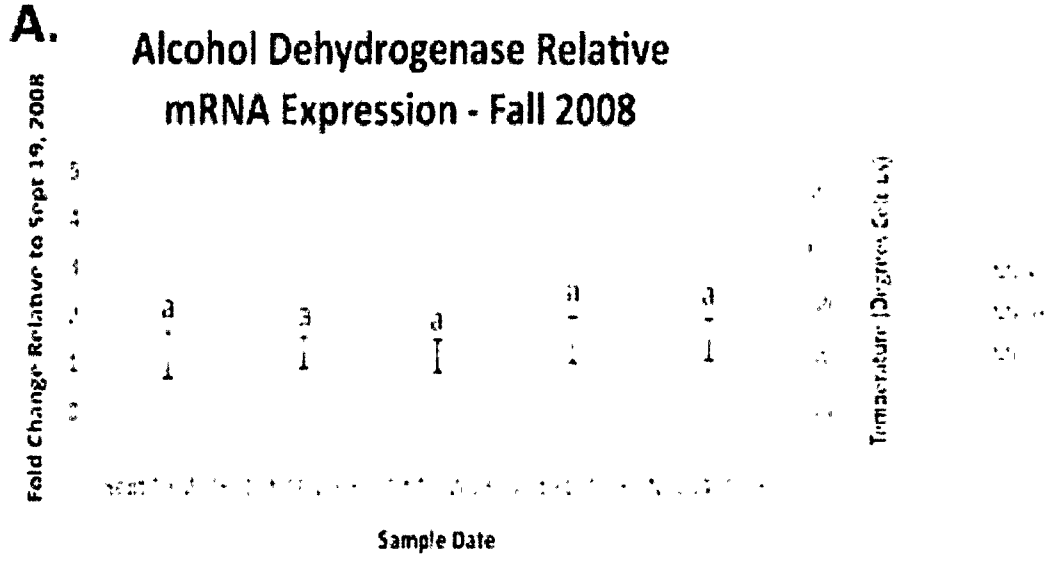

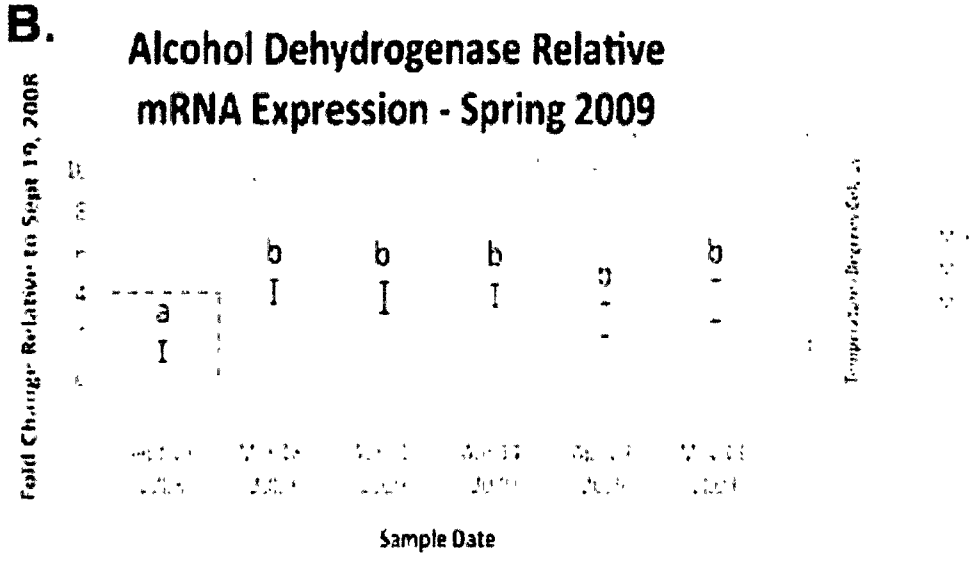

Figure 4.9 – Geometric mean fold change in *D. ponderosae* alcohol dehydrogenase transcript accumulation relative to 19 September, 2008 and corresponding daily seasonal thermal data at the larval collection site for (A) fall 2008, and (B) spring 2009 study periods. Gene transcript accumulation values were obtained from 4-8 *D. ponderosae* larval biological replicates, collected from two separate lodgepole pine trees, with 95% confidence intervals being displayed. One-way ANOVA were conducted for alcohol dehydrogenase transcript accumulation data followed by Tukey's HSD *post-hoc* test for pair-wise multiple comparisons. Means found to be statistically different ($p<0.05$) are denoted with different lowercase letters.

4.3.6.4.2 Triosephosphate Isomerase (TPI)

Seasonal triosephosphate isomerase (TPI) transcript accumulation trends exhibited throughout the fall 2008 study period (Figure 4.10A) were found to be different from those found for GS transcript accumulation for spring 2009 study period (Figure 4.10B).

A small but significant increase in TPI transcript accumulation was found across the fall 2008 study period (Figure 4.10A). A 1.02-fold increase in TPI transcript accumulation was obtained for the 3 October, 2008 treatment group, which was not significantly different than the 19 September transcript accumulation level. The geometric mean-fold change for 17 October, 2008 TPI transcript accumulation was found to be a 1.57-fold increase and significantly not different from the 19 September, 2008 control group. A 1.64-fold increase in TPI transcript accumulation was returned for the 31 October, 2008 treatment group, which was found to be significantly different from the 3 October, 2008 treatment group.

A significant decrease in TPI transcript accumulation was found for the spring 2009 study period (Figure 4.10B). Geometric mean-fold changes for TPI transcript accumulation, compared to the control group, started at a maximum of a 3.26-fold increase for the 18 March, 2009 treatment group and reached a minimum of a 0.68-fold change for the 14 April, 2009 treatment group. The geometric mean-fold change for 18 March, 2009 GS transcript accumulation was found to be significantly different from all other spring 2009 treatment groups. Decreasing from 18 March, 2009 levels, all other treatment groups did not return statistically different transcript accumulation values from

the control group or from each other. TPI transcript accumulation changes observed for 1 April, 29 April and May 13, 2009 were 1.05-fold, 0.90-fold and 0.92-fold respectively.

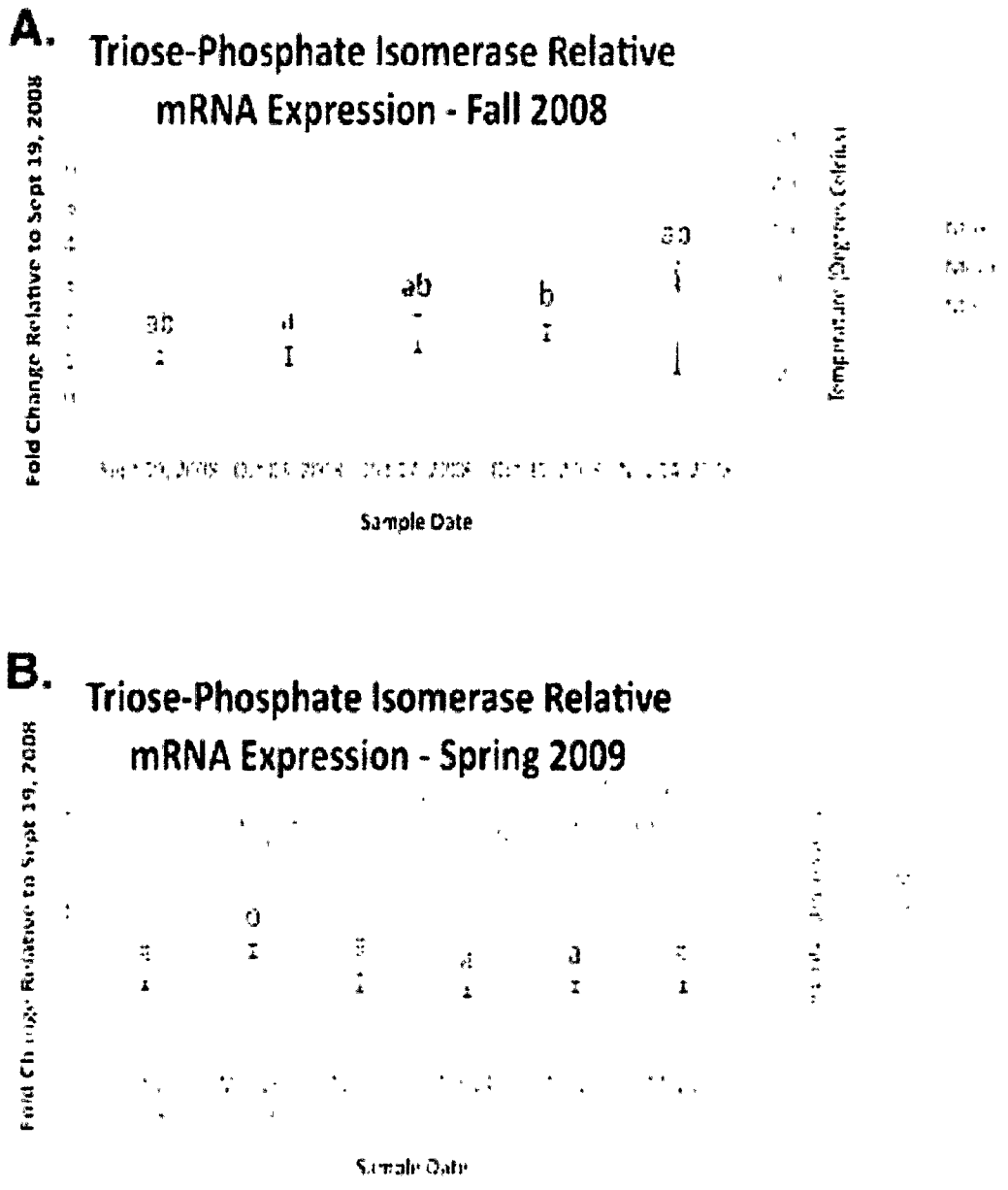

Figure 4.10 – Geometric mean fold change in *D. ponderosae* triose-phosphate isomerase transcript accumulation relative to 19 September, 2008 and corresponding daily seasonal thermal data at the larval collection site for (A) fall 2008, and (B) spring 2009 study periods. Gene transcript accumulation values were obtained from 4-8 *D. ponderosae* larval biological replicates, collected from two separate lodgepole pine trees, with 95% confidence intervals being displayed. One-way ANOVA were conducted for triosephosphate isomerase transcript accumulation data followed by Tukey's HSD *post-hoc* test for pair-wise multiple comparisons. Means found to be statistically different ($p<0.05$) are denoted with different lowercase letters.

4.3.6.4.3 Glycerol-3-phosphate Dehydrogenase (G3PDH)

Seasonal glycerol-3-phosphate dehydrogenase (G3PDH) transcript accumulation trends exhibited throughout the fall 2008 study period (Figure 4.11A) were found to be different from those found for G3PDH transcript accumulation for spring 2009 study period (Figure 4.11B).

A statistically significant increase in G3PDH transcript accumulation was found for the fall 2008 study period (Figure 4.11A). A 1.72-fold increase in G3PDH transcript accumulation was obtained for the 3 October, 2008 treatment group, which was not significantly different than the 19 September 2008 control group's transcript accumulation level. The geometric mean-fold change for 17 October, 2008 G3PDH transcript accumulation was found to be a 9.10-fold increase and significantly different from both the control and 3 October, 2008 treatment groups. G3PDH transcript accumulation reached an observed maximum transcript accumulation level in the 31 October, 2008 treatment group with a 10.79-fold increase over the control group. The geometric mean-fold change in G3PDH transcript accumulation for 31 October, 2008 was found to be significantly different from both the 19 September and 03 October, 2008 treatment groups and not significantly different from the 17 October and 14 November, 2008 treatment groups. The geometric mean-fold change for 14 November, 2008 G3PDH transcript accumulation was found to be a 5.88-fold increase and significantly different from the control group.

A statistically significant decrease in G3PDH transcript accumulation was found for the spring 2009 study period (Figure 4.11B). Geometric mean-fold changes for G3PDH transcript accumulation, compared to the 19 September, 2008 control group,

started at a maximum of a 16.88-fold increase for the 18 March, 2009 treatment group and reached a minimum of a 1.01-fold change for the 14 April, 2009 treatment group. With exception of the 1 April, 2009 treatment group, the geometric mean-fold change for 18 March, 2009 G3PDH transcript accumulation was found to be significantly different from all other spring 2009 treatment groups. Decreasing from 18 March, 2009 levels, the geometric mean fold change for 1 April, 2009 G3PDH transcript accumulation was found to be a 5.92-fold increase and significantly different from all subsequent spring 2009 treatment groups. G3PDH transcript accumulation levels observed for the 29 April and 13 May, 2009 treatment groups were found to be 1.06-fold and 1.30-fold increases respective to the control group. These transcript accumulation values were not found to be significantly different from one another or the 19 September, 2008 control group but were found to be significantly different from the 18 March and 1 April, 2009 treatment groups.

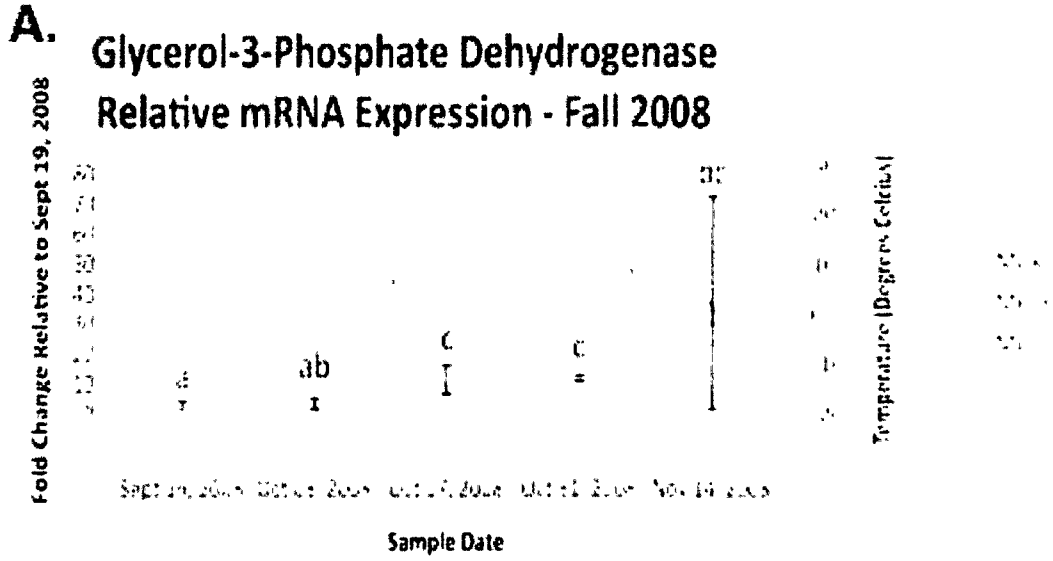

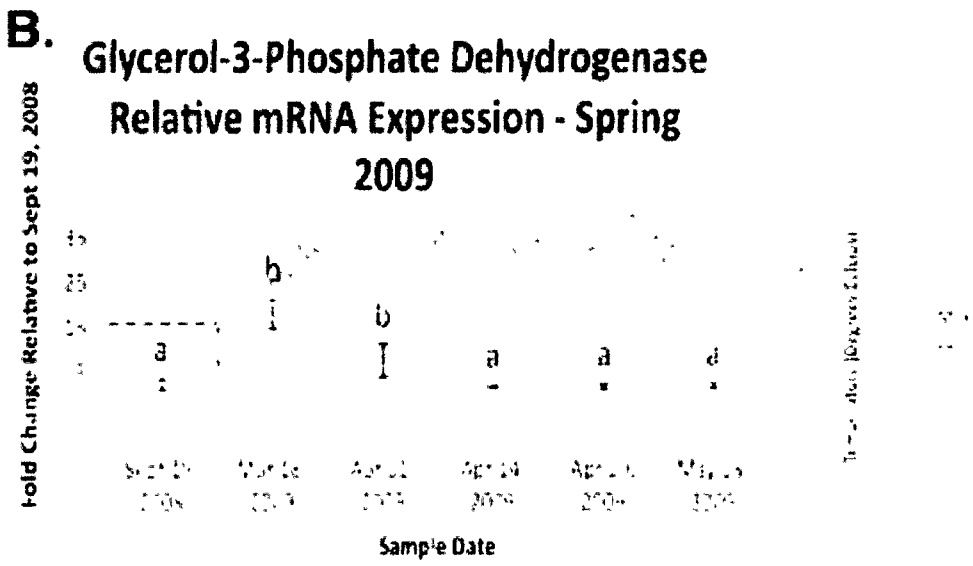

Figure 4.11 – Geometric mean fold change in *D. ponderosae* glycerol-3-phosphate dehydrogenase transcript accumulation relative to 19 September, 2008 and corresponding daily seasonal thermal data at the larval collection site for (A) fall 2008, and (B) spring 2009 study periods. Gene transcript accumulation values were obtained from 4-8 *D. ponderosae* larval biological replicates, collected from two separate lodgepole pine trees, with 95% confidence intervals being displayed. One-way ANOVA were conducted for glycerol-3-phosphate dehydrogenase transcript accumulation data followed by Tukey's HSD *post-hoc* test for pair-wise multiple comparisons. Means found to be statistically different ($p<0.05$) are denoted with different lowercase letters.

4.3.6.4.4 Glycerol Kinase (GK)

Seasonal glycerol kinase (GK) transcript accumulation trends exhibited throughout the fall 2008 study period (Figure 4.12A) were found to be different from those found for GK transcript accumulation for the spring 2009 study period (Figure 4.12B).

A small significant increase in GK transcript accumulation was found across the fall 2008 study period (Figure 4.12A). A 1.45-fold increase in GK transcript accumulation was obtained for the 3 October, 2008 treatment group, which was not significantly different than the 19 September transcript accumulation level. The geometric mean-fold change for 17 October, 2008 GK transcript accumulation was found to be a 3.84-fold increase and significantly different from the 19 September, 2008 control and 3 October, 2008 treatment groups. From 17 October, 2008, GK did not return statistically different transcript accumulation results, with the observed maximum transcript accumulation level reaching a 4.64-fold increase for the 14 November, 2008 treatment group and a 3.75-fold increase for the 14 November, 2008 treatment group.

A significant decrease in GK transcript accumulation was found for the spring 2009 study period (Figure 4.12B). Geometric mean-fold changes for GK transcript accumulation, compared to the control group, started at a maximum of a 10.05-fold increase for the 18 March, 2009 treatment group and reached a minimum of 1.36-fold for the 13 May, 2009 treatment group. The geometric mean-fold change for 18 March, 2009 GK transcript accumulation was found to be significantly different from all other spring 2009 treatment groups. Decreasing from 18 March, 2009 levels, the geometric mean fold change for 1 April, 2009 GK transcript accumulation was found to be a 4.25-fold

increase and significantly different from the control group. GK transcript accumulation levels observed in 14 April and 13 May 2009 treatment groups were found to be 2.77-fold and 2.25-fold increases respectively and significantly different from the control and 18 March 2009 treatment groups. The transcript accumulation value for the 13 May 2009 treatment group was not found to be significantly different from the control group but was found to be significantly different from all other spring 2009 treatment groups.

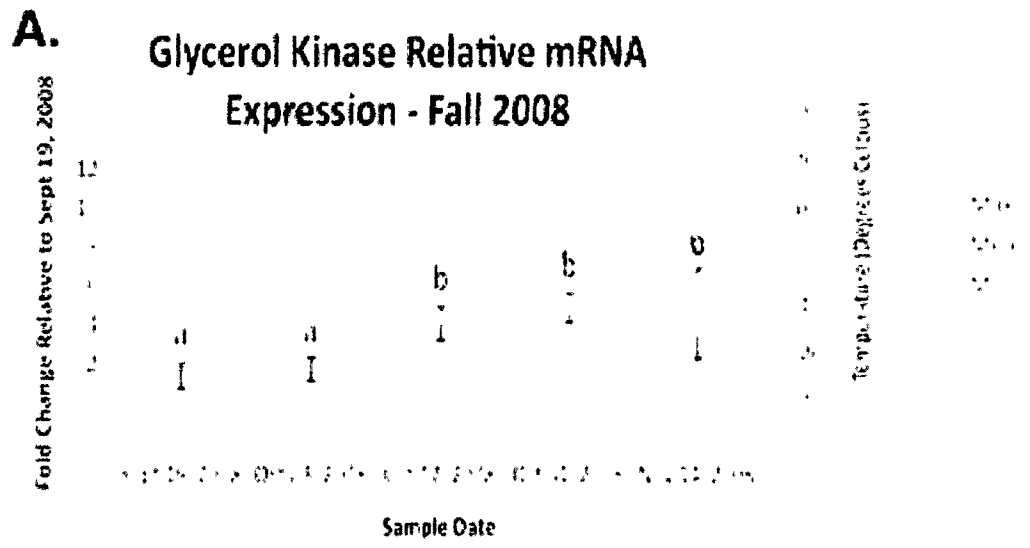

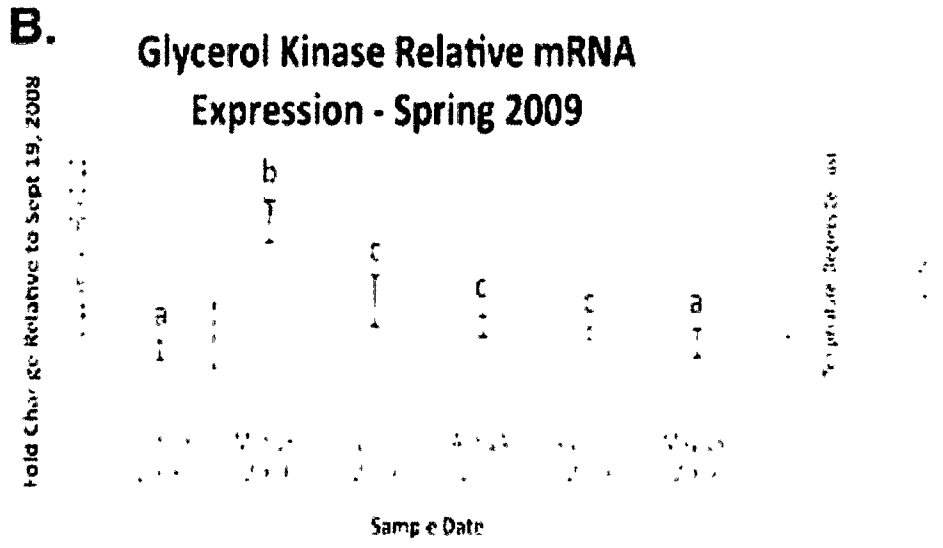

Figure 4.12 – Geometric mean fold change in *D. ponderosae* glycerol kinase transcript accumulation relative to 19 September, 2008 and corresponding daily seasonal thermal data at the larval collection site for (A) fall 2008, and (B) spring 2009 study periods. Gene transcript accumulation values were obtained from 4-8 *D. ponderosae* larval biological replicates, collected from two separate lodgepole pine trees, with 95% confidence intervals being displayed. One-way ANOVA were conducted for glycerol kinase transcript accumulation data followed by Tukey's HSD *post-hoc* test for pair-wise multiple comparisons. Means found to be statistically different ($p<0.05$) are denoted with different lowercase letters.

4.3.6.5 GOI Associated with the Pentose Phosphate Pathway

4.3.6.5.1 6-Phosphoglucolactonase (6-PGL)

6-phosphoglucolactonase (6-PGL) exhibited constant transcript accumulation throughout the fall 2008 (Figure 4.13A) and spring 2009 (Figure 4.13B) study periods. Geometric mean-fold change values for 6-PGL did not produce significant differences both within and among the 2008 and 2009 study periods.

For the fall 2008 study period, relative decreases and increases were obtained, with fold changes ranging from a 0.75-fold change for 3 October, 2008 to a 1.53-fold increase for 14 November, 2008.

For the spring 2009 study period, the 18 March and 29 March, 2009 treatment groups did not return fold changes significantly different from the 19 September, 2008 control group (i.e. fold change of 1.00). The 14 April and 13 May, 2009 treatment groups returned transcript accumulation changes of 0.82-fold and 0.91-fold respective to the control group. The 1 April, 2009 treatment group returned a transcript accumulation increase of a 1.28-fold change.

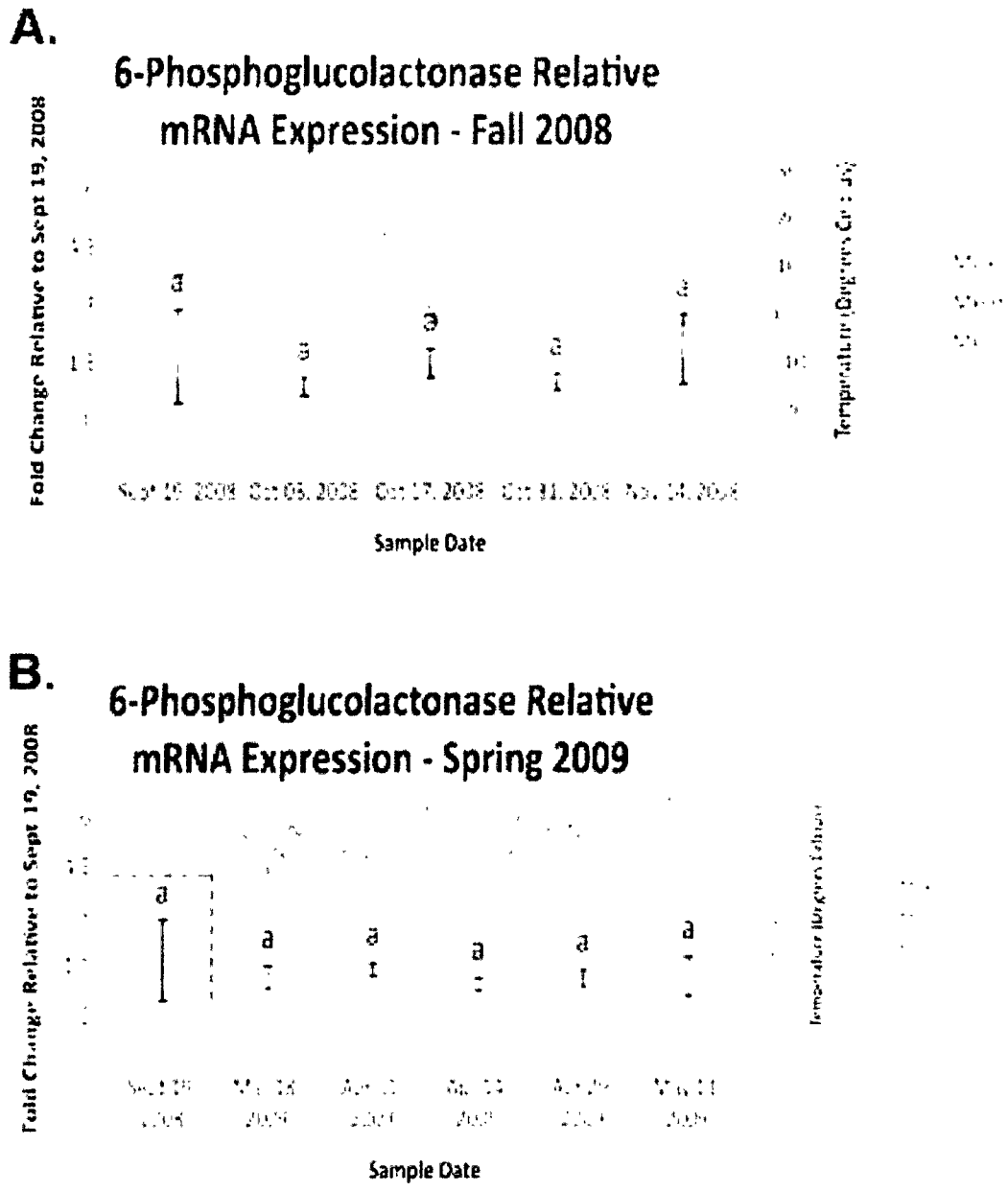

Figure 4.13 – Geometric mean fold change in *D. ponderosae* 6-phosphoglucolactonase transcript accumulation relative to 19 September, 2008 and corresponding daily seasonal thermal data at the larval collection site for (A) fall 2008, and (B) spring 2009 study periods. Gene transcript accumulation values were obtained from 4-8 *D. ponderosae* larval biological replicates, collected from two separate lodgepole pine trees, with 95% confidence intervals being displayed. One-way ANOVA were conducted for 6-phosphoglucolactonase transcript accumulation data followed by Tukey's HSD *post-hoc* test for pair-wise multiple comparisons. Means found to be statistically different ($p<0.05$) are denoted with different lowercase letters.

4.3.6.5.2 Glucose-6-phosphate dehydrogenase (G6PDH)

Glucose-6-phosphate dehydrogenase (G6PDH) exhibited constant transcript accumulation throughout the fall 2008 (Figure 4.14A) and spring 2009 (Figure 4.14B) study periods. Geometric mean-fold change values for G6PDH did not produce significant differences both within and among the 2008 and 2009 study periods.

For the fall 2008 study period, relative decreases and increases were obtained, with fold changes ranging from a 0.75-fold change for 3 October, 2008 to a 1.53-fold increase for 14 November, 2008.

For the spring 2009 study period, the 18 March treatment group did not return fold changes different from the control group (i.e. fold change of 1.01). The 1 April, 14 April and 29 April, 2009 treatment groups returned transcript accumulation of 0.64-fold, 0.81-fold and 0.70-fold respective to the control group. The 13 May, 2009 treatment group returned a transcript accumulation increase of 1.25-fold.

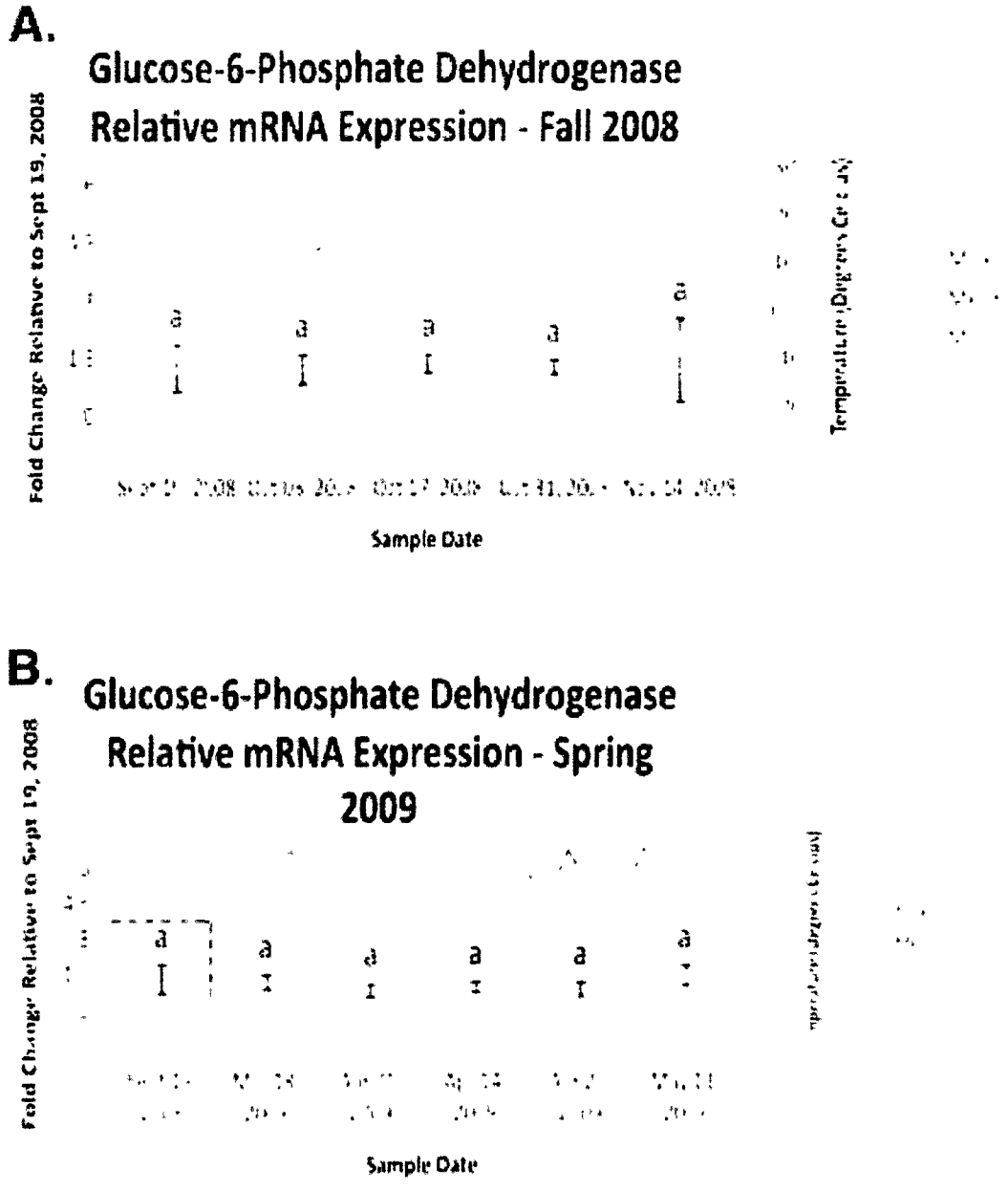

Figure 4.14 – Geometric mean fold change in *D. ponderosae* glucose-6-phosphate dehydrogenase transcript accumulation relative to 19 September, 2008 and corresponding daily seasonal thermal data at the larval collection site for (A) fall 2008, and (B) spring 2009 study periods. Gene transcript accumulation values were obtained from 4-8 *D. ponderosae* larval biological replicates, collected from two separate lodgepole pine trees, with 95% confidence intervals being displayed. One-way ANOVA were conducted for glucose-6-phosphate dehydrogenase transcript accumulation data followed by Tukey's HSD *post-hoc* test for pair-wise multiple comparisons. Means found to be statistically different ($p<0.05$) are denoted with different lowercase letters.

4.3.6.6 GOI Associated with the Citric Acid Cycle

4.3.6.6.1 Pyruvate kinase (PK)

Pyruvate kinase (PK) exhibited constant transcript accumulation throughout the fall 2008 (Figure 4.15A) and spring 2009 (Figure 4.15B) study periods. Geometric mean-fold change values for PK did not produce significant differences both within and among the 2008 and 2009 study periods.

For the fall 2008 study period, all treatment groups returned relative increases in PK transcript accumulation, with fold increases ranging from 1.09-fold for 17 October, 2008 to 1.20-fold for 3 October, 2008.

For the spring 2009 study period, all treatment groups returned relative increase in PK transcript accumulation, with fold increases ranging from 1.22-fold for both 1 April and 13 May, 2009 to 1.75-fold for 29 April, 2009.

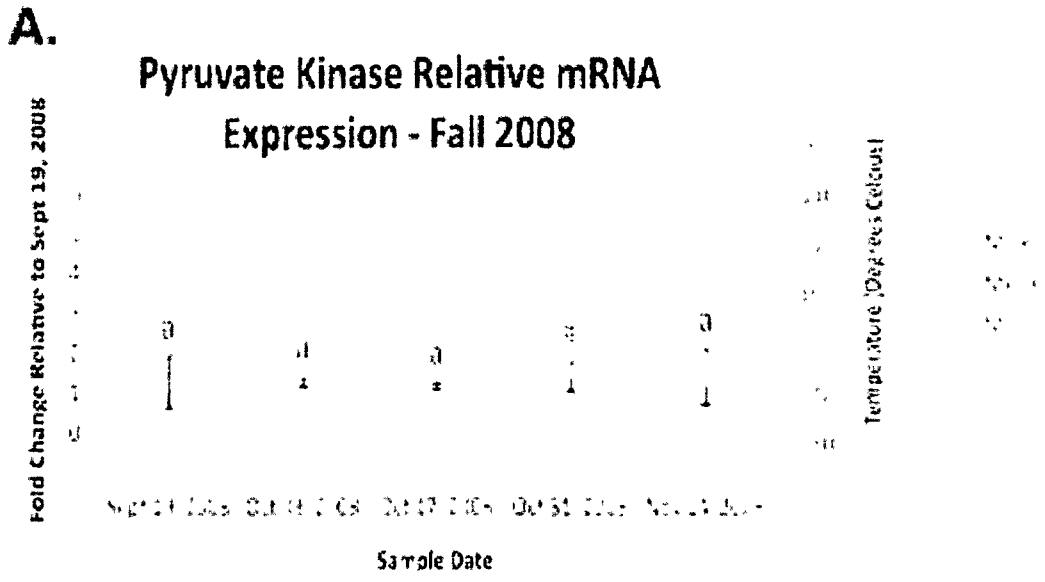

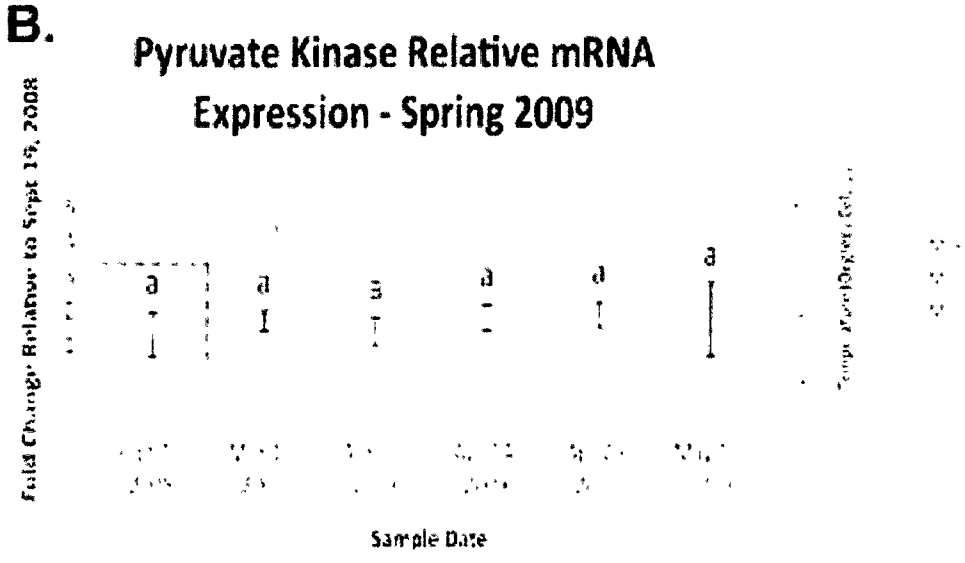

Figure 4.15 – Geometric mean fold change in *D. ponderosae* pyruvate kinase transcript accumulation relative to 19 September, 2008 and corresponding daily seasonal thermal data at the larval collection site for (A) fall 2008, and (B) spring 2009 study periods. Gene transcript accumulation values were obtained from 4-8 *D. ponderosae* larval biological replicates, collected from two separate lodgepole pine trees, with 95% confidence intervals being displayed. One-way ANOVA were conducted for pyruvate kinase transcript accumulation data followed by Tukey's HSD *post-hoc* test for pair-wise multiple comparisons. Means found to be statistically different ($p<0.05$) are denoted with different lowercase letters.

4.3.6.6.2 Citrate synthase (CS)

Citrate synthase (CS) exhibited constant transcript accumulation throughout the fall 2008 (Figure 4.16A) and spring 2009 (Figure 4.16B) study periods. Geometric mean-fold change values for CS did not produce significant differences both within and among the 2008 and 2009 study periods.

For the fall 2008 study period, the 14 November, 2008 treatment group returned a transcript accumulation change of 0.87-fold. 3 October, 17 October and 31 October, 2008 treatment groups all returned transcript accumulation increases of 1.55-fold, 1.19-fold and 1.17-fold respective to the control group.

For the spring 2009 study period, the 1 April, 2009 treatment group returned a transcript accumulation increases of 1.20-fold. All other spring 2009 treatment groups returned transcript accumulation changes ranging from a 0.60-fold change for 29 April, 2009 to 0.88-fold change for 13 May, 2009.

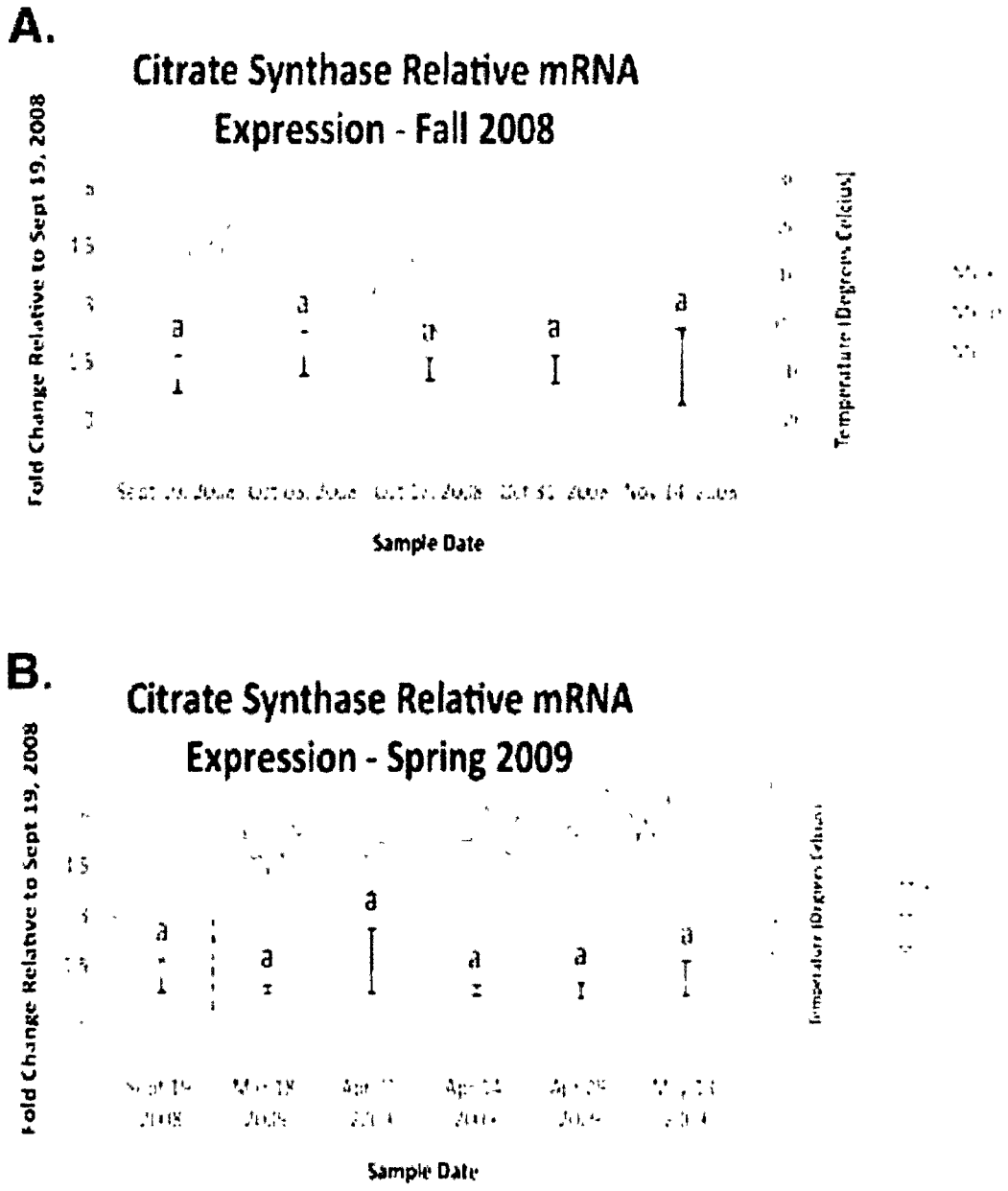

Figure 4.16 – Geometric mean fold change in *D. ponderosae* citrate synthase transcript accumulation relative to 19 September, 2008 and corresponding daily seasonal thermal data at the larval collection site for (A) fall 2008, and (B) spring 2009 study periods. Gene transcript accumulation values were obtained from 4-8 *D. ponderosae* larval biological replicates, collected from two separate lodgepole pine trees, with 95% confidence intervals being displayed. One-way ANOVA were conducted for citrate synthase transcript accumulation data followed by Tukey's HSD *post-hoc* test for pair-wise multiple comparisons. Means found to be statistically different ($p<0.05$) are denoted with different lowercase letters.

4.4 Discussion

4.4.1 Introduction to Challenges of GOI Analysis

The main goals of this study were: i) to assess transcript accumulation of genes of interest (GOI) in *D. ponderosae* that are important in glycerol production in other insects and ii) to identify potential seasonal and/or thermal cues inducing any observed changes in transcript accumulation. Identifying a correlative relationship between relative transcript accumulation levels for GOI associated with glycerol production and seasonal temperatures can provide inferences as to how *D. ponderosae* achieve a state of cold tolerance, however, other phenomena that act concurrently with seasonal temperature changes complicate an understanding of the two primary study variables.

Our cold tolerance study period spanned from 19 September, 2008 to 13 May, 2009. In addition to weathering seasonal temperature changes throughout this period, *D. ponderosae* must also, but not limited to: i) undergo a state of quiescence, ii) incur continual development, iii) endure a prolonged period of fasting and, iv) experience potential periods of hypoxia and/or anoxia. All of these phenomena tax limited energy stores of larvae; stores required for the production of cryoprotectants. Also, polyols are not exclusively produced for cryoprotectant purposes, further complicating our analysis of transcript accumulation. Additional complexities arise due to the limitations inherent to using RT-qPCR as a proxy measure of active enzyme abundance.

4.4.1.1 Diapause, Quiescence and Overwintering Development

Gene transcript accumulation studies probing the cause of polyol accumulation in eggs of *Bombyx mori* showed a positive correlation between declining temperatures and polyol production, suggesting that increased GOI transcript accumulation associated

with the production of polyols are induced by cold treatment in order to obtain a state of cold tolerance (Niimi *et al.*, 1993). Subsequent studies however identified that polyol production was too small to function as a form of cold tolerance and that elevated polyol levels were instead produced as necessary requirements to signal an arrest to diapause (Horie *et al.*, 2000). Similar studies conducted with two other diapausing insects, *Achaearanea tepidariorum*, the American house spider (Pullin *et al.*, 1991; Pullin, 1992) and *Pieris brassicae*, the cabbage butterfly (Tanaka, 1995) further support the hypothesis that polyol production occurs as a diapause termination signal. As declining temperatures and diapause are two interrelated factors, both requiring the production of polyols, a singular effect of temperature on polyol production cannot be adequately separated from that of diapause (Li *et al.*, 2002). Interestingly, some researchers have gone so far as to suggest that cryoprotection is simply a by-product of the metabolic suppression mediated by diapause and not a primary objective of polyol production at all (Pullin *et al.*, 1991; Pullin, 1992; Tanaka, 1995).

While a state of diapause has not been observed for *D. ponderosae* (Logan and Bentz, 1999; Powell and Logan, 2005), it is important to maintain an evolutionary perspective when interpreting gene transcript accumulation results (Harshman and James, 1998). An absence of a comprehensive evolutionary history for *D. ponderosae* fails to rule out potential vestigial physiological processes, such as polyol production for diapause signaling, which could influence correlations between observed phenomena, such as polyols produced for cryoprotection given declining temperatures. *D. ponderosae* do however experience a state of quiescence during the winter months (Powell and Logan, 2005), which, similar to diapause in other insects, has shown to

significantly alters the metabolism of stored energy reserves (Han and Bauce, 1998; Li *et al.*, 2002; Kostal *et al.*, 2004; Hahn and Denlinger, 2007). As cryoprotectant production employs these same pre-existing metabolic pathways, assessment of GOI transcript accumulation variation would not allow us to discriminate to what extent seasonal changes observed for *D. ponderosae* were shaped by endogenous quiescent cues versus exogenous thermal/seasonal cues that occur simultaneously. Continual overwintering development of non-diapausing insects similarly occurs concurrent to seasonal temperature changes, which was shown to alter both the quantity and type of energy reserve metabolized (Ding *et al.*, 2003; Tanaka, 1995).

4.4.1.2 Fasting

Bale (2002) states that, in the process of cold hardening, freeze avoidant insects cease feeding and void their gut contents so to rid themselves of potential ice-nucleating agents. Using phloem temperatures and larval supercooling points, mechanistic models support these two events occurring prior to the onset of glycerol accumulation within *D. ponderosae* (Regniere and Bentz, 2007). To maintain basal metabolism during periods of prolonged fasting, organisms will up-regulate mRNA expression involved in the process of gluconeogenesis and down-regulate mRNA expression associated with glycolysis and the citric acid cycle (Azzout *et al.*, 1986; Hagopian *et al.*, 2008; Weickert and Pfeiffer, 2006). As these pathways are directly, if not indirectly, involved in the production of glycerol upon exposure to cold temperatures, a synchronous period of fasting and declining winter temperatures complicates determining what relationship may exist between mRNA expression associated with glycerol production and thermal treatments.

4.4.1.3 Hypoxia and Anoxia

Freezing facilitates a state of ischemia that induces anaerobic metabolism when insects can no longer adequately circulate oxygen to tissues (Storey, 2004; pg 492 and 489). This insufficient supply of oxygen – referred to as hypoxia – and its more extreme form whereby all oxygen is depleted known as anoxia, has been shown to significantly influence an insect's capacity to produce glycerol when presented with declining temperatures. When experiencing a decline in temperature from 16°C to -4°C, freeze avoidant *Epiblema scudderianna* larvae under anoxic conditions only increased glycerol production by 50% compared to a 1000% increase experienced by larvae under aerobic conditions (Churchill and Storey, 1989). Similarly, freeze tolerant *Eurosta solidaginis* under anoxic conditions, first acclimated to 23°C and then exposed to 13°C, produced 57% of the glycerol that larvae under aerobic conditions produced (Storey and Storey, 1990). As with the aforementioned factors of quiescence, potential vestigial processes, continual development, and starvation, it is apparent that both hypoxia and anoxia, potentially experienced overwinter in *D. ponderosae*, also complicate determining what relationship may exist between transcript accumulation associated with glycerol production and thermal treatments. It is important to keep these factors in mind and their increased potential to create autocorrelation between variables, while analyzing this study's results.

4.4.2 Glycerol Metabolism Involves Both Glycogenolysis and Gluconeogenesis

One of the predominant carbohydrate energy reserves used by overwintering insects is glycogen (Li *et al.,* 2002; Han and Bauce, 1997; Klowden, 2002), whereas the most common lipid store comes in the form of triglycerides (Klowden, 2002).

Overwintering in a non-feeding larval state (Regniere and Bentz, 2007; personal observation), *D. ponderosae* must efficiently allocate limited energetic stores between maintaining basal metabolic levels and producing cryoprotectants, mainly glycerol (Bentz and Mullins, 1999). Measures of how overwintering metabolic rates vary and which energetic substrates are consumed in the production of glycerol have yet to be obtained for *D. ponderosae*. As both glycogen and triglycerides have the potential to metabolize glycerol (Figure 4.1), genes involved in both glycogenolysis (i.e. glycogen phosphorylase; GP) and lipolysis (triacylglycerol lipase; TAGL) were selected for investigation.

Transcript accumulation for TAGL did not reveal any observable connection with temperature data for either the fall 2008 (Figure 4.4A) or spring 2009 (Figure 4.4B) study periods. This result fails to support the hypotheses that glycerol is produced from the metabolism of triglycerides and triglycerols are used as an energy source post-quiescence. This finding runs contrary to that found for a study of the closely related *Ips pini* (Lombardero *et al.*, 2000) which indicated that lipids were indeed the source of overwintering glycerol metabolism. Mixed evidence has been generated from similar metabolite assays conducted within *Eurosta solidagensis*. Early observations found a concomitant decline in lipid content and an increase in glycerol accumulation (Morrissey and Baust, 1976), but subsequent studies observed stable overwintering lipid levels for this same insect species (Storey and Storey, 1986), which mirror our findings for TAGL.

In the fall 2008 study period a statistically significant increase in GP transcript accumulation from 19 September to 17 October was observed corresponding to an observably large decrease in temperature. Conversely, during the spring 2009 study

period a statistically significant decrease in GP transcript accumulation occured from 18 March to 1 April, corresponding to an observably large increase in temperature. The negative correlation observed between GP transcript accumulation and temperature in both the fall of 2008 (Figure 4.5A) and the spring of 2009 (Figure 4.5B) support the hypothesis that glycerol production is the result of the metabolism of glycogen in *D. ponderosae.* This conclusion is similar to the findings of numerous other studies investigating the overwintering accumulation of glycerol, such as: metabolite assays observing glycogen depletion (Storey *et al.*, 1981a; Storey and Storey, 1986; Pullin and Bale, 1989; Churchill and Storey, 1989; Han and Bauce, 1998; Li *et al.*, 2002), increased glycogenolytic enzyme activities (Storey and Storey, 1981b; Joanisse and Storey, 1994a; Joanisse and Storey, 1995; Clow *et al.*, 2008) and increased glycogenolytic gene transcript accumulation (Richards *et al.*, 2010).

While Storey and Storey (1986) concluded that glycogen was the "sole source" for synthesis of glycerol in overwintering *Eurosta solidaginis*, studies involving both cold treated *Chilo suppressalis* (Li *et al.*, 2002) and *Pyrrhocoris apterus* (Kostal *et al.*, 2004) observed that glycerol accumulation exceeded glycogen depletion, requiring an additional source from which glycerol could be metabolized. Clow *et al.* (2008) observed that cold-treated *Osmerus mordax* hepatocypes cultured in a media containing either glucose, pyruvate or lactate produced glycerol levels exceeding those of controls cultured in absence of these substrates. This enhanced glycerol production is consistent with the theory that, in response to cold treatment, glycerol can be produced by gluconeogenic means (Liebsher *et al.*, 2006).

In the fall 2008 study period a statistically significant increase in phosphoenolpyruvate carboxykinase (PEPCK) transcript accumulation from 3 October to 17 October was observed corresponding to an observably large decrease in temperature. Conversely, in the spring 2009 study period a statistically significant decrease in PEPCK transcript accumulation occurred from 1 April to 14 April, corresponding to an observably large increase in temperature. The negative relationship observed between temperature and PEPCK transcript accumulation for both the fall of 2008 (Figure 4.6A), and spring of 2009 (Figure 4.6B), study periods supports the hypothesis that, in addition to glycogenolysis, gluconeogenesis contributes to the production of overwintering glycerol in *D. ponderosae.*

A two-week lag period between fall GP and PEPCK transcript up-regulation indicates that gluconeogenesis may serve as a secondary source for glycerol production subsequent to the potential exhaustion of the primary glycogenolytic source; a successive "one-two" punch of glycerol production. Further supporting this theory are the comparative intensities at which GP mRNA and PEPCK mRNA up-regulation occur. Between 3 October and 17 October, 2008, GP relative fold-change values increased a little more that 282%. Over this same period of time, PEPCK relative fold change values increased 3.25 times as much (i.e. 919%). Where GP mRNA up-regulation appears to be gradual over a four-week period, PEPCK mRNA up-regulation displays much larger fold-change increase over a shorter two-week period of time.

Increased PEPCK activity has been reported in cultured hepatocytes from fasted mammals (Azzout *et al.*, 1986) and fasted mammal liver tissues (Hagopian *et al.*, 2008). Gluconeogenesis has been observed in other species of insects post-fasting (Zhou *et al.*,

2004) and it is possible that increased PEPCK transcript accumulation in *D. ponderosae* could be induced by experiencing prolonged fasting overwinter instead of declining fall temperatures. While our study cannot differentiate between potential nutritional or thermal cues that occur simultaneously, findings from rainbow smelt indicate increased PEPCK transcript accumulation could, at least in part, be in response to thermal cues. Seasonal variation in PEPCK transcripts within liver tissue of *Osmerus mordax*, were found to increase overwinter, with declining ambient temperatures, and decrease in the spring, with increased ambient temperatures (Liebsher *et al.*, 2006). PEPCK transcript accumulation for *Osmerus mordax* was also found to be positively correlated to smelt plasma glycerol concentrations. Both of these findings support our hypotheses that gluconeogenesis, as indicated by PEPCK transcript accumulation, is both involved in seasonal glycerol production and is upregulated in response to declining seasonal temperatures for *D. ponderosae*.

Further supporting the hypothesis that gluconeogenesis is induced during winter in *D. ponderosae* are the seasonal fructose-1,6-bisphosphatase (FBP) transcript accumulation results (Figure 4.7). FBP catalyzes reactions downstream of a mechanism branch point that could route carbon produced from the catabolism of amino acids to glycerol production (Figure 4.1). The FBP seasonal transcript accumulation profile produced for *D. ponderosae* suggests that, in addition to glycerol production, gluconeogenesis may produce additional glucose as well. In addition to producing glycerol, cold treatment of *Osmerus mordax* hepatocypes also produced glucose (Clow *et al.*, 2008), suggesting that additional glucose is either: i) produced to maintain basal metabolism, or ii) exported for glycerol production in other tissues. Different from our

results, however, enzyme activity assays for both *Eurosta solidaginis* (Joanisse and Storey, 1994a) and *Chilo suppressalis* (Li *et al.*, 2002) indicated that FBP activity was lowest during maximal glycerol production. These differences could be in part explained if FBP in *D. ponderosae* was regulated at the transcriptional level versus at a protein activity control level apparent in some other insect species.

4.4.3 Glycerol is Not Reconverted to Glycogen by Glycogenesis

While the majority of this study's objectives were concerned with GOI associated with the *production* of glycerol, further aspects related to GOI associate with glycerol *consumption* within *D. ponderosae* after spring temperatures had increased and cryoprotection was no longer essential. While several overwintering studies using radioisotope (Kukal *et al.*, 1988) and metabolite (Han and Bauce, 1998; Li *et al.*, 2002) assays have concluded that glycerol is reconverted to glycogen post-winter, contrary results and subsequent justification have also been presented elsewhere (Storey, 1997). Metabolite profiles in *Eurosta solidaginis* found that while the cryoprotectant sorbitol was reconverted to glycogen, glycerol was not (Storey and Storey, 1986). Similarly Richards *et al.*, (1987) found that spring clearance of glycerol in *Epiblema scudderiana* could only account for 20% of spring glycogen synthesized. One potential explanation for these results is that reconversion of glycerol to glycogen does not impact the surplus of reducing equivalents assumed to be accumulated during the overwintering production of glycerol (Storey, 1997). Using this reasoning, alternate fates for spring glycerol stores have been suggested such as lipid biosynthesis (Storey and Storey, 1986; Storey, 1997) and metabolism within the citric acid cycle (Storey and Storey, 1986; Joanisse and Storey, 1994a).

These results indicate a negative relationship exists between spring 2009 glycogen synthase (GS) transcript accumulation and temperature, a result that fails to support the hypothesis that glycerol is reconverted to glycogen in the spring (Figure 4.8A). It was unexpected to observe the GS transcript accumulation profile paralleling the GP transcript accumulation profile, as these two enzymes catalyze competing glycogenolytic and glycogenic reactions (Figure 4.1).

4.4.4 Glycerol is Metabolized from a DHAP Intermediate and by Glyceroneogenesis

Within arthropods there has been much debate about which intermediary substrates glycerol is produced from. Thoughtful review of this debate can be found elsewhere (Storey, 1997). Consensus within the field has centered around two triose-phosphate substrates, both produced in the process of glycogenolysis: dihydroxacetone phosphate (DHAP) and glyceraldehyde 3-phosphate (GAP). The metabolism of glycerol from these two intermediate substrates occurs by two unique two-step pathways each involving different enzymes. While the enzymes within DHAP and GAP pathways are different, these different enzymes are common in the reactions they catalyze – reduction and dephosphorylation – and differ only in the order in which these reactions occur (Figure 4.1).

The synthesis of glycerol from GAP begins with glyceraldehyde 3-phosphatase (GAPase) facilitated dephosphylation, which produces a glyceraldehyde (GA) intermediate. The reduction of the GA intermediate to produce the cryoprotectant glycerol is catalyzed by the enzyme alcohol dehydrogenase (ADH), also commonly referred to as polyol dehydrogenase with aldehyde activity. Alternatively, reduction of DHAP to glycerol 3-phosphate (G3P) is catalyzed by the enzyme glycerol 3-phosphate

dehydrogenase (G3PDH). G3P is further dephosphorylated by glycerol 3-phosphatase (G3Pase) to produce the cryoprotectant glycerol, however, it has also been predicted to occur by increased glycerol kinase (GK) activity (Kapil *et al.*, 2004).

Findings from *in vivo* studies comparing enzyme activity levels for G3PDH and G3Pase versus GAPase and ADH within *Chilo suppressalis* (Li et al., 2002) and *Eurosta solidaginis* (Joanisse and Storey, 1994a) support metabolism of GAP, versus DHAP, as a glycerol intermediate. These studies, and other metabolite based ones (Storey and Storey, 1981b), however, did not detect the presence of GK and more importantly, did not explain high activity levels of G3PDH in both their and the findings of others (Hayayakawa and Chino, 1982; Clow *et al.,* 2008). Furthermore, accumulation of G3P during the cessation of glycerol synthesis (Storey *et al.*, 1981a) and increased transcript accumulation of G3PDH both prior and during glycerol production (Liebsher *et al.*, 2006; Richards *et al.*, 2010) present the metabolism of DHAP as plausible source of glycerol synthesis. While the debate often presents DHAP and GAP metabolism as mutually exclusive options for glycerol production, enzyme activity assays in *Epiblema scudderianna* indicate that both pathways can play an important role in glycerol synthesis (Joanisse and Storey, 1994b).

Where no relationship was observed between fall 2008 temperature and ADH transcript accumulation (Figure 4.9), a negative relationship was detected for triose-phosphate isomerase (TPI) (Figure 4.10), G3PDH (Figure 4.11) and GK (Figure 4.12). These results support the hypothesis that glycerol is metabolized from a DHAP intermediate and fail to support the hypothesis that glycerol is metabolized from a GAP intermediate.

The up-regulation of TPI transcript accumulation during periods of cold was much less than that observed for either G3PDH or GK, indicating a possible regulatory role for TPI in the production of glycerol. An interesting alternative interpretation of these TPI results is that, in addition to glycogenolysis and gluconeogenesis, glyceronogenesis is facilitating the production of glycerol. Glyceroneogenesis is an abbreviated form of gluconeogenesis that leads from the catabolism of amino acid precursors to produce G3P (Hanson and Reshef, 2003). Shown previously to be important in fat metabolism in other insects (Okamura *et al.*, 2007), glyceroneogenesis, like gluconeogenesis, is highly regulated by the transcript accumulation of PEPCK. Fold-change increases for PEPCK mRNA during periods of cold exposure were far greater than any other GOI investigated within this study, reaching a high of 58.64-fold 18 March, 2009. This increased PEPCK transcript accumulation is consistent with patterns expected during periods of cold-induced glyceroneogenesis and provides the conditions required for GK to produce glycerol from G3P.

As previously mentioned, cold tolerance studies almost exclusively focus on G3Pase as the catalyst to convert G3P to glycerol. GK has only been investigated as a means of reconverting glycerol to G3P when spring temperatures rise and cryoprotection is no longer required. Should glyceroneogenesis contribute to producing G3P in excess during times of energy depletion (i.e. ADP is in excess), GK would favor the production of glycerol and ATP, both of which would be beneficial to the overwintering *D. ponderosae*. While metabolite and proteomic data would be required before theoretical cold-induction of glyceroneogenesis and consequent production of glycerol from GK

could be confirmed, if this is indeed the case, this would be this study's most significant finding.

As was indicated from the aforementioned GS transcript accumulation analysis (Figure 4.8B), when spring temperatures increase and cryoprotectant reserves are no longer essential to maintain, it is likely that glycerol is not reconverted into glycogen. Others have hypothesized that glycerol is metabolized through the citric acid cycle (Storey and Storey, 1986; Joanisse and Storey, 1994a). Our study did not observe mRNA up-regulation during the spring 2009 study period for: i) citrate synthase (CS; Figure 4.16B), an enzyme involved in the citric acid cycle, ii) pyruvate kinase (PK; Figure 4.15B), a required glycolytic enzyme, and/or, iii) enzymes from either of the two possible glycerol producing pathways – ADH or GK, G3PDH and TPI – which catalyze reversible glycerol metabolizing reactions. Failure to observe mRNA up-regulation of these enzymes indicates that glycerol is likely metabolized by means other than within the citric acid cycle.

Other authors have suggested that when metabolized in the spring, glycerol contributes to lipid biosynthesis (Storey and Storey, 1986; Storey, 1997). In order to be converted to lipid, glycerol would first need to be phosphorylated by GK to produce G3P. A prerequisite for the subsequent acetylation of G3P and eventual production of triacylglycerol would be a spring up-regulation of GK mRNA, which was not observed in my study. One possibility could be that lipid biosynthesis arises from the direct acetylation of glycerol, which through use of radioisotrope assays, has been found to occur within mammalian myoblasts and hepatocytes (Lee *et al.*, 2001). While metabolite assays would need to confirm its occurrence within *D. ponderosae*, endogenous juvenile

hormone has been shown to stimulate production of acyl-glycerols in the firebug, *Pyrrhocoris apterus* (Jedlicka *et al.*, 2009). The presence of juvenile hormone within *D. ponderosae* has been confirmed within the context of detoxification experiments, making this hypothesis relatively plausible.

It should be noted at this point that carnitine acyltransferase I (CATI), an enzyme involved in the synthesis of long-chain fatty acid derivatives, was originally selected as a GOI for this study. While template specific primers and probes were successfully designed and seasonal transcript accumulation data obtained, the standard curve for CATI did not produce an acceptable gene efficiency value (i.e. >110%). Once an acceptable gene efficiency value has been obtained for CATI, a hypothesis regarding the consumption of glycerol for purposes of lipid biosynthesis, specifically with respect to long chain fatty acids, can be assessed.

4.4.5 Glycerol Production Does Not Involve the Pentose Phosphate Pathway

No comprehensive overwintering account of insect glycerol production is complete without discussion of the flux that exists between oxidizing (i.e. NAD^+ or $NADP^+$) and reducing (i.e. NADH or NADPH) equivalents during glycerol synthesis. Function of a few key enzymes involved in glycerol metabolism are dependent on a steady supply of reducing agents. Several cold tolerance studies employing radioisotope assays during cold stress under both aerobic (Wood and Nordin, 1980; Tsumuki *et al.*, 1987) and anaerobic conditions (Meyer, 1978; Storey and Storey, 1990) have shown an increased activity of the pentose phosphate pathway (PPP) during cold induced cryoprotectant synthesis. In a further investigation of prior work (Storey and Storey, 1981b), an elegant set of metabolite experiments conducted with the goldenrod gall fly,

Eurosta solidaginis, under both aerobic and anoxic conditions provided clear evidence of a coupling between glycogenolytic and PPP reactions (Storey and Storey, 1990). In this study, carbon was shuttled into the PPP where reactions synthesized reducing agents for the purpose of being consumed by enzymes catalyzing polyol producing reactions. Contrary to these findings, GOI transcript accumulation of two key PPP enzymes – 6-phosphoglucolactonase (6PGL; Figure 4.13) and glucose-6-phosphate dehydrogenase (G6PDH; Figure 4.14) – within our study did not show any relationship to either temperature data or transcript accumulation of significant glycogenolytic GOI (see GP or G3PDH) within *D. ponderosae*. While these results fail to support the hypothesis that the PPP is involved in the production of glycerol, regulation of these enzymes' function could instead be present at a protein activity control level as observed in other insect species (Joanisse and Storey, 1995; Kostal *et al.*, 2004), however others' results have varied (Li *et al.*, 2002; Joanisse and Storey, 1994a; Joanisse and Storey, 1995).

4.4.6 During Glycerol Production, the Citric Acid Cycle Remains Unaffected

Suppression of metabolism has been proposed as a means to conserve limited overwintering energy reserves (Joanisse and Storey, 1994b). It was expected that transcription of both the glycolytic enzyme PK and the mitochondrial enzyme CS would be down-regulated overwinter in *D. ponderosae* because they are important to aerobic metabolism. However neither transcript exhibited an accumulation profile that suggested a connection to temperature data (Figure 4.15A and Figure 4.16A). Supporting our findings, a microarray transcript analysis for the yeast *Saccharomyces cerevisiae* grown at low temperature also did not reveal thermally induced down-regulation of PK (Tai *et al.*, 2007). While an early *in vitro* metabolite assay indicated an inactivation of PK in

cold treated *E. solidaginis* (Storey and Storey, 1981b), subsequent assays observed constant enzyme activity for PK under similar thermal stress (Joanisse and Storey, 1994a; Joanisse and Storey, 1995). This latter result was similarly found during *in vivo* studies of the rice stem borer, *Chilo suppressalis* (Li *et al.*, 2002) and *E. scudderianna* (Joanisse and Storey, 1994b).

While complicated by multiple phases of overwintering diapause and quiescence, RT-qPCR gene transcript accumulation for *in vitro* chilling experiments with *P. apterus* indicated a downregulation of CS during both diapause initiation and termination phases. Seasonal CS activity levels for two cold-hardy gall moths declined significantly from September to Novemeber, as much as 50% in the case of *Eurosta solidaginis* (Joanisse and Storey, 1995). A similar seasonal decline in enzyme activity was found in *Euphausia superba*, the Antarctic krill, (Cullen *et al.*, 2003), suggesting further investigation into protein activity control may be warranted within *D. ponderosae*.

4.5 Conclusion

This study successfully optimized RT-qPCR reaction conditions for assessment of transcript accumulation of GOI associated with glycerol metabolism. Glycerol production seems to occur through both glycogenolytic, gluconeogenic and potentially glyceroneogenic patways versus lipolytic means. Aerobic metabolism, as indicated by activity within the citric acid cycle, seems to remain constant during periods of increased glycerol production. The pentose phosphate pathway appears to be uninvolved with glycerol production and an alternative source for reducing equivalents must exist, assuming they are indeed required. Glycerol kinase transcripts were found to be present within *D. ponderosae* and its transcript accumulation was up-regulated, along with TPI and G3PDH transcripts, indicating production of glycerol from a DHAP intermediate. Constant ADH transcript accumulation indicated that a GAP is not involved in the production of glycerol. Glycogenesis does not appear to occur in the spring when glycerol is no longer needed as a cryoprotectant for *D. ponderosae*. This study provides a starting point from which subsequent metabolite and proteomic investigation can further elucidate thermal cues, and levels of regulation other than transcriptional, of seasonal production of glycerol in *D. ponderosae*.

4.6 Bibliography

Alberts, B., Johnson, A., Lewis, J., Raff, M., Roberts, K., and Walter, P. (2002). *Molecular Biology of the Cell* (4th ed.). New York, New York: Garland Science, (pp. 379).

Applied Biosystems. (2008). Real-time PCR: understanding CT. Application Note (136AP01-01), pp. 1-6.

Aukema, B.H., Carroll, A.L., Zheng, Y., Zhu, J., Raffa, K.F., Moore, R.D., Stahl, K., and Taylor, S.W. (2008). Movement of outbreak populations of mountain pine beetle: influences of spatiotemporal patterns and climate. *Ecography* 31: 348-358.

Azzout, B., Bois-Joyeux, B., Chanez, M., and Peret, J. (1986). Development of gluconeogenesis from various precursors in isolated rat hepatocytes during starvation or after feeding a high protein, carbohydrate-free diet. *J. Nutr.* 117:164-169.

Bale, J. S. (2002). Insects and low temperatures: from molecular biology to distributions and abundance. *Phil. Trans. R. Soc. Lond. B* 357: 849-862.

Baust, J.G. (1983). Protective agents: regulation of synthesis. *Cryobiology* 20: 357-364.

Bentz, B.J., Mullins, D.E. (1999). Ecology of mountain pine beetle (Coleoptera: Scolytidae) cold hardening in the intermountain West. *Environmental Entomology* 28: 577–587.

Churchill, T.A., and Storey, K.B. (1989) Metabolic correlates to glycerol biosynthesis in a freeze-avoiding insect, *Epiblema scudderiana. J. Comp. Physiol. B* 15: 461-472

Clow, K.A., Ewart, K.V., and Driedzic, W.R. (2008). Low temperature directly activates the initial glycerol antifreeze response in isolated rainbow smelt (*Osmerus mordax*) liver cells. *Am. J. Physiol. Regulatory Integrative Comp. Physiol.* 295: 961-970.

Cole, W.E. (1981). Some risks and causes of mortality in mountain pine beetle populations: a long-term analysis. *Researches on Population Ecology* 23: 116-144.

Danks, H.V. (2006). Insect adaptations to cold and changing environments *Can. Entomol.* 138: 1-23.

Delinger, D.L., and Lee, R.E. (1998). Physiology of cold sensitivity. (pp. 55-96) In: Hallman, G.J. and Delinger, D.L. (Eds.), *Temperature sensitivity in insects and application in integrated pest management* Westview Press, Boulder, Colo.

Delinger, D.L. (2002). Regulation of diapause. *Annu. Rev. Entomol.* 47: 93-122.

Ding, L., Li, Y., and Goto, M. (2003). Physiological and biochemical changes in summer and winter diapause and non-diapause pupae of the cabbage armyworm, *Mamestra brassicae* L. during long-term cold acclimation. *Journal of Insect Physiology* 49: 1153-1159.

Duman, J.G. (2001). Antifreeze and ice nucleator proteins in terrestrial arthropods. *Annu. Rev. Physiol.* 63: 327-357.

Hagopian, K., Ramsey, J.J., and Weindruch, R. (2008). Enzymes of glycerol and glyceraldehyde metabolism in mouse liver: effects of caloric restriction and age on activities *Biosci. Rep.* 28: 107-115.

Hahn, D.A., and Denlinger, D.L. (2007). Meeting the energetic demands of insect diapause: nutrient storage and utilization. *Journal of Insect Physiology* 53: 760-773.

Han, E., and Bauce, E. (1998). Timing of diapause initiation, metabolic changes and overwintering survival of the spruce budworm, *Choristoneura fumiferana. Ecological Entomology* 23: 160-167.

Hanson, R.W., and Reshef, L. (2003). Regulation of phosphoenolpyruvate carboxykinase (GTP) gene expression. *Annu. Rev. Biochem.* 66: 581-611.

Harshman, L.G., and James, A.A. (1998). Differential gene expression in insects: transcriptional control. *Annu. Rev. Entomol.* 43: 671-700.

Hayayakawa, Y., and Chino, H. (1982). Phosphofructokinase as a possible key enzyme regulating glycerol or trehalose accumulation in diapausing insects. *Insect Biochem.* 12(6): 639-642.

Horie, Y., Kanda, T., and Mochida, Y. (2000). Sorbitol as an arrester of embryonic development in diapausing eggs of the silkworm, *Bombyx mori. Journal of Insect Physiology* 46: 1009-1016.

Jedlicka, P., Cvacka, J., and Slama, K. (2009). Juvenile hormone-stimulated synthesis of acyl-glycerols and vitamin E in female accessory sexual glands of the fire bug, *Pyrrhocoris apterus* L. *Archives of Insect Biochemistry and Physiology* 72(1): 48-59.

Joanisse, D.R., and Storey, K.B. (1994a). Enzyme activity profiles in an overwintering population of freeze-tolerant larvae of the gall fly, *Eurosta solidaginis. J. Comp. Physiol. B.* 164:247-255.

Joanisse, D.R., and Storey, K.B. (1994b). Mitochondrial enzymes during overwintering in two species of cold-hardy gall insects. *Insect Biochem. Molec. Biol.* 24(2): 145-150.

Joanisse, D.R., and Storey, K.B. (1995). Temperature acclimation and seasonal responses by enzymes in cold-hardy gall insects. *Archives of Insect Biochemistry and Physiology* 28: 339-349.

Kapil, K.G., Doyle, F.J., Edwards, J.S., and Mahadevan, R. (2004). Estimating optimal profiles of genetic alterations using constraint-based models. *Biotechnol. Bioeng.* 89(2): 243-251.

Klowden, M.J. (2002). *Physiological systems in insects.* San Diego, CA: Academic Press, (pp. 1-415).

Kostal, V., Tamura, M., Tollarova, M., and Zahradnickova, H. (2004). Enzymatic capacity for accumulation of polyol cryoprotectants changes during diapause development in the adult red firebug, *Pyrrhocoris apterus. Physiological Entomology* 29: 344-355.

Kukal, O., Serianni, A.S., and Duman, J.G. (1988). Glycerol metabolism in a freeze-tolerant arctic insect: an *in vivo* ^{13}C NMR study. *J. Comp. Physiol. B* 158:175-183.

Lee, D.P., Deonarine, A.S., Kienetz, M., Zhu, Q., Skrzypczak, M., Chan, M., and Choy, P.C. (2001). A novel pathway for lipid biosynthesis: the direct acylation of glycerol. *Journal of Lipid Research* 42: 1979-1986.

Li, N., Andorfer, C.A., and Duman, J.G. (1998). Enhancement of insect antifreeze protein activity by solutes of low molecular mass. *The Journal of Experimental Biology* 201: 2243-2251.

Li, Y., Ding, L., and Goto, M. (2002). Seasonal changes in glycerol content and enzyme activities in overwintering larvae of the Shonai ecotype of the rice stem borer, *Chilo suppressalis* Walker. *Archives of Insect Biochemistry and Physiology* 50: 53-61.

Liebsher, R.S., Richards, R.C., Lewis, J.M., Short, C.E., Muise, D.M., Driedzic, W.R., and Ewart, K.V. (2006). Seasonal Freeze Resistance of rainbow smelt (*Osmerus mordax*) is generated by differential expression of glycerol-3-phosphate dehydrogenase, phosphoenolpyruvate carboxykinase, and antifreeze protein genes. *Physiological and Biochemical Zoology* 79(2):411-423.

Logan, J.A., and Bentz, B.J. (1999). Model analysis of mountain pine beetle (Coleoptera: Scolytidae) seasonality. *Environmental Entomology* 28(6): 924-934.

Lombardero M.J., Ayres, M.P., Ayres, B.B., and Reeve, J.D. (2000). Cold tolerance in four species of bark beetle (Coleoptera: Scolytidae) in North America. *Environ. Entomol.* 29(3): 421-432.

Meyer, S.G.E. (1978). Effects of heat, cold, anaerobiosis and inhibitors on metabolite concentrations in larvae of *Callitroga macellaria. Insect Biochem.* 6: 471-477.

Morrissey, R.E., and Baust, J.G. (1976). The ontogeny of cold tolerance in the gall fly, *Eurosta solidagensis. J. Insect Physiol.* 22: 431-437.

Niimi, T., Yamashita, O., and Yaginuma, T. (1993). A cold-inducible *Bombyx* gene encoding a protein similar to mammalian sorbitol dehydrogenase. *Eur. J. Biochem.* 213: 1125-1131.

Okamura, T., Shimizu, H., Nagao, T., Ueda, R., and Ishii, S. (2007). ATF-2 regulates fat metabolism in *Drosophila. Molecular Biology of the Cell* 18: 1519-1529.

Powell, J.A., and Logan, J.A. (2005). Insect seasonality: circle map analysis of temperature-driven life cycles. *Theoretical Population Biology* 67:161-179.

Pullin, A.S., and Bale, J.S. (1989). Effects of low temperature on diapausing *aglais urticae* and *Inachis io* (Lepidoptera: Nymphalidae): overwintering physiology. *J. Insect Physiol.* 35(4): 283-290.

Pullin, A.S., Bale, J.S., and Fontaine, L.R. (1991). Physiological aspects of diapause and cold tolerance during overwintering in *Pieris brassicae. Physiol. Entomol.* 16: 447-456.

Pullin, A.S. (1992). Diapause metabolism and changes in carbohydrates related to cryoprotection in *Pieris brassicae. J. Insect Physiol.* 38: 319-327.

Regniere, J., and Bentz, B. (2007). Modeling cold tolerance in the mountain pine beetle *Dendroctonus ponderosae. Journal of Insect Physiology* 53: 559-572.

Richards, J.C., Kelleher, M.J., and Storey, K.B. (1987). Strategies of freeze avoidance in larvae of the goldenrod gall moth, *Epiblema scudderiana*: winter profiles of a natural population. *J. Insect Physiol.* 33: 443-450.

Richards, R.C., Short, C.E., Driedzic, W.R., and Ewart, K.V. (2010). Seasonal changes in hepatic gene expression reveal modulation of multiple processes in rainbow smelt (*Osmerus mordax*). *Mar. Biotechnol.* 12: 650-663.

Safranyik, L. (1978). Effects of climate and weather on mountain pine beetle populations.(pp. 77-84) In Kibbee, D.L., Berryman, A.A., Amman, G.D., and Stark, R.W. (Eds.), *Theory and practice of mountain pine beetle management in lodgepole pine forests.* Symposium Proceedings, University of Idaho, Moscow, ID.

Safranyik, L., Carroll, A., (2006). The biology and epidemiology of the mountain pine beetle in lodgepole pine forests. (pp. 3-66) In: Safranyik, L., Wilson, B. (Eds.), *The mountain pine beetle, a synthesis of biology, management and impacts on lodgepole pine.* Natural Resources Canada, Canadian Forest Service, Pacific Forestry Centre, Victoria, BC.

Stahl, K., Moore, R.D., and McKendry, I.G. (2006). Climatology of winter cold spells in relation to mountain pine beetle mortality in British Columbia, Canada. *Clim. Res.* 32: 13-23.

Storey, K.B., Baust, J.G., and Storey, J.M. (1981a). Intermediary metabolism during low temperature acclimation in the overwintering gall fly larvae, *Eurosta solidaginis. J. Comp. Physiol.* 144: 183-190.

Storey, K.B., and Storey, J.M. (1981b). Biochemical strategies of overwintering in the gall fly larvae, *Eurosta solidaginis*: effect of low temperature acclimation on the activities of enzymes of intermediary metabolism. *J. Comp. Physiol.* 144: 191-199.

Storey, J.M, and Storey, K.B. (1986). Winter survival of the gall fly larvae, *Eurosta solidaginis*: profiles of fuel reserves and cryoprotectants in a natural population. *J. Insect Physiol.* 32(6): 549-556.

Storey, J.M. and Storey, K.B. (1990). Carbon balance and energetics of cryoprotectant synthesis in a freeze-tolerant insect: responses to perturbation by anoxia. *J. Com. Physiol. B* 160: 77-84.

Storey, K.B. (1997). Organic solutes in freezing tolerance. *Comp. Biochem. Physiol.* 117A(3): 319-326.

Storey, J.M., and Storey, K.B. (2004). *Cold hardiness and freeze tolerance.* In *Functional Metabolism: Regulation and Adaptation* (ed. K. B. Storey), New York: Wiley-Liss, (pp. 473-503).

Tai, S.L., Daragan-Lapujade, P., Luttik, M.A.H., Walsh, M.C., Diderich, J.A., Krijger, G.C., van Gulik, W.M., Pronk, J.T., and Daran, J. (2007). Control of the glycolytic flux in *Saccharomyces cerevisiae* grown at low temperature. *The Journal of Biological Chemistry* 282(14) 10243-10251.

Tanaka, K. (1995). Seasonal change in glycogen and inositol/sorbitol contents of the house spider, *Achaearanea tepidariorum* (Araneae: Theridiidae). *Comp. Biochem. Physiol.* 110(B): 539-545.

Tian, Q., Stepaniants, S.B., Mao, M., Weng, L., Feetham, M.C., Doyle, M.J., Yi, E.C., Dai, H., Thorsson, V., Eng, J., Goodlett, D., Berger, J.P., Gunter, B., Linseley, P.S., Stoughton, R.B., Aebersold, R., Collins, S.J., Hanlon, W.A., and Hood, L.E. (2004). Integrated genomics and proteomic analyses of gene expression in mammalian cells. *Mol. Cell. Proteomics* 3(10): 960-969.

Tsumuki, H., Rojas, R.R., Storey, K.B., and Baust, J.G. (1987). The fate of [^{14}C]Glucose during cold-hardening in *Eurosta solidaginis* (Fitch). *Insect Biochem.* 17(2): 347-352.

Weickert, M.O., and Pfeiffer, A.F.H. (2006). Signalling mechanisms linking hepatic glucose and lipid metabolism. *Diabetologia* 49: 1732-1741.

Willems, E., Leyns, L., and Vandesompele, J. (2008). Standardization of real-time PCR gene expression data from independent biological replicates. *Analytical Biochemistry* 379: 127-129.

Wood, F.E., and Nordin, J.H. (1980). Activation of the hexose monophosphate shunt during cold-induced glycerol accumulation by *Protophormia terranovae. Insect Biochem.* 10: 87-93.

Zhou, G., Flowers, M., Friedrich, K., Horton, J., Pennington, J., Wells, M.A. (2004). Metabolic fate of [^{14}C]-labeled meal protein amino acids in *Aedes aegypti mosquitoes. J Insect Physiol* 50: 337–349.

Conclusions

My evaluation of seasonal mRNA expression as it relates to glycerol biosynthesis and cold tolerance in overwintering *Dendroctonus ponderosae* has provided a significant amount of novel information. This information that I have generated both advances the field of insect cryobiology and provides potential new guidelines for the appropriate application of RT-qPCR methods to many insect species. My results are summarized below:

1. Insect RNA integrity analysis reveal that as much as an approximate 9-fold decrease in mRNA expression can be falsely detected due solely to compromised RNA integrity. Thermal, but not chemical, denaturing conditions – both of which are inherent to MCE – were found to cause cleavage of the 28S rRNA in *D. ponderosae*. The advantage that thermal treatment provides with respect to MCE in decreasing secondary structure of insect RNA must therefore be compared against the potential cost of complicating the assessment of insect RNA integrity on a case-by-case basis.

2. Area quotients, defined as the division of late phase area over early phase area, were found to strongly correlate with the amount of apparent decrease in mRNA transcript levels due to compromised insect RNA integrity and can be used as a measure of insect RNA integrity. An area quotient threshold value of ≤ 0.3 is suggested as an indicator level where the likelihood of obtaining compromised data are probable.

3. Considerable treatment-to-treatment variation was detected when analyzing the stability of endogenous controls for seasonal *D. ponderosae* samples, indicating the importance of assessing endogenous control stability prior to conducting an mRNA expression study.

4. Variation in endogenous control stability was influenced by insect development. When conducting a long-term time course study of mRNA expression on larvae, where insect development is inevitable, the importance of assessing endogenous control stability increases significantly.

5. mRNA transcript levels indicated that glycerol production in *D. ponderosae* occurs through both glycogenolytic, gluconeogenic and potentially glyceroneogenic pathways, but not from the metabolism of lipids. A two-week lag period between fall GP and PEPCK transcript up-regulation indicates that gluconeogenesis may serve as a secondary source for glycerol production subsequent to the potential exhaustion of the primary glycogenolytic source; a successive "one-two" punch of glycerol production.

6. Aerobic metabolism, as indicated by mRNA transcript levels from genes within the citric acid cycle, remains constant during periods of increased glycerol production. The pentose phosphate pathway appears to be uninvolved with glycerol production and so an alternative source for reducing equivalents must exist, assuming they are indeed required.

7. Glycerol kinase was found to be present within *D. ponderosae* and its mRNA transcript levels increased in the autumn, along with those of TPI and G3PDH, to produce glycerol from a DHAP intermediate. Constant ADH transcript levels indicated that a GAP intermediate is not involved in production of glycerol in *D. ponderosae*.

8. Glycogenesis does not appear to occur in the spring when glycerol is no longer needed as a cryoprotectant for *D. ponderosae*.

Figure A. The increasing employment of microfluidics capilliary electrophoresis as a means by which to assess RNA integrity, demonstrated by none other than LL Cool J. Illustrating its rise in popular culture, LL has traded his boombox (left) for a Biorad Experion system (right). Image modified by Tiffany R. Clarke.

Figure B. Ashton Kutcher (above, in lab goggles) stars in "Dude, Where's My Band?", a new documentary exploring the challenges involved in assessing insect RNA integrity via conventional microfluidic capillary electrophoresis measures. This has become an issue of growing interest to both scientists and Hollywood film directors alike, as illustrated here. Image modified by Tiffany R. Clarke.

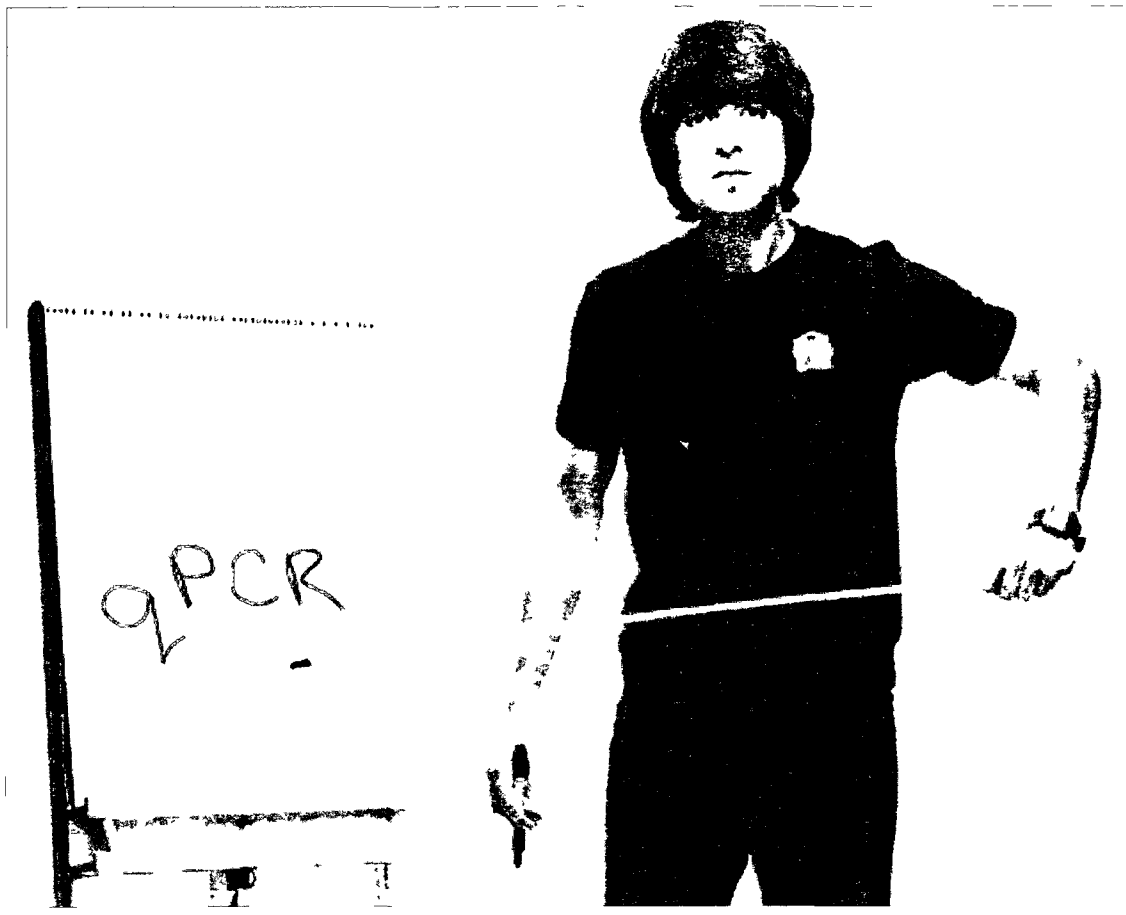

Figure C. Illustrating how qPCR methods qualify as an Important Thing. Important Things are drawn on a large pad with markers and pointed at with a pointer. "qPCR" appears both on the large pad (seen above) and is pointed at with a pointer, fulfilling both conditions of being an Important Thing. Image modified by Tiffany R. Clarke.